JRC TECHNICAL REPORTS

Evaluation of Copernicus Atmosphere Monitoring Service methane products

Koffi, E.N. and Bergamaschi, P.

2018

Joint
Research
Centre

EUR 29349 EN

This publication is a Technical report by the Joint Research Centre (JRC), the European Commission's science and knowledge service. It aims to provide evidence-based scientific support to the European policymaking process. The scientific output expressed does not imply a policy position of the European Commission. Neither the European Commission nor any person acting on behalf of the Commission is responsible for the use that might be made of this publication.

Contact information
Name: Ernest N. Koffi
Address: European Commission Joint Research Centre, Via E. Fermi, 2749, I-21027 Ispra (VA), Italy
Email: ernest.koffi@ec.europa.eu
Tel.: +39 0332 786610

JRC Science Hub
https://ec.europa.eu/jrc

JRC112816

EUR 29349 EN

PDF	ISBN 978-92-79-93409-4	ISSN 1831-9424	doi:10.2760/906932
Print	ISBN 978-92-79-93410-0	ISSN 1018-5593	doi:10.2760/765162

Luxembourg: Publications Office of the European Union, 2018

How to cite this report: Koffi, E.N. and Bergamaschi, P., *Evaluation of Copernicus Atmosphere Monitoring Service methane products*, EUR 29349 EN, Publications Office of the European Union, Luxembourg, 2018, ISBN 978-92-79-93409-4, doi:10.2760/906932, JRC112816

Contents

Acknowledgements

We thank Ed Dlugokencky and Colm Sweeney for providing CH_4 data from the NOAA / ESRL global cooperative air sampling network and from NOAA aircraft and AirCore profiles. We are grateful to Eric Kort for the provision of the ORCAS data, to Andreas Zahn for the CARIBIC data, and to Toshinobu Machida for the CONTRAIL data.

This work has been supported by the Administrative Arrangement "Copernicus No. 2" [JRC No. 34732-2017 NFP] between the European Commission's Directorate-General for Internal Market, Industry, Entrepreneurship and SMEs (DG GROW) and the Joint Research Centre (JRC).

Authors

Ernest N. Koffi and Peter Bergamaschi

Abstract

The Copernicus Atmosphere Monitoring Service (CAMS) provides continuous data and information on atmospheric composition in an operational mode. The CAMS products include analyses/re-analyses of the greenhouse gases (carbon dioxide, methane, and nitrous oxide) for recent years. In this report, we evaluate the quality of the CAMS methane (CH_4) products, focussing on the "near real time analyses" of the atmospheric CH_4 concentrations (from the ECMWF IFS assimilation system) and the re-analyses of CH_4 concentrations and fluxes (from the TM5-4DVAR inverse modelling system, provided by TNO / SRON). The CAMS CH_4 products are compared to comprehensive independent observational data sets (from surface monitoring stations, ship cruises, various aircraft programmes, AirCore balloon soundings up to the middle stratosphere, and measurements of column averaged CH_4 mole fractions) during 2010-2017. Furthermore, CH_4 flux inversions from the JRC TM5-4DVAR system (which was used as prototype of the operational CAMS inversion system) are included in the analysis, providing a benchmark to evaluate the CAMS CH_4 flux inversion products.

Overall, the CAMS and JRC inversions show very similar performance and compare well to observations over remote regions near the surface and within the free troposphere, confirming that in general CH_4 mole fractions in the background troposphere far from CH_4 emissions are realistically simulated. Due to the relatively coarse horizontal resolution of 3^o (longitude) x 2^o (latitude), however, both CAMS and JRC inversions show clear limitations in simulating regional surface monitoring stations (which are influenced by regional CH_4 emissions), in most cases underestimating measured CH_4 mole fractions in these areas. Furthermore, the inversions show large differences to the observed CH_4 mole fractions in the lower to middle stratosphere at mid to high latitudes, most likely due to shortcomings in simulating the transport and/or chemistry in the stratosphere and the stratospheric-tropospheric exchange.

In contrast to the flux inversions, the CAMS "near real time analyses" show generally large biases (varying in space and time) in the simulated CH_4 mole fractions compared to observations in the background troposphere. These large biases are probably mainly due to the assimilation strategy of including only satellite retrievals (but no surface observations) and potential biases in the assimilated satellite products, while the flux inversions assimilate satellite retrievals and surface observations simultaneously and thus correct for biases in the satellite data (along with potential biases of the models to simulate the stratosphere).

The surface CH_4 fluxes derived from the CAMS inversion system are in general similar to the JRC estimates. However, the latitudinal gradients of the fluxes are slightly different between the two inversion systems, probably in part due to the two different convection schemes applied.

1 Introduction

Methane (CH_4) is the second most important anthropogenic greenhouse gas (GHG) after carbon dioxide (CO_2), with 28 times the global warming potential of CO_2 over a 100-year time horizon [*IPCC*, 2013]. Global atmospheric CH_4 concentrations have increased by a factor of ~2.5 since preindustrial times [*Etheridge et al.*, 1998] and contribute to ~17% of the direct anthropogenic radiative forcing of all long-lived GHGs in 2016, relative to 1750 (NOAA Annual Greenhouse Gas Index, AGGI; [*Butler and Montzka*, 2018]). Monitoring of atmospheric GHGs is essential in order to support international efforts to limit climate change, in particular the Paris Agreement, which aims to hold "the increase in the global average temperature to well below 2°C above pre-industrial levels and pursuing efforts to limit the temperature increase to 1.5°C above pre-industrial level".

To support climate change mitigation and adaptation strategies, but also for efficient management of emergency situations and to improve the security of European citizens, the European Union (EU) has established the Copernicus programme (http://www.copernicus.eu/), the EU's earth observation programme, providing operational data and information services on the state of the environment including land, sea, and atmosphere. These earth observation data are processed by six thematic Copernicus services: Atmosphere, Marine, Land, Climate, Emergency, and Security services. The Copernicus Atmosphere Monitoring Service (CAMS; https://atmosphere.copernicus.eu/), has been developed through the series of pilot projects GEMS ("Global and regional Earth-system (Atmosphere) Monitoring using Satellite and in situ data"), PROMOTE ("PROtocol MOniToring for the GMES Service Element on Atmospheric Composition") and MACC ("Monitoring Atmospheric Composition and Climate"; http://www.gmes-atmosphere.eu/) until July 2015. In operational mode CAMS provides continuous data and information on atmospheric composition, including reactive gases (e.g. carbon monoxide, oxidised nitrogen compounds, sulphur dioxide, ozone), aerosols and GHGs (CO_2, CH_4, and nitrous oxide (N_2O)). The purpose of the CAMS GHG analyses is to provide realistic global 3D fields (as function of time) of the atmospheric CO_2, CH_4, and N_2O mole fractions (e.g. for use as boundary conditions for regional atmospheric models). Furthermore, the CAMS GHG flux inversions aim at estimating global and regional GHG fluxes and their evolution in time.

In this report, we evaluate the quality of the CAMS CH_4 products, focussing on the "near real time analyses" of the atmospheric CH_4 concentrations (from the ECMWF IFS assimilation system) and the re-analyses of CH_4 concentrations and fluxes (from the TM5-4DVAR inverse modelling system, provided by TNO / SRON). The evaluation presented in this report has been performed in the framework of the administrative arrangement "Copernicus 2" between Directorate-General for Internal Market, Industry, Entrepreneurship and SMEs (DG GROW) and the Joint Research Centre (JRC), which has been established to further support the development of the Copernicus services and to monitor their technical performance. While CAMS already includes some regular validation of the different products, the purpose of this work is to provide a more comprehensive overall evaluation of the CH_4 products by comparison with comprehensive independent observational data sets (from surface monitoring stations, ship cruises, various aircraft programmes, AirCore balloon soundings up to the middle stratosphere, and total column measurements). Furthermore, CH_4 flux inversions from the JRC TM5-4DVAR inversion system (which was used as prototype of the operational

CAMS inversion system) are included in the analysis, providing a benchmark to evaluate the specific model setup and further model updates of the CAMS TM5-4DVAR system.

2 Evaluated products

We evaluate two fundamentally different types of CAMS CH_4 products: (1) the CAMS "near real time analyses" that provide 3D fields of CH_4 dry air mole fractions based on the ECMWF Integrated Forecasting System (IFS) assimilation system; and (2) the CAMS CH_4 flux inversions, that primarily aim to estimate global and regional CH_4 fluxes [*Segers and Houweling*, 2017a; 2017b], but also provide 3D fields of CH_4 dry air mole fractions. The TM5-4DVAR inversion system used in CAMS (operated by TNO/SRON) was originally developed by JRC during the GEMS/MACC projects, but includes further model updates and partly different model settings. Therefore, we also include JRC CH_4 inversion products in the analysis (based on the current JRC TM5-4DVAR system), to provide a benchmark to evaluate the impact of the specific model setup and model updates of the CAMS TM5-4DVAR system.

2.1 CAMS "near real time analyses" of CH_4 concentrations

The CAMS assimilation system was developed during the series of MACC research projects [*Agusti-Panareda et al.*, 2017; *Massart et al.*, 2014], based on the ECMWF IFS, including 4DVAR data assimilation. The system assimilates CH_4 satellite retrievals in 12-hour assimilation windows. Within each single assimilation, the initial 3D fields of CH_4 concentrations ("initial state of the atmosphere") at 00, 06, 12, and 18 UTC are optimised using the available satellite observations during the 12 hours assimilation window. The CAMS IFS assimilation system uses prescribed CH_4 emissions, similar to those used in the CAMS inversion system and described in the following Section.

The IFS system assimilates XCH_4 retrievals from the TANSO ("Thermal And Near-infrared Sensor for carbon Observation") instrument onboard GOSAT, using the "proxy retrievals" based on the RemoTeC algorithm [*Butz et al.*, 2010]. In addition, also CH_4 retrievals from the IASI (Infrared Atmospheric Sounding Interferometer) instruments on board the Metop family of satellites are assimilated [*Crevoisier et al.*, 2009; *Crevoisier et al.*, 2013], providing mainly information about mid- to upper-tropospheric CH_4 concentrations in the tropics.

In this report, we analyse the CAMS "near real time analyses" (also called "delayed-mode production stream") during 2016-2017, covered by the CAMS assimilation experiment IDs gg5m, gm3p, and gqiq (Table 1), denoted "CAMS_assim" in this report. Some further details ("Change log") are given at the ECMWF / CAMS website: https://atmosphere.copernicus.eu/gda-global-production-log-files#delayed.

Table 1: CAMS near real time analyses ("delayed-mode production") production streams evaluated in this report.

Experiment ID	**Spatial resolution** (km x km x nlevel)	**Period of outputs used in this study**
gg5m	39 x 39 x 137	20151201 - 20161122
gm3p	30 x 30 x 137	20161101 - 20170802
gqiq	30 x 30 x 137	20170101 - 20171231

2.2 Flux inversions

CAMS and JRC inversion products are generated using the TM5-4DVAR inverse modelling system [*Bergamaschi et al.*, 2013; *Meirink et al.*, 2008; *Segers and Houweling*, 2017a; 2017b]. This system is built around the atmospheric transport model TM5 [*Krol et al.*, 2005] and its adjoint and uses a 4DVAR variational technique that iteratively minimises the cost function. The inversion system uses surface measurements and satellite retrievals as observational constraints to optimise emissions from individual grid cells of four source categories (wetlands[1], rice, biomass burning, and "other" CH_4 emission sources (mainly anthropogenic sources)). The inversion system takes into account a priori information on emissions from available emission inventories (as detailed below) and uses prescribed 3D fields of photochemical CH_4 sinks in the troposphere (OH) and stratosphere (OH, Cl, and $O(^1D)$) [*Bergamaschi et al.*, 2013]. The meteorological fields used by the TM5 model are from ECMWF ERA-Interim reanalyses [*Dee et al.*, 2011].

Since the CAMS TM5-4DVAR system is largely based on the TM5-4DVAR system developed by JRC during the GEMS/MACC projects, the current CAMS and JRC systems share the main components and are very similar. However, there are several model updates and differences in the model settings. The most important differences are:

- Both the CAMS and JRC inversions have now increased horizontal resolution of 3^o (longitude) x 2^o (latitude) (compared to 6^o x 4^o of the MACC inversions). Furthermore, the vertical resolution of the CAMS inversions has been increased (34 vertical layers, compared 25 layers of the JRC inversion).
- The CAMS inversions use archived convective mass fluxes from ERA-Interim [*Dee et al.*, 2011], while the JRC inversions used in this report still apply the convection parameterisation of *Tiedtke* [1987].
- The CAMS inversions apply the a priori emission inventories as described by *Bergamaschi et al.* [2013], including the wetland emission inventory of J. O. Kaplan [*Bergamaschi et al.*, 2007]. In contrast, the JRC inversions analysed in this report use as prior for the wetland emissions the mean values of seven wetland inventories from the WETCHIMP ("Wetland and Wetland CH_4 Inter-comparison of Models") project [*Melton et al.*, 2013].
- Both the CAMS and JRC inversions are run in 2 iterations: First, a coarse resolution (6^o x 4^o) inversion is run consecutively in yearly blocks (plus 6-monthly spin-down periods; and for CAMS also including 6-monthly spin-up periods [*Segers and Houweling*, 2017a; 2017b] to generate a consistent inversion over the entire target period. Optimised 3D fields of CH_4 mole fractions from these coarse resolution inversions are then used as initial fields for the high-resolution inversions run over 3 years (plus 6 months spin-up and spin-down) for the CAMS inversion, and over 1 year (plus 6 months spin-down) for the JRC inversion.
- For the inversions which include satellite retrievals in addition to the surface measurements from the NOAA Earth System Research Laboratory (ESRL) global cooperative air sampling network, different bias corrections are applied to account for biases in the satellite retrievals as well as model transport biases. The CAMS inversion applies a bias correction based on the comparison of GOSAT

[1] excluding emissions from permafrost thawing

XCH_4 with a TM5-4DVAR inversion using only NOAA surface observations (CAMS_inv S1(NOAA)), as described by *Pandey et al.* [2016]. The same bias correction (as function of latitude and month) is applied for all years and is not further optimised in the CAMS inversion. In contrast, the JRC inversion derives the bias correction (as function of latitude, month, and year) during the inversion of the satellite data [*Bergamaschi et al.*, 2013].

- The CAMS GOSAT inversions exclude GOSAT retrievals over Antarctica (south of 60°S) and include all retrievals at high northern latitudes, while the JRC inversions only include retrievals between 50°S and 50°N. Furthermore, the CAMS inversions include GOSAT retrievals over the ocean, while they are excluded in the JRC inversions.

The different inversion products evaluated in this report are compiled in Table 2 and briefly summarized in the following Section.

Table 2: CAMS and JRC inversion products.

Institution	**Inversion ID**	**Spatial resolution** (lon x lat x level)	**Inversion Period**	**Assimilated observations**
TNO/SRON	CAMS_inv S1(NOAA)[1]	3° x 2° x 34	2000-2016	NOAA
	CAMS_inv S2(GOSAT)[2]	3° x 2° x 34	2009-2016	NOAA+GOSAT
JRC	JRC_inv S1(NOAA)[3]	3° x 2° x 25	2009-2016	NOAA
	JRC_inv S2(GOSAT)[4]	3° x 2° x 25	2009-2015	NOAA+GOSAT

[1]CAMS CH_4 release v16r1

[2]CAMS CH_4 release v16r1s

[3]RUNID: VAR_M07B_ECC_CH4_glb32_NOAA015_E42FI_WETE_G3_TM_EC_V01_I3

[4]RUNID:VAR_M07B_ECC_CH4_glb32_SRPR238_E42FI_WETE_G3_TM_EC_V01_I3

2.2.1 CAMS CH_4 flux inversions

The CAMS CH_4 flux inversions are described in detail by *Segers and Houweling* [2017a; 2017b] and are available through the CAMS data server: http://apps.ecmwf.int/datasets/data/cams-ghg-inversions/

- The first inversion stream (CAMS CH_4 release v16r1) only uses NOAA surface observations over the period 2000-2016 (plus spin-down until 06/2017). This stream is denoted "CAMS_inv S1(NOAA)" in this report.
- The second inversion stream (CAMS CH_4 release v16r1s) uses XCH_4 satellite retrievals from GOSAT (PROXY retrieval data set v2.3.8 [*Detmers and Hasekamp*, 2016] as well as the NOAA surface observations (and is denoted "CAMS_inv S2(GOSAT)" in this report). This dataset covers the period 2009-2016 (plus spin-down until 06/2017) for which GOSAT data are available.

2.2.2 JRC CH_4 flux inversions

- Inversion "JRC_inv S1(NOAA)" uses only NOAA surface observations (similar to "CAMS_inv S1(NOAA)") and is run over the period 2009-2016 (plus spin-down until 06/2017).
- "JRC_inv S2(GOSAT)" uses both NOAA surface observations and GOSAT XCH_4 retrievals from SRON (PROXY retrieval data set v2.3.8) in the inversion (similarly as "CAMS_inv S2(GOSAT)") and it covers the period 2009-2015 (plus spin-down until 06/2016).

In this report, we evaluate the products from 2010 until 2017, depending on the availability of the products and observations.

3 Observations

For the evaluation of the different CH_4 model products (described in section 2), we use various observational data sets, including measurements at surface monitoring stations, ship cruises, various aircraft programmes, AirCore balloon soundings, and surface based total column measurements. Figure 1 shows the locations of the measurements, and the data sets are described in the following subsections.

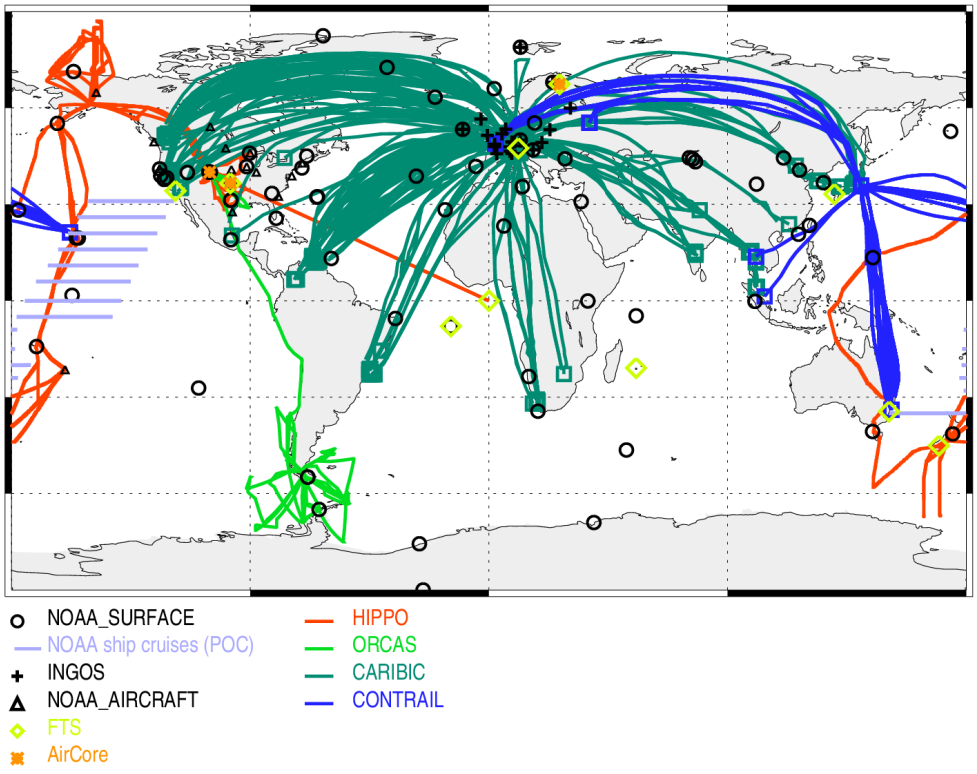

Figure 1: Observational data of atmospheric CH_4 mole fractions used for the evaluation of the models. The map shows the locations of NOAA and InGOS surface sampling sites, NOAA aircraft profile sites, TCCON FTS sites, and AirCore sites. Furthermore, the regions of NOAA ship cruises (POC) and aircraft routes of different measurement programs (HIPPO, ORCAS, CARIBIC, and CONTRAIL) are shown.

3.1 Surface observations

To evaluate the model simulations near the surface, we use the NOAA measurements of discrete air samples taken at the NOAA ESRL global cooperative air sampling network (including regular ship cruises through the Pacific Ocean), and quasi-continuous *in situ* measurements at European monitoring stations (using the harmonised data set generated within the European FP7 project InGOS).

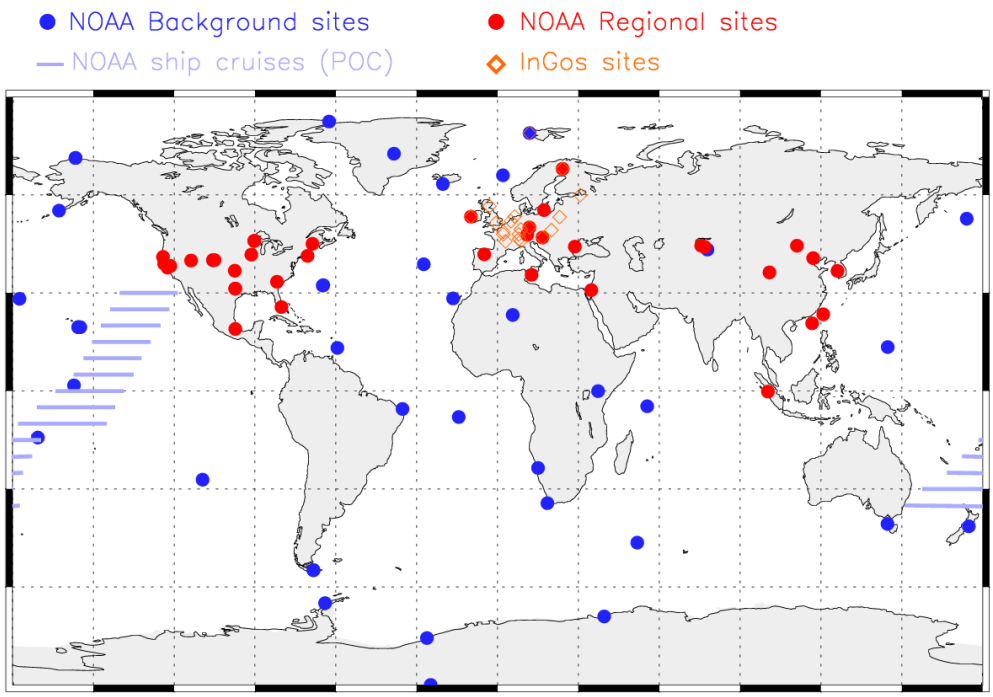

Figure 2: Map showing the locations of NOAA and InGOS surface sites. Furthermore, the regions of NOAA ship cruises (Pacific Ocean (POC)) are shown.

3.1.1 NOAA

Figure 2 shows the locations of the discrete air sampling sites of the NOAA ESRL global cooperative air sampling network [*Dlugokencky et al.*, 1994; 2003; 2009]. In order to analyse the performance of the different CH_4 model products separately for the remote atmosphere and over the continents, respectively, we have separated the sites into two groups: (1) "background sites", including mainly marine background sites and coastal sites (at which air samples are usually taken under background conditions), and (2) "regional sites" over the continents which are usually affected by regional CH_4 emissions.

Furthermore, we use measurements of discrete air samples taken along the lines of regular ship cruises over the Pacific Ocean (POC; Figure 2), which mainly sample air masses over the remote ocean and downwind of continental sources. Due to a gap in time of these measurements, the POC measurements are available only during two periods: 2010-2012 and 2015 to mid-2017 (see Figure 5). The NOAA measurements were calibrated against the NOAA2004 CH_4 standard scale, which is equivalent to the WMO-CH_4-X2004 CH_4 mole fraction scale [*Dlugokencky et al.*, 2005].

3.1.2 InGOS

We also use the quality-controlled and harmonised data set of *in situ* measurements from 18 European atmospheric monitoring stations generated within the European FP7 project InGOS ("Integrated non-CO2 Greenhouse gas Observing System") [*Bergamaschi et al.*, 2018]. The InGOS network includes surface stations and tower sites with quasi-continuous measurements. Most of the

InGOS stations are influenced by regional CH_4 emissions and therefore considered as "regional sites" (Figure 2). However, we do not use the full diurnal cycle of the measurements, but only data during 12:00-15:00 Local Time (LT) for stations in the boundary layer and during 0:00-03:00 LT for mountain stations. For the tall towers in the network, which sample at different heights above surface, we use only the measurements from the highest sampling level, which are generally less affected by local sources and can therefore be better represented by the atmospheric models. Here, we use the InGOS "release 2014" data set [*Bergamaschi et al.*, 2018]. The InGOS measurements were also calibrated against the NOAA-2004 standard scale [*Dlugokencky et al.*, 2005].

3.2 Aircraft observations

The aircraft observations used in this report include the regular NOAA aircraft profile measurements, the CARIBIC and CONTRAIL measurements onboard of commercial flights, and the experimental aircraft campaigns HIPPO and ORCAS. The locations of the NOAA aircraft profile sites and the flight routes of the other aircraft measurements are shown in Figure 1.

3.2.1 NOAA regular aircraft

Within the NOAA aircraft program, air samples are collected regularly in vertical profiles (https://www.esrl.noaa.gov/gmd/ccgg/aircraft/). The aircraft profiles sites are located mainly over the US but also include some sites over the Pacific Ocean (Figure 1). Most of the aircraft profiles range between the surface and around 8 km.

3.2.2 HIPPO

Furthermore, we use the measurements of the "HIAPER Pole-to-Pole Observations" (HIPPO) programme (http://hippo.ornl.gov/) [*Wofsy et al.*, 2011]. HIPPO measured cross sections of atmospheric concentrations of GHGs approximately pole-to-pole, from the surface to the lower stratosphere [*Wofsy et al.*, 2011]. We use the HIPPO-3 to HIPPO-5 campaigns, performed in March/April 2010 (HIPPO-3), June/July 2011 (HIPPO-4), and August/September 2011 (HIPPO-5), respectively. HIPPO measurements were carried out mainly over the Pacific Ocean, North America, and the Atlantic Ocean (Figure 1). The CH_4 mole fraction measurements were performed onboard of the aircraft at high frequency using a quantum cascade laser spectrometer (QCLS) [*Kort et al.*, 2011; *Kort et al.*, 2012]. In addition, air samples were collected using the NOAA Programmable Flask Package and analysed at NOAA ESRL. The comparison of the QCLS measurements with these flask samplings showed a small average bias of -5.8, -4.4, and -5.0 ppb for HIPPO-3, HIPPO-4, and HIPPO-5, respectively. In this study, we subtracted this bias from the QCLS measurements.

3.2.3 ORCAS

In addition, measurements of the recent aircraft observational campaign in the Southern Ocean ORCAS ("O_2/N_2 Ratio and CO_2 Airborne Southern Ocean Study"; https://www.eol.ucar.edu/field_projects/orcas; *Stephens et al.* [2017]) have been used. The ORCAS aircraft campaigns took place over the Southern Ocean (35°N - 75°S region; Figure 1) and within 0-13 km altitude during January until early March 2016.

3.2.4 CARIBIC

Aircraft measurements of CH_4 mole fractions provided by the CARIBIC ("Civil Aircraft for the Regular Investigation of the atmosphere Based on an Instrument Container"; http://www.caribic-atmospheric.com/) program are also used. Air samples were collected onboard a Lufthansa Airbus A340-600 passenger aircraft [*Brenninkmeijer et al.*, 2007; *Schuck et al.*, 2010; *Schuck et al.*, 2012; *Zahn et al.*, 2000]. The CARIBIC flights start from Frankfurt (Germany) to various destinations around the world (Figure 1). The air samples were analysed at the Max Planck Institute (MPI) Mainz laboratory and the data were calibrated against the NOAA2004 scale. The CARIBIC measurements cover mainly the upper troposphere and lower stratosphere (8-13 km altitude). We analyse CARIBIC data collected onboard of 222 flights during 2010-2016.

3.2.5 CONTRAIL

Further aircraft measurements of CH_4 mole fractions were provided by the CONTRAIL ("Comprehensive Observation Network for TRace gases by AIrLiner"; http://www.cger.nies.go.jp/contrail/index.html) project, which is jointly conducted by NIES (National Institute for Environmental Studies), the MRI (Meteorological Research Institute), JAL (Japan Airlines), and JAMCO (JAMCO Corporation) and JAL-F (JAL Foundation). The CH_4 mole fractions were measured from an Automatic air Sampling Equipment (ASE) for flask sampling installed onboard Japan Airlines Boeing 747-400 and Boeing 777-200ER aircraft or from a Manual air Sampling Equipment (MSE) carried by operator onboard of Boeing 777-300ER aircraft [*Machida et al.*, 2008; *Matsueda et al.*, 2008; *Sawa et al.*, 2015; *Umezawa et al.*, 2012]. The JAL flights start from Tokyo (Japan) to Asia, Australia, Europe, and Hawaii (Figure 1). The measurements were conducted mainly between 10-12 km altitude and partly below 10 km. We analyse 123 CONTRAIL flights during the 2011-2015 period.

3.3 AirCore measurements

The AirCore instrument developed by NOAA/ESRL is an atmospheric sampling system that can be launched on balloons and that consists of a long stainless steel tube, which can sample the surrounding atmosphere and preserve a profile of the trace gas of interest from the middle stratosphere to the ground (https://www.esrl.noaa.gov/gmd/ccgg/aircore/; *Karion et al.* [2010]). The AirCore system is open at one end and relies on positive changes in ambient pressure for passive sampling of the atmosphere. The system gradually evacuates the filled air while ascending to a high altitude and collects a sample of the ambient air as it descends. Comparisons of AirCore observations with flask data from aircraft flights indicate a standard deviation of differences of less than 5 ppb for CH_4 concentrations with no apparent bias [*Karion et al.*, 2010; *Membrive et al.*, 2017]. The AirCore measurements are useful for the evaluation of modelled CH_4 mole fractions especially in the lower and middle stratosphere. In this report we use data from NOAA AirCore balloon soundings at two sites in the US (Boulder and Lamont) and one site in Finland (Sodankyla). The site locations are shown in Figure 1.

3.4 FTS: Total column measurements

The Total Carbon Column Observing Network (TCCON; https://tccon-wiki.caltech.edu/) is a global network of ground-based Fourier Transform

Spectrometers (FTS) that record spectra of the sun in the near-infrared. From these spectra, column-averaged abundances of atmospheric constituents including CO_2 and CH_4 are retrieved [*Wunch et al.*, 2011]. The TCCON data are scaled to the WMO scale by comparison with *in situ* aircraft profile measurements [*Wunch et al.*, 2010], which however cover only the altitudes between the surface and the lower stratosphere. For consistent comparison of the TCCON column-averaged mixing ratios (XCH_4) with model simulations, the TCCON averaging kernels and the a priori profiles are applied to the model fields.

4 Evaluation of simulated CH_4 mole fractions

We evaluate the simulated 3D fields of CH_4 mole fractions from the CAMS "near real time analyses" and from the CAMS and JRC inversions by comparing them with the various observational data sets described in the previous Section 3. For a consistent comparison between the models and observations, the model simulations are sampled at the same time and location of the observations, extracted either directly during the model runs (e.g. TM5-4DVAR station output) or extracted from daily (TM5-4DVAR system) or 6-hourly (CAMS "near real time analyses") 3D output fields using 3D linear interpolation in space (i.e. horizontally and vertically) and linear interpolation in time. For the comparison of model simulations with FTS observations, the FTS averaging kernels and a priori profiles (provided by TCCON) are applied.

In the following, we first analyse the performance of the different CH_4 products near the surface, including both the remote atmosphere (by comparing with measurements at the NOAA background sites and along the routes of the NOAA ship cruises) and regions affected by regional CH_4 emissions (by comparing with "regional" NOAA discrete air sampling sites and InGOS stations) (section 4.1). In section 4.2, we analyse the ability of the models to simulate the vertical gradients of CH_4 concentrations (including the boundary layer, the free troposphere, and the lower stratosphere) by comparison with various aircraft data sets (including NOAA regular aircraft profiles, HIPPO, ORCAS, CARIBIC, and CONTRAIL). In section 4.3, AirCore measurements are used to evaluate the simulated vertical gradients of CH_4 concentrations in the stratosphere. Finally, the column-averaged CH_4 mole fractions are evaluated by comparison with TCCON FTS measurements (section 4.4).

4.1 Comparison with surface observations

Figure 3 shows the comparison of model simulations with measurements at several selected NOAA background sites. The average bias between model simulations and measurements (using all available NOAA background sites) as function of latitude and time (averaged in monthly 5^o latitude bins) is displayed in Figure 4. Both CAMS and JRC "NOAA-only" inversions (CAMS_inv_S1(NOAA) and JRC_inv_S1(NOAA)) show very good agreement with observations during the entire period (2010-2017). In the Southern Hemisphere (SH), the CAMS_inv_S1(NOAA) shows a small positive bias (~4 ppb) during SH summer (Figure 4). The overall very good performance of the CAMS and JRC "NOAA-only" inversions is due to the fact that the observations of most of these sites are used in the inversions. Including the GOSAT retrievals in the inversions slightly reduces the agreement with the NOAA surface measurements. CAMS_inv_S2(GOSAT), however, shows a small positive bias during 2010 and 2011, as diagnosed also in the CAMS validation report ([*Segers and Houweling*, 2017b]; Figure 8), potentially either due to the initial CH_4 concentrations for the first 3-yearly NOAA+GOSAT inversion [*Segers and Houweling*, 2017a; 2017b], or to the mean bias corrections applied (see Section 2.2), which cannot correct any inter-annual variations in the biases of the satellite retrievals. In contrast to the inversions, the CAMS "near real time analyses" show significant differences compared with the observations (Figures 3, 4) with large biases (often exceeding 20 ppb) and varying sign (depending on latitude and time) (Figure 4). These large discrepancies compared to the measurements are probably due to the fact that the CAMS "near real time analyses" assimilate only satellite data (which may have some biases), but do not include any surface

measurements. The general picture emerging from the comparison with the NOAA background sites is largely confirmed by the comparison with the NOAA ship measurements in the Pacific, shown in Figure 5. All inversions show excellent agreement with very low average biases, confirming that the inversions represent the background atmosphere at the surface (marine boundary layer) in this area quite well. In contrast, the CAMS "near real time analyses" show significant average biases during 2016 (gg5m), but lower average biases in 2017.

The comparison of model simulations with measurements at regional sites (regional NOAA discrete air sampling sites and InGOS stations) is shown in Figures 6, 7, 8, and 9. At the regional continental sites, CH_4 concentrations typically show large diurnal cycles. These are clearly visible in the continuous measurements from the InGOS stations (Figure 8), but not in the ~weekly NOAA discrete air samples (Figure 6), which selectively sample air under background conditions (conditions with low influence of local/regional sources). Despite this sampling strategy, however, the agreement between the inversions and the measurements is somewhat poorer than that for the background sites. For the comparison of model simulations with InGOS measurements, we use only daytime data (between 12:00 and 15:00 LT) for stations in the boundary layer and only night-time data (between 0:00 and 3:00 LT) for mountain stations [*Bergamaschi et al.*, 2018]. Furthermore, for tall towers with multiple sampling heights, generally only the uppermost level is used (which has the smallest impact from local and smaller-scale regional sources and which should be easier to represent by the models than the lower levels closer to the surface). Although the background CH_4 concentrations observed at the InGOS stations and the regional NOAA sites are in general relatively well represented by the inversions (Figures 6 and 8), some small average biases are visible (for the InGOS sites between 45 and 60° N mainly negative bias; Figure 9). This is partly explained by the fact that the regional stations cannot be very well represented by the relatively coarse spatial resolution (3° x 2°) used in the inversions. The CAMS "near real time analyses" for NOAA regional sites also show significant biases (varying with time; Figures 6 and 7), probably largely related to the significant biases visible at the NOAA background stations (Figures 3 and 4).

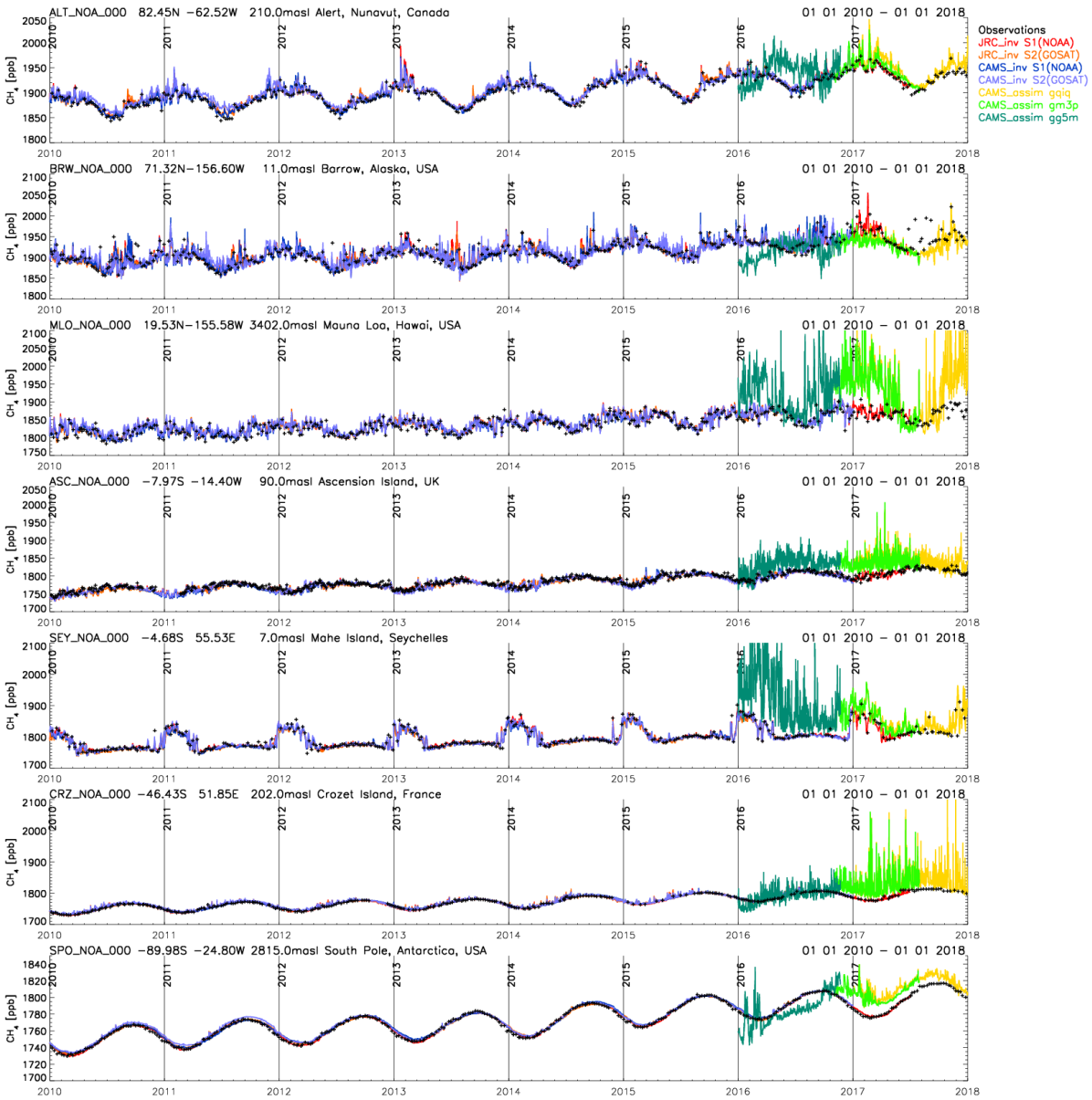

Figure 3: Comparison of simulated and observed CH_4 mole fractions at NOAA background surface stations.

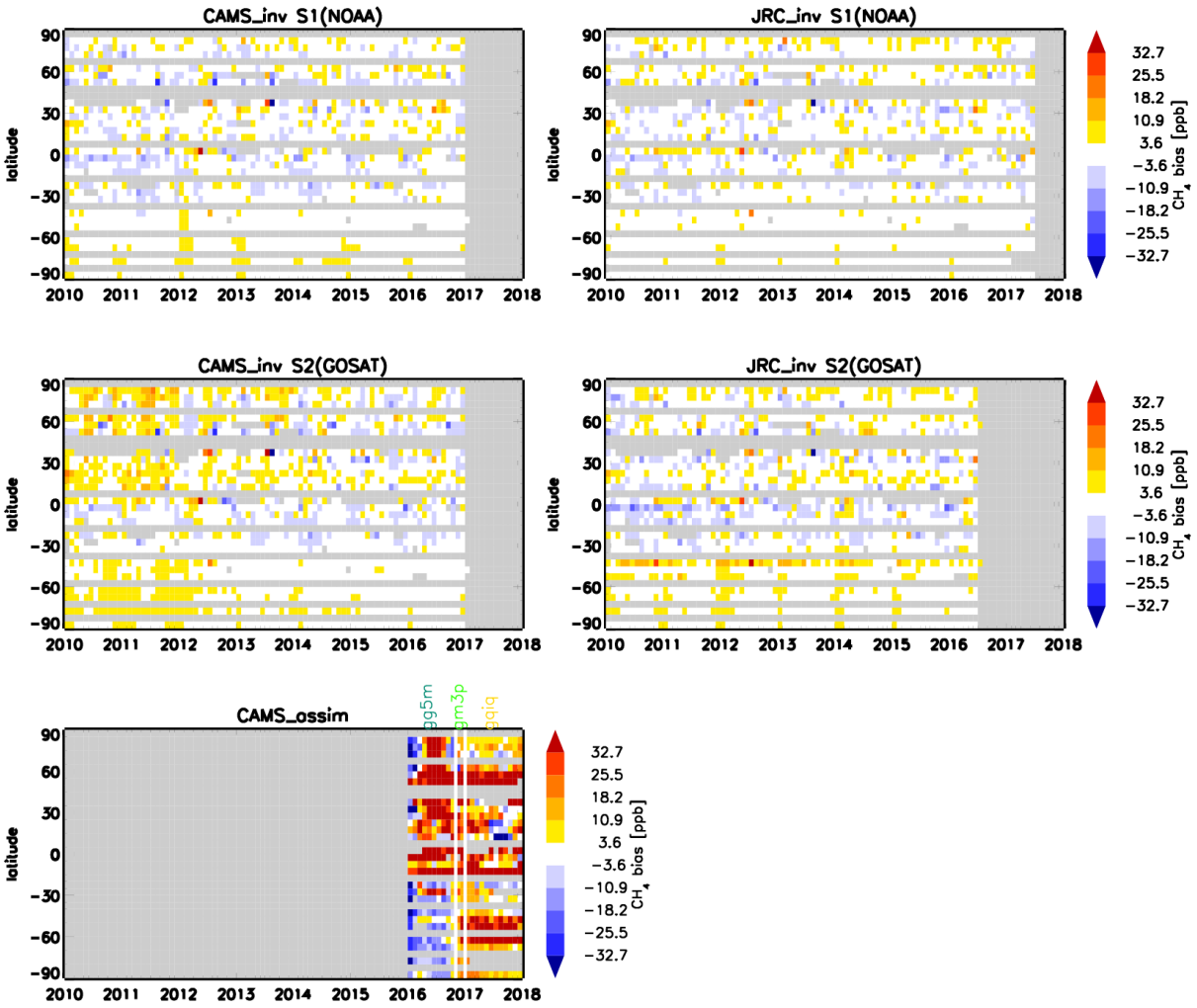

Figure 4: Average bias between simulated and observed CH_4 mole fractions at NOAA background sites as function of time and latitude. Measurements and model simulations are averaged in monthly 5° latitude bins. For CAMS "near real time analyses", when two experiments have overlapping periods, the data for the most recent assimilation stream are shown.

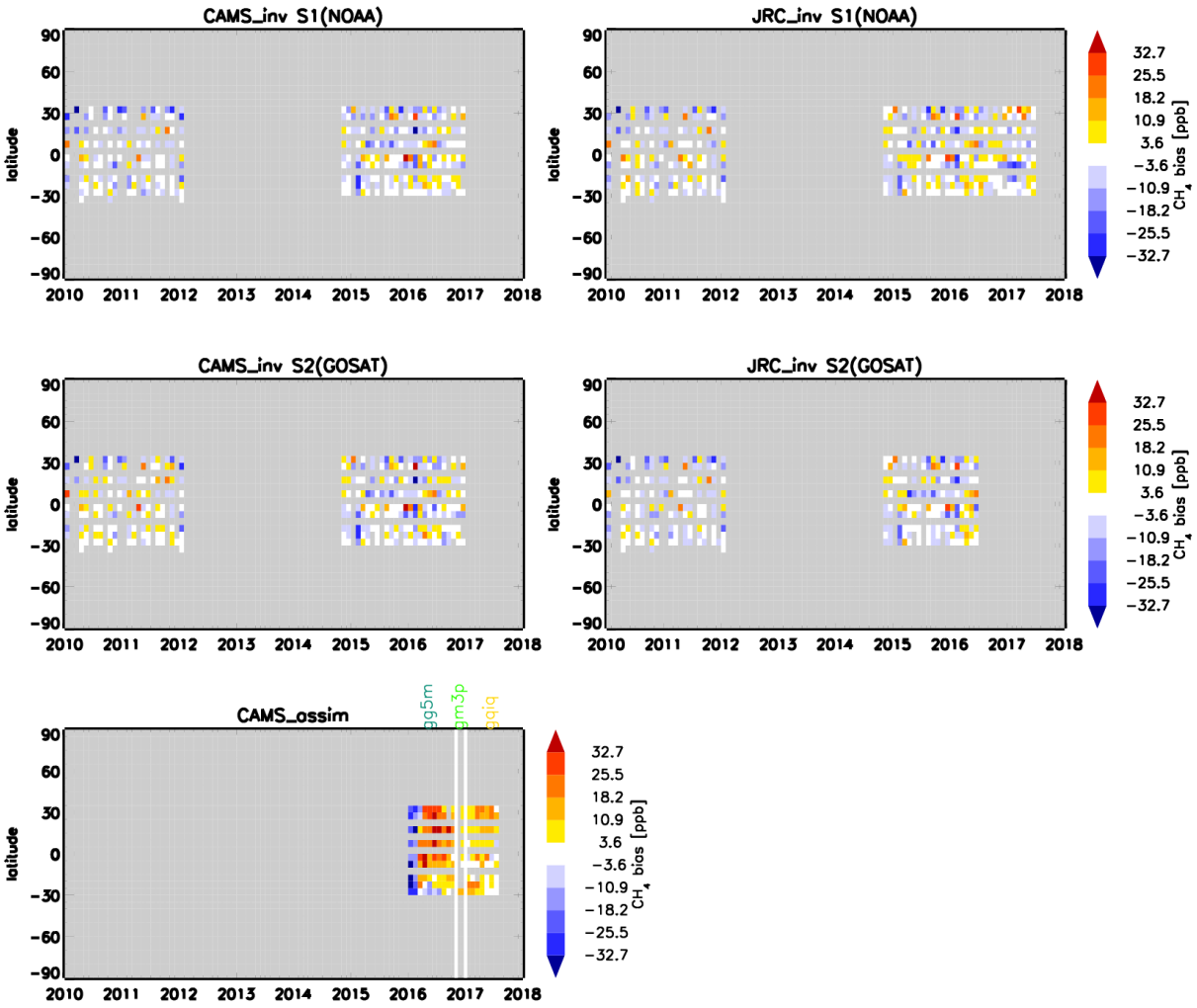

Figure 5: Average latitudinal biases between simulated and observed CH_4 mole fractions for NOAA measurements on samples collected regularly on commercial ship lines across the Pacific Ocean (POC). Measurements and model simulations are averaged in monthly 5° latitude bins.

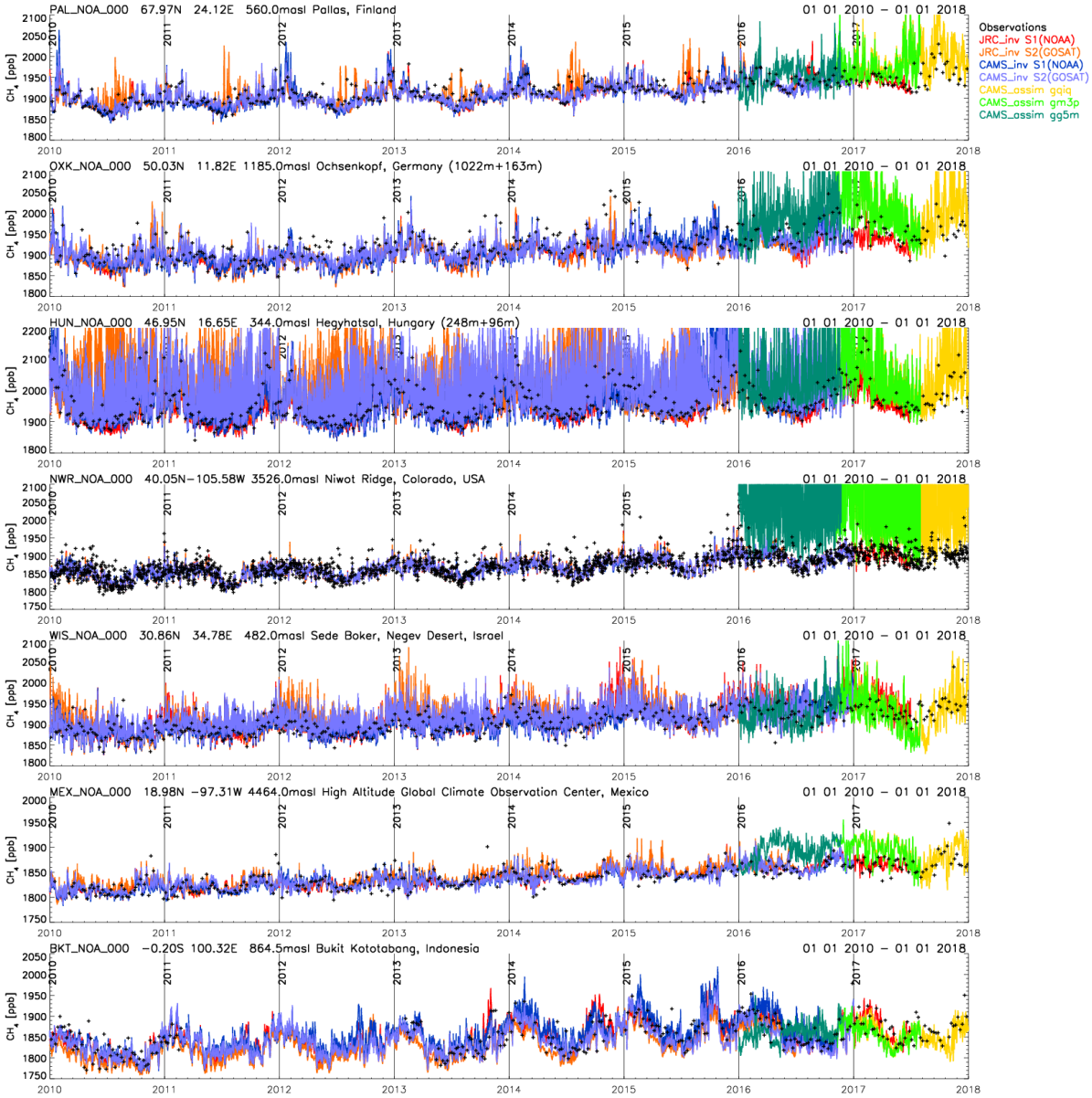

Figure 6: Comparison of simulated and observed CH_4 mole fractions at "regional" NOAA surface stations.

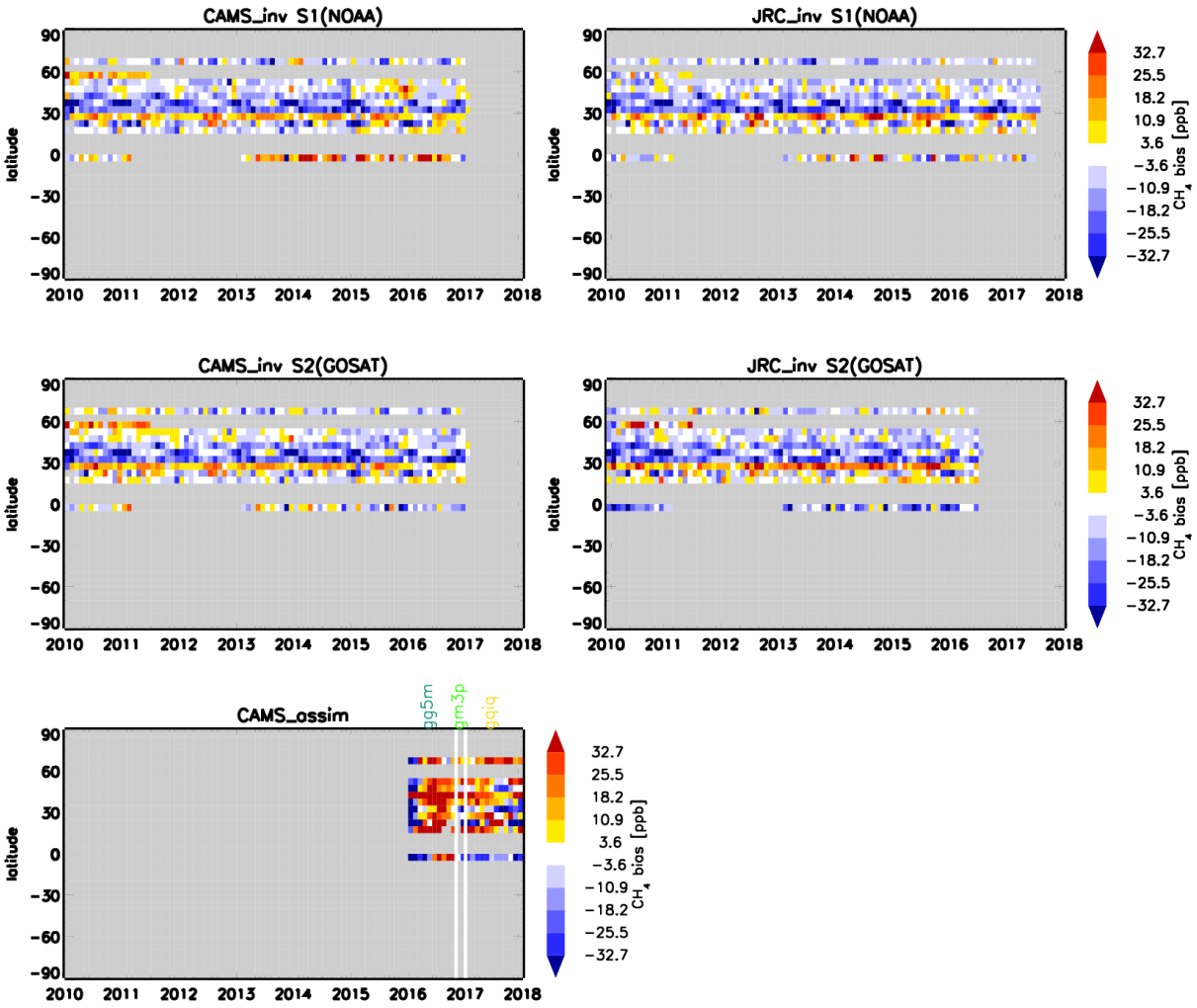

Figure 7: As Figure 4, but for "regional" NOAA sites.

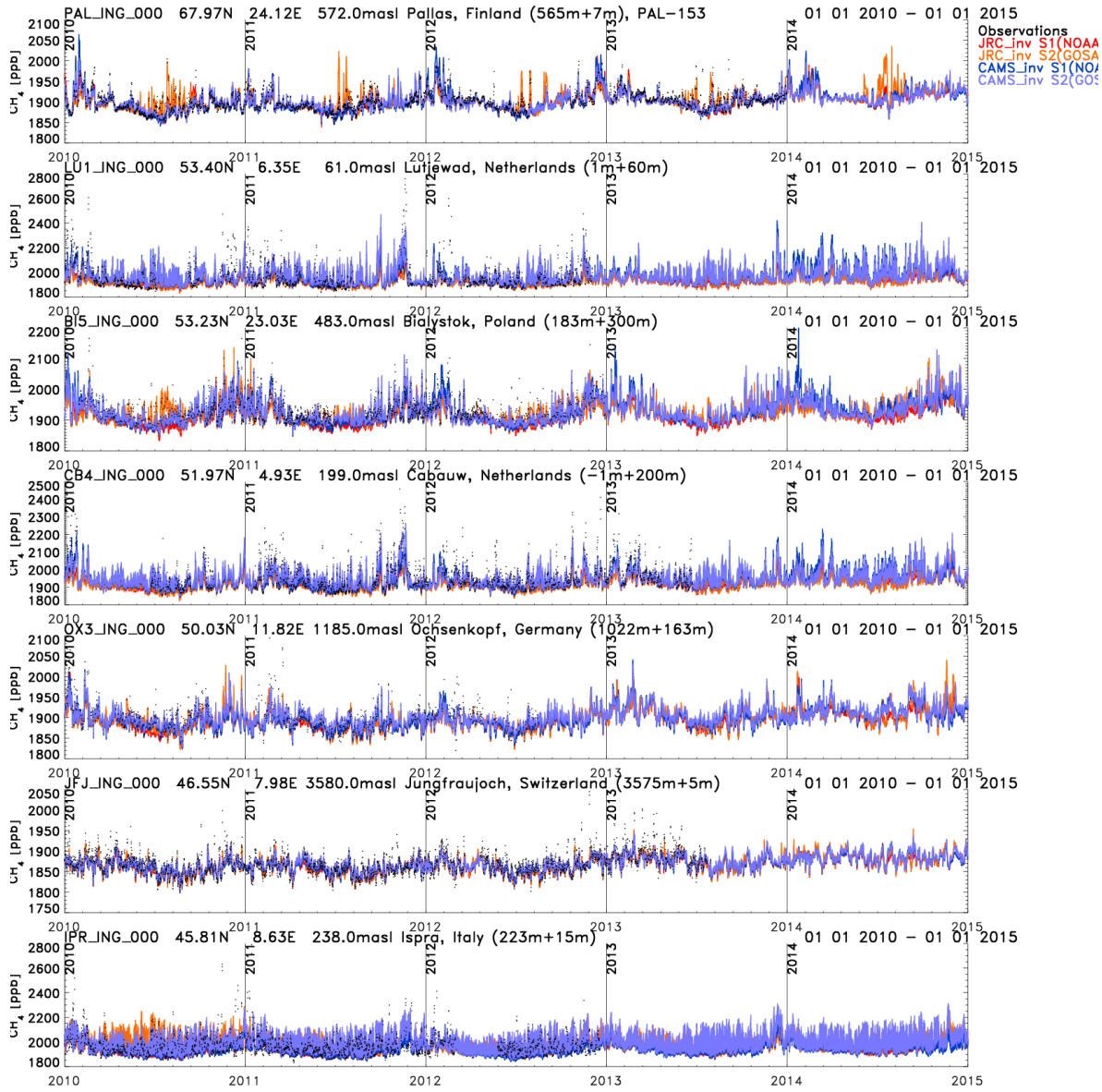

Figure 8: Comparison of simulated and observed CH_4 mole fractions at InGOS stations.

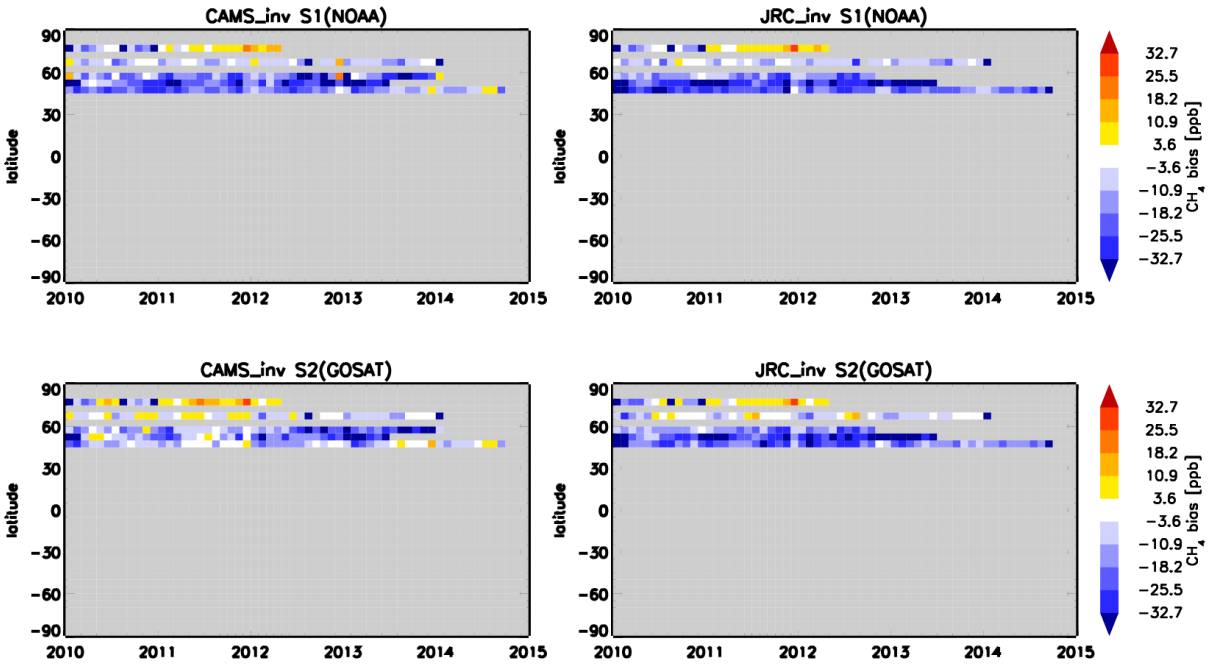

Figure 9: Average bias between simulated and observed CH_4 mole fractions at InGOS stations as function of time and latitude. The bias is averaged in monthly 5^o latitude bins.

4.2 Comparison with aircraft measurements

Figure 10 shows the mean vertical profiles of CH_4 mole fractions at the different NOAA aircraft profile sites during 2016 (the year for which we have data from all models; for JRC_inv_S2(GOSAT), however, only for the first half of 2016 (spin-down period of this inversion)). Figures 11a and 11b show the average bias as function of time and latitude for the boundary layer and for the free troposphere, respectively, while Figure 12 shows the average bias as function of time and altitude. The comparison shows that the optimised CH_4 concentrations from CAMS and JRC NOAA-only inversions are in quite good agreement with the observations in the free troposphere with average biases close to zero. Including the GOSAT retrievals in the inversions results in similarly good agreement with measurements in case of JRC_inv_S2(GOSAT), but shows a small significant positive bias for CAMS_inv_S2(GOSAT), especially during 2010-2011, similarly (but even more pronounced) as the comparison with the global background sites (Figure 4). Within the boundary layer, the average bias between the optimised CH_4 concentrations from the inversions and the measurements is more variable (as function of time and latitude; Figure 11a) and shows on average a tendency to small negative biases (Figure 12), similar to the comparison at the "regional" NOAA sites (Figure 7). Compared to the inversions, the CAMS "near real time analyses" show in general poorer agreement, with significant average biases (of variable sign) (Figures 11a, 11b, and 12) both within the boundary layer (Figures 11a and 12) and in the free troposphere (Figure 11b and 12), especially for gg5m, and then slightly decreasing for gm3p (with smaller average positive bias) and gqiq (with bias varying with time).

While the regular NOAA aircraft profiles are primarily over the US (but covering the entire evaluation period 2010-2017), the HIPPO measurements provide pole-to-pole transects from the surface to the lower stratosphere, but as "snapshots" in time. Figure 13 shows the average bias between simulated and observed CH_4 mole fractions as function of latitude and altitude (average bias from HIPPO-3, 4, and 5 during 2010-2011), while the comparison for the individual HIPPO campaigns is shown in Annex 1 (Figures A11, A12, and A13). On average, the "NOAA-only" inversions show only very small biases in the free troposphere (but there are some negative biases near the surface over the continent in the Northern Hemisphere between 25°N and 50°N). CAMS_inv_S2(GOSAT), however, shows a significant positive average bias in the NH troposphere, as diagnosed also from the comparison with the regular NOAA aircraft profiles (Figures 11b and 12). Above the tropopause, all inversions show large biases, in most cases significantly overestimating observed CH_4 mole fractions in the lower stratosphere, similar to previous analyses [*Alexe et al.*, 2015; *Bergamaschi et al.*, 2009; 2013], especially at mid to high latitudes.

A similar picture emerges from the comparison with the ORCAS data (Figure 14 and Figures A21-25 in Annex 2). The inversions perform remarkably well within the entire troposphere (including the boundary layer) in the Southern Hemisphere (some varying biases are visible in the NH troposphere; however the NH data are from a single flight only). Above the tropopause, however, significant positive biases are apparent for all inversion products, similarly to the comparison with the HIPPO data. The CAMS "near real time analyses" shows large negative biases (<-30 ppb; Figure 14), consistent with the finding that during the period of the ORCAS campaign beginning of 2016 the gg5m "near real time analyses" show significant negative biases in many world regions (e.g. Figures 3, 4, 5, 11a, 11b, 12).

The model deficiencies in simulating the vertical gradients in the stratosphere are also clearly visible in the comparison with the CARIBIC and CONTRAIL data. Figures 15 and 17 show the average bias as function of time and latitude, and Figures 16 and 18 as function of time and altitude for CARIBIC and CONTRAIL, respectively. Within the upper troposphere, the CH_4 mole fractions from the inversions show on average small negative biases (which become zero or slightly positive just below the tropopause) and above the tropopause large positive biases. Please note that the tropopause height shows significant seasonal variation (as indicated by the black dotted lines in Figures 16 and 18) - therefore, the average bias within the altitude range of the tropopause reflects comparison of data of varying fractions of tropospheric and stratospheric air masses. The increase of the average bias with latitude visible in Figures 15 and 17 is mainly due to the increase in the fraction of data in the stratosphere with increasing latitude.

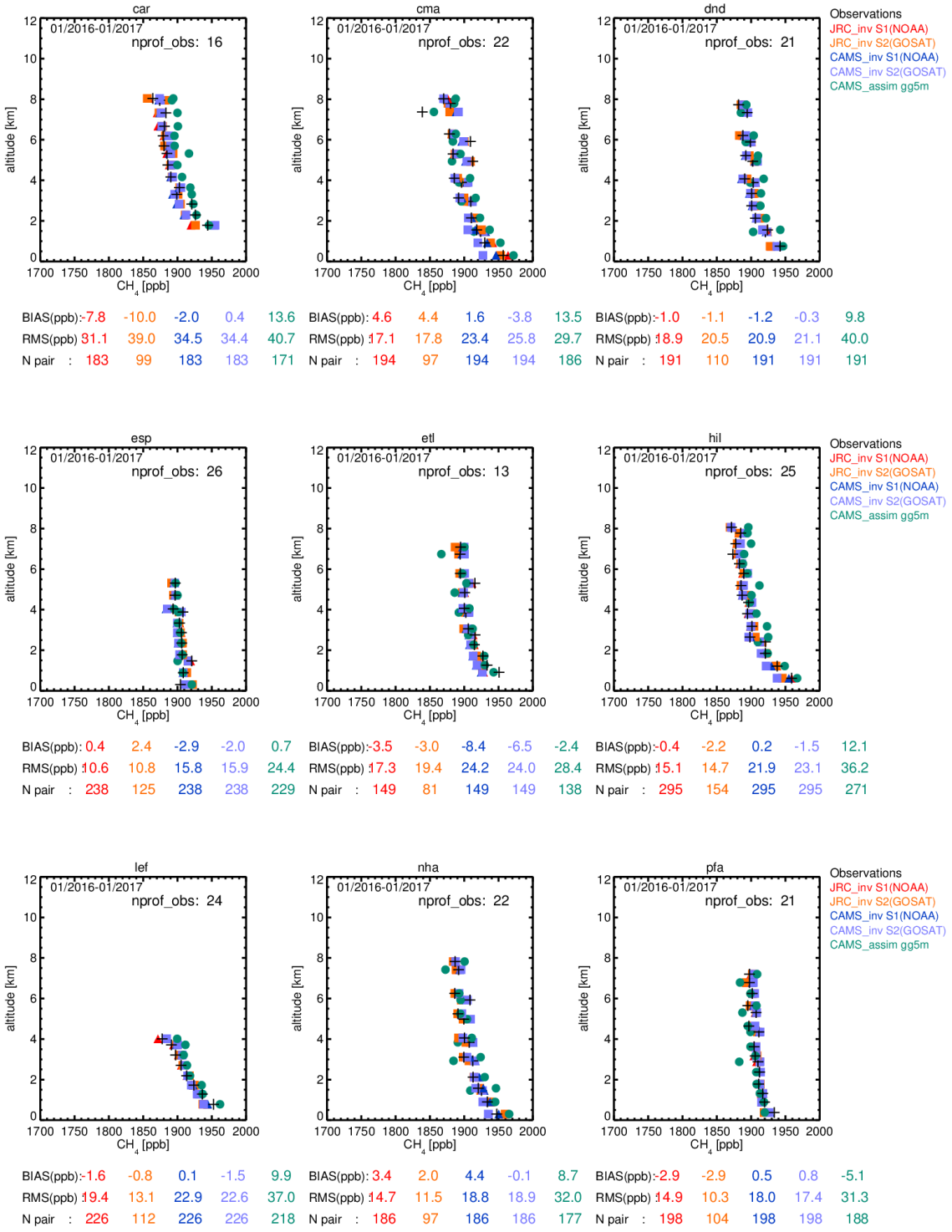

Figure 10: Mean vertical profiles of CH_4 mole fractions for the different NOAA aircraft sites during 2016. The mean bias (BIAS) and root mean square (RMS) difference between simulated CH_4 mole fractions and observations are given below each panel. N pair is the number of available paired data. The model data for JRC_inv_S2(GOSAT) cover only the first half of 2016 (spin-down period of 2015 inversion), and for the CAMS "near real-time analyses" only until 22 November 2016.

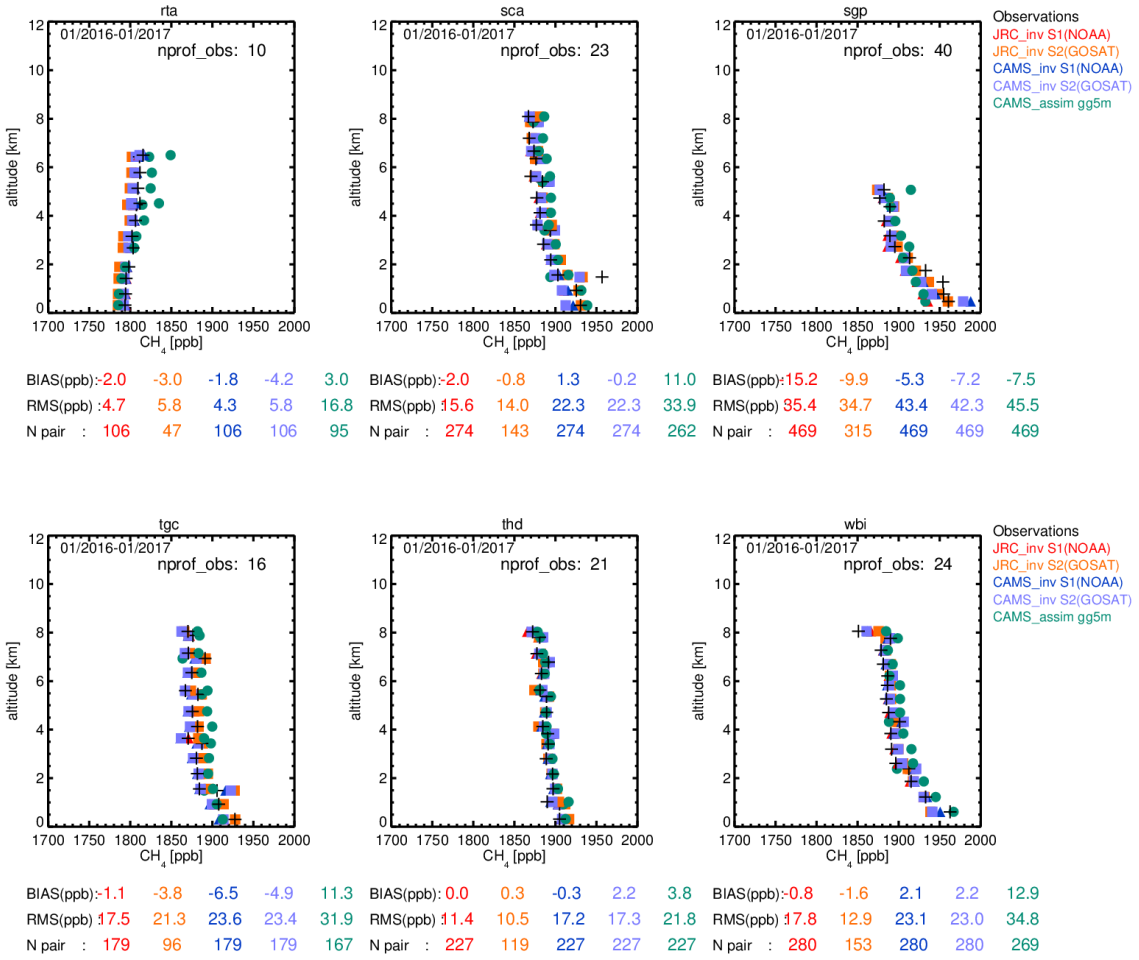

Figure 10: continued

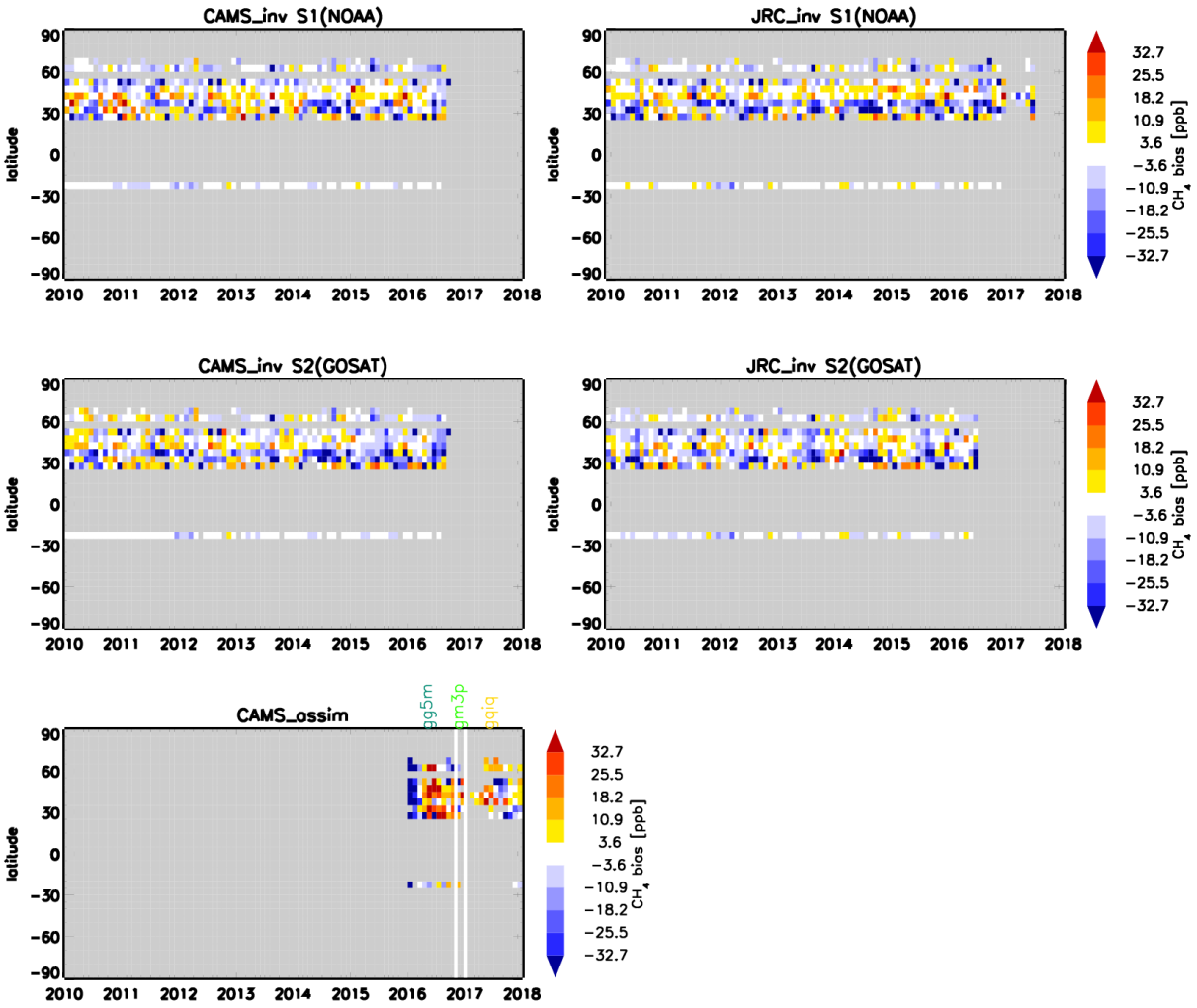

Figure 11a: Average bias between simulated and observed CH_4 mole fractions as function of time and latitude for NOAA aircraft data within the boundary layer (height < 1500 m). The bias is averaged in monthly 5° latitude bins.

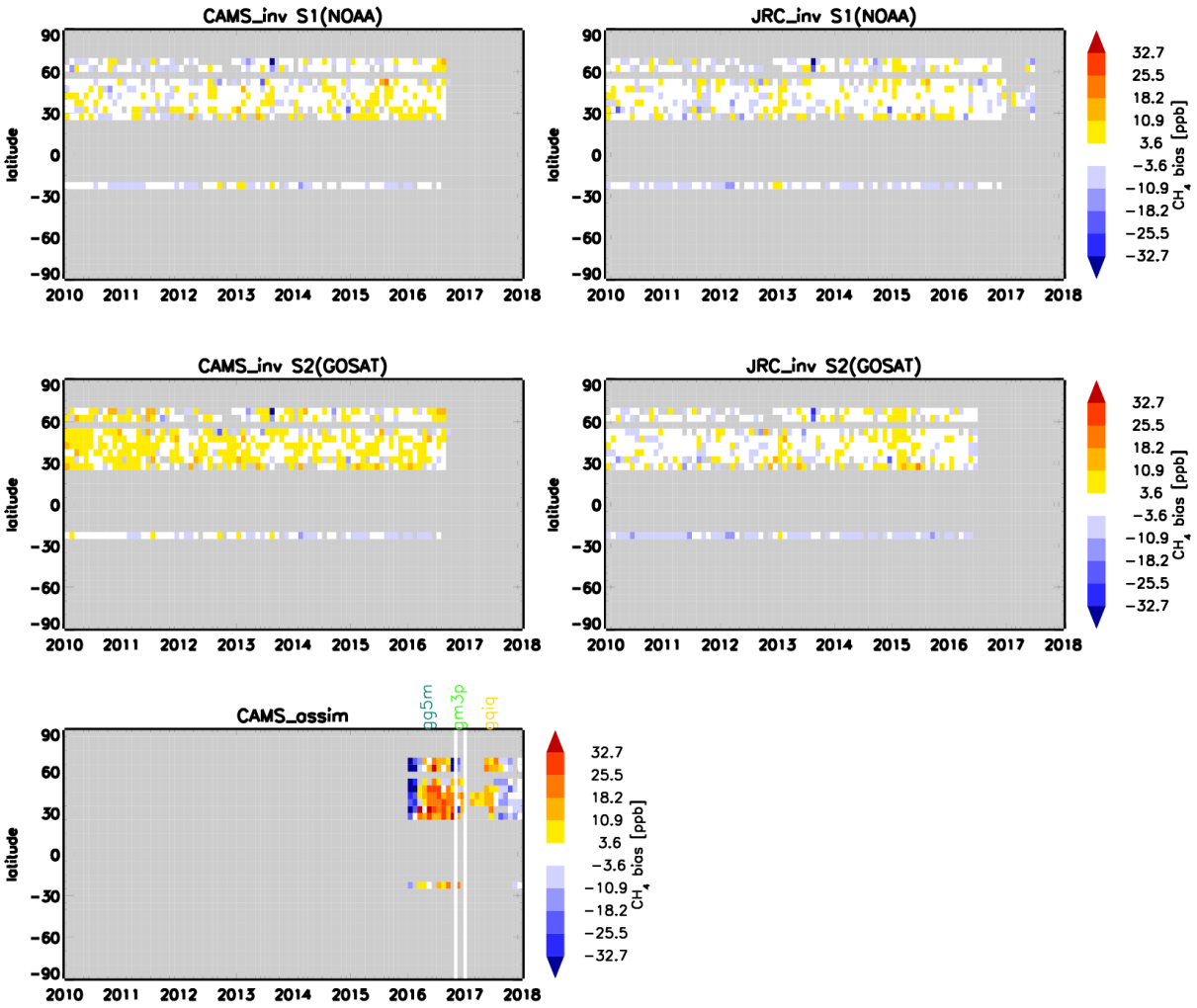

Figure 11b: Same as Figure 11a, but for NOAA aircraft data within the free troposphere (height range: 1500-8500 m).

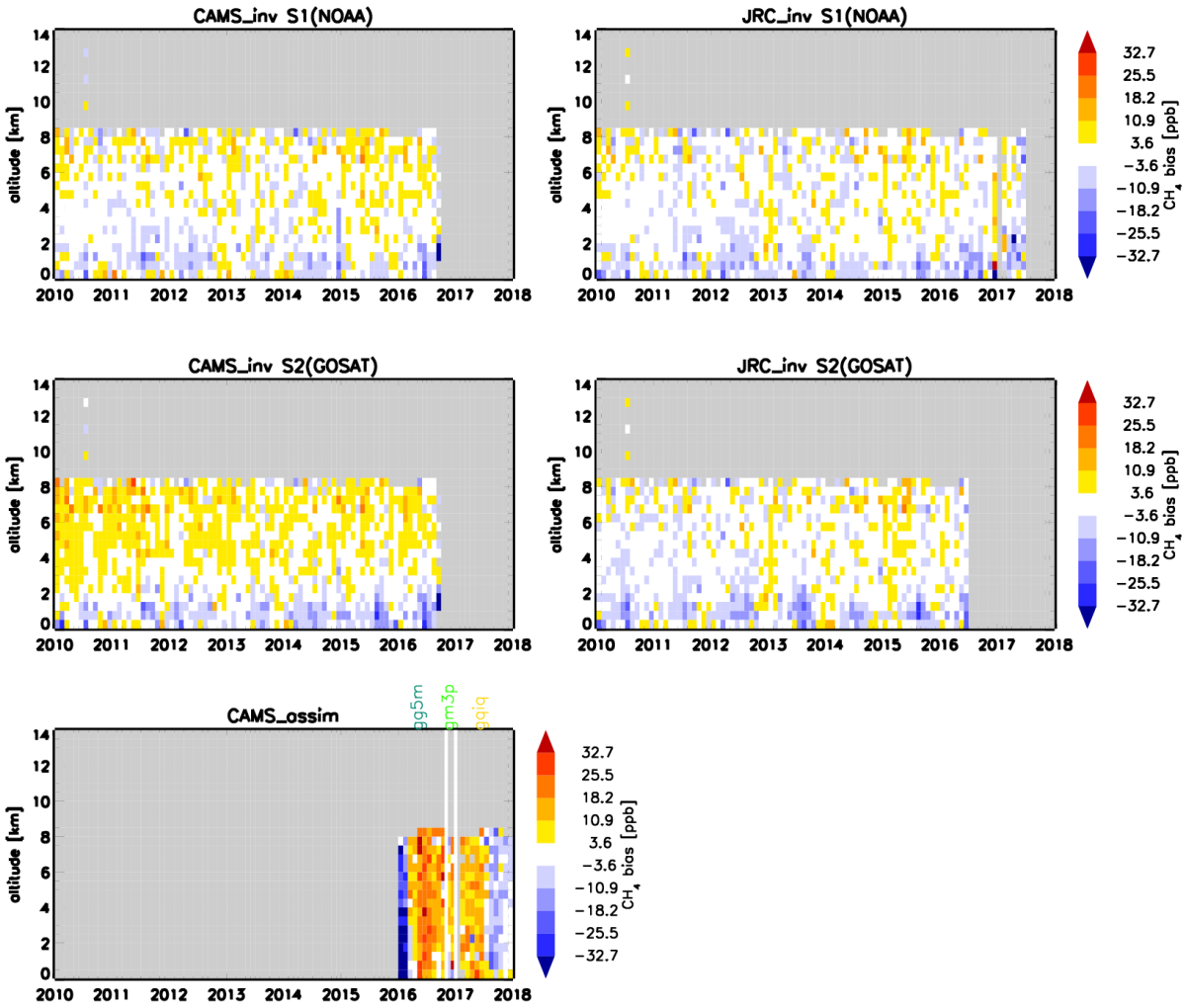

Figure 12: Average bias between simulated and observed CH_4 mole fractions as function of time and altitude for NOAA aircraft data. The bias is averaged in bins of 500 m altitude.

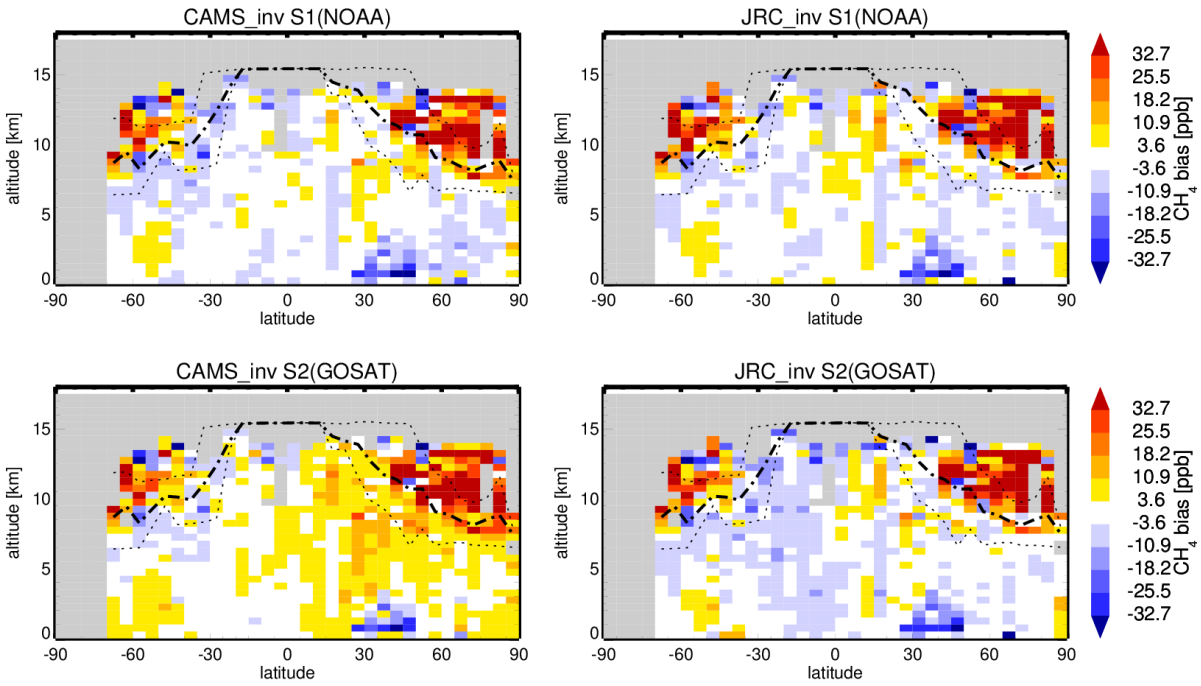

Figure 13: Average bias between simulated and observed CH_4 mole fractions as function of latitude and altitude for HIPPO aircraft data (2010-2011). The bias is averaged in bins of 5° latitude and 500 m altitude. The mean tropopause height as diagnosed by the TM5 model is shown by the black dash-dotted line (and minimum and maximum tropopause heights by black dotted lines).

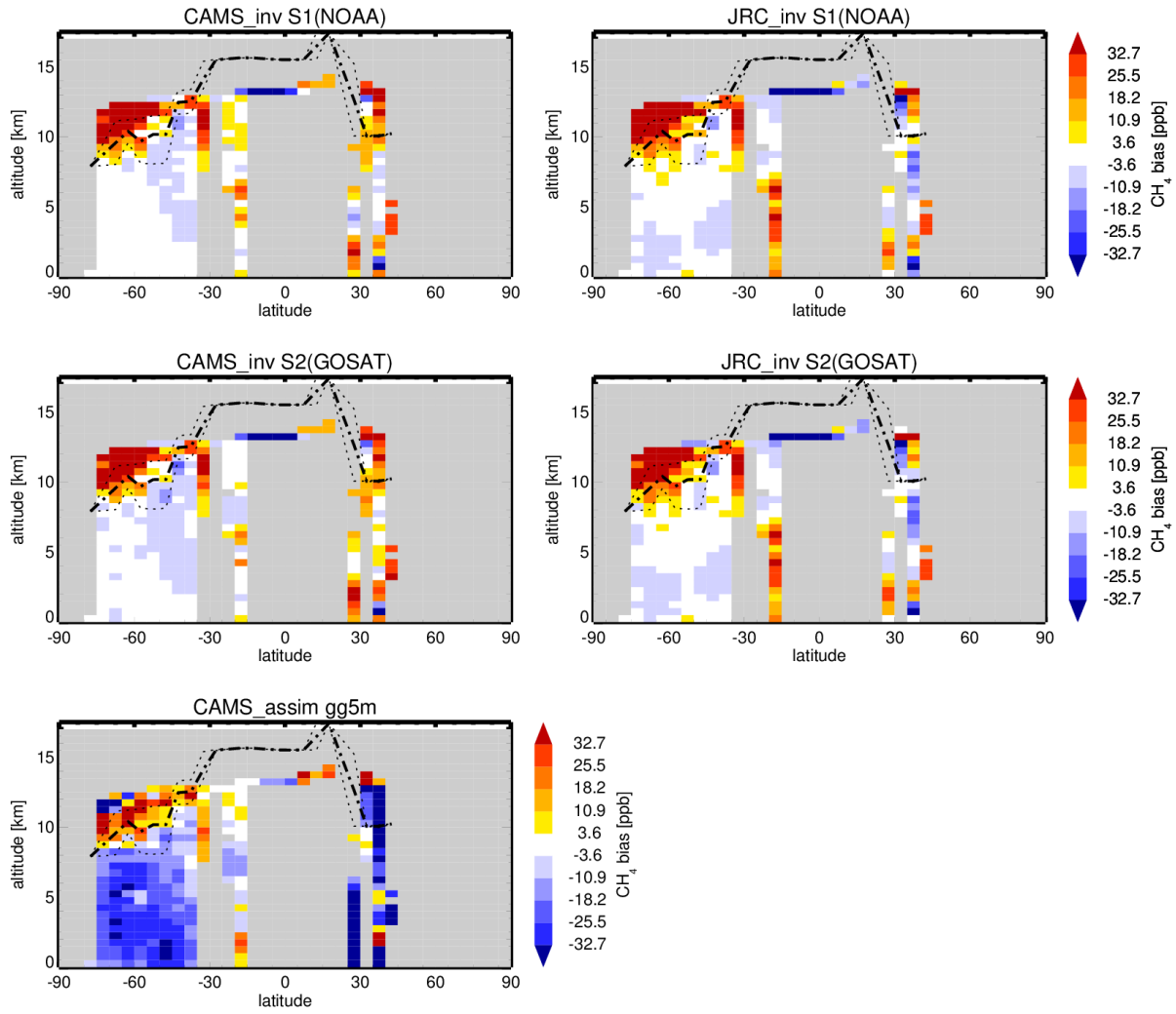

Figure 14: As Figure 13, but for ORCAS data.

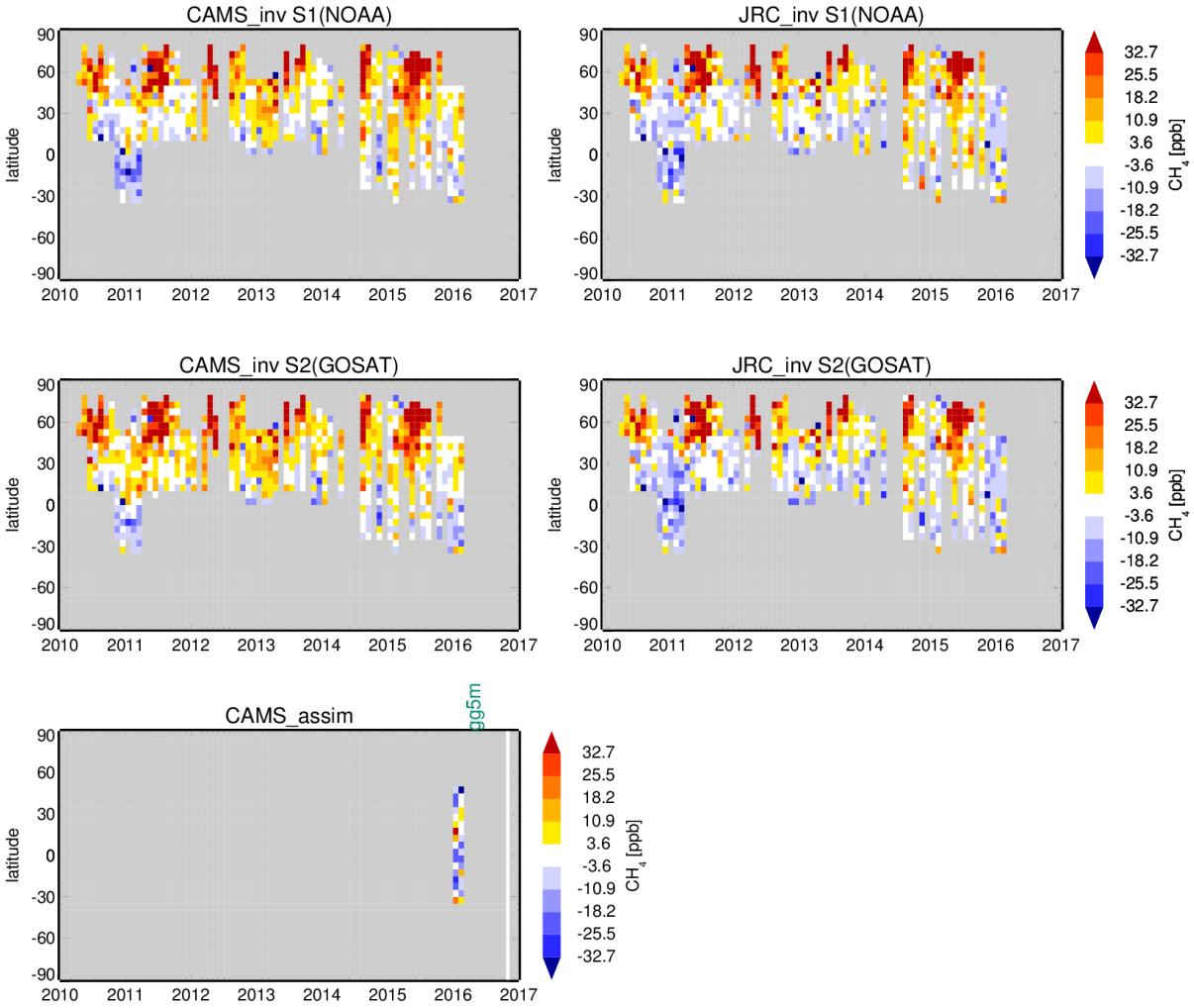

Figure 15: Average bias between simulated and observed CH_4 mole fractions as function of time and latitude for CARIBIC aircraft data. Measurements and model simulations are averaged in monthly 5° latitude bins.

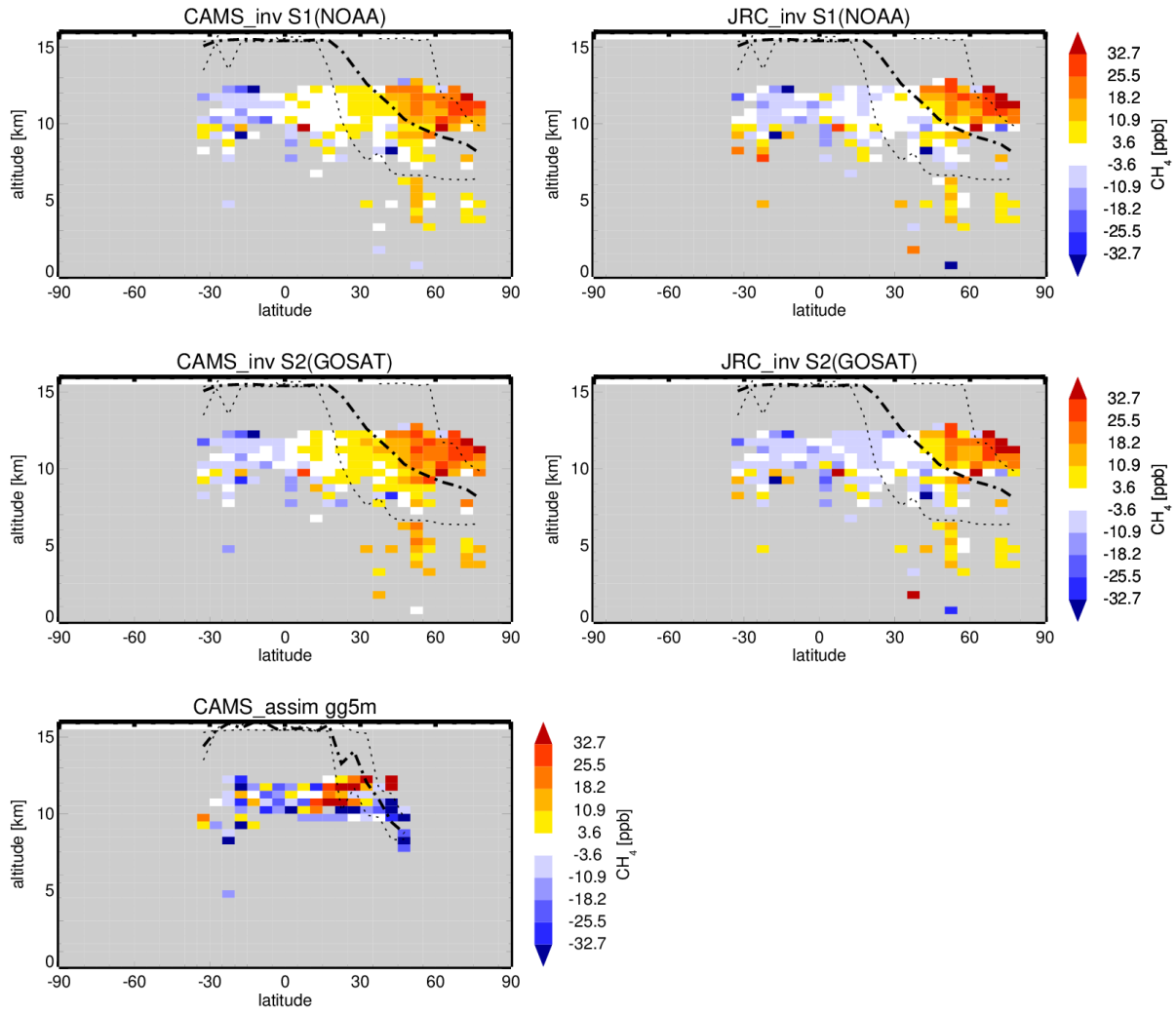

Figure 16: Average bias between simulated and observed CH_4 mole fractions as function of latitude and altitude for CARIBIC aircraft data. The bias is averaged in bins of 5° latitude and 500 m altitude. The mean tropopause height as diagnosed by the TM5 model is shown by the black dash-dotted line (and minimum and maximum tropopause heights by black dotted lines).

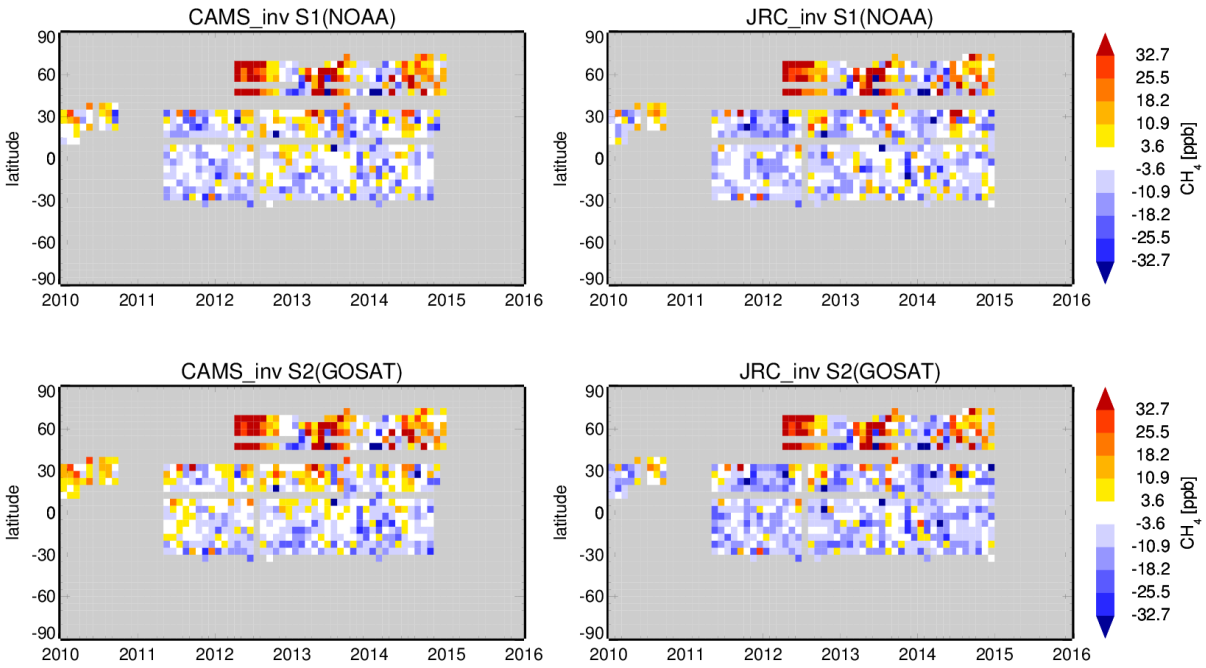

Figure 17: Average bias between simulated and observed CH_4 mole fractions as function of time and latitude for CONTRAIL aircraft data. Measurements and model simulations are averaged in monthly 5° latitude bins.

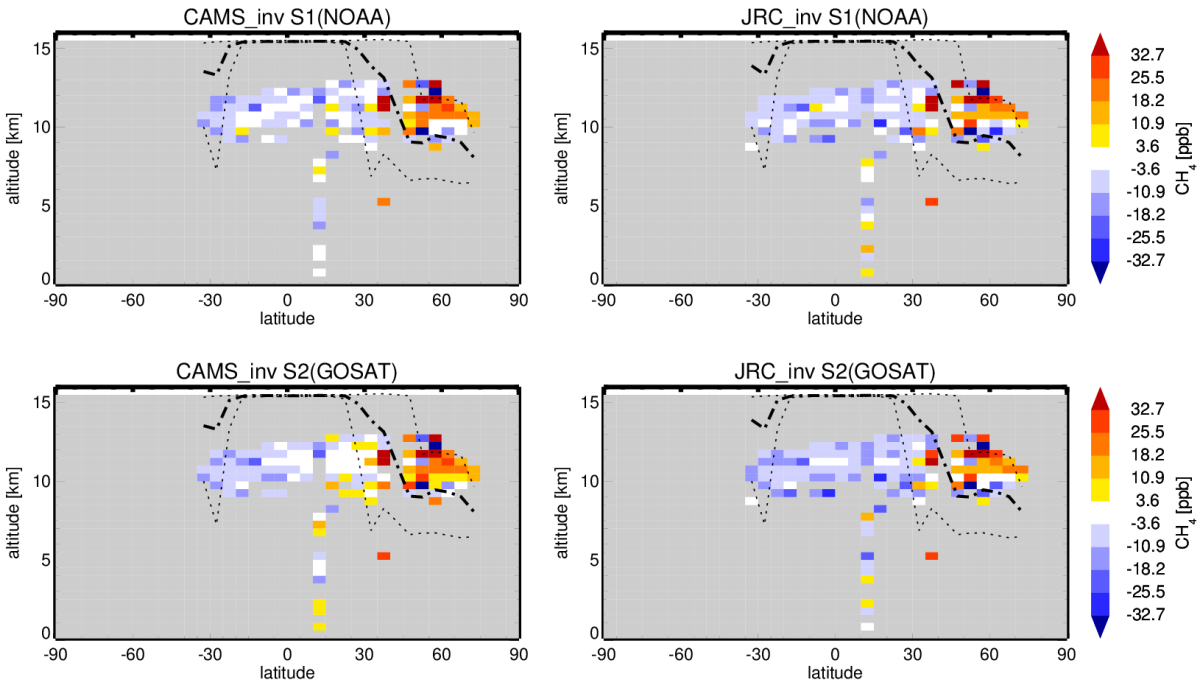

Figure 18: Average bias between simulated and observed CH_4 mole fractions as function of latitude and altitude for CONTRAIL aircraft data. The bias is averaged in bins of 5° latitude and 500 m altitude. The mean tropopause height as diagnosed by the TM5 model is shown by the black dash-dotted line (and minimum and maximum tropopause heights by black dotted lines).

4.3 Comparison with AirCore measurements

The NOAA AirCore profiles provide measurements of CH_4 mole fractions up to the middle stratosphere, providing a unique data set to evaluate the quality of the model simulations in the stratosphere. The mean vertical profiles at Boulder and Lamont are shown in Figure 19a (2016) and 19b (2017) and the individual AirCore balloon soundings during 2012-2017 in Annex 3 (including also profiles at Sodankyla). The comparison with the mean profiles shows that the models largely overestimate the observed CH_4 concentrations within the stratosphere, with a mean bias of 19-27 ppb at Boulder and 141-147 ppb at Lamont for the flux inversions and 35 ppb at Boulder and 122 ppb at Lamont for the CAMS "near real time analyses" in 2016, while the CAMS "near real time analyses" in 2017 show better agreement with the observations, with a mean bias between 3 and 21 ppb in the stratosphere at the two sites (Figure 19b). However, when considering the data over the 2012-2017 period, the average bias is relatively small (Figure 26), since the biases of the individual profiles show large variations and are varying in sign (Annex 3; Figures A31-A33). Furthermore, the average bias varies as a function of altitude above the tropopause (Figure 20). Both in the troposphere and the stratosphere the AirCore profiles often show significant "fine structures" in the vertical gradients, which are usually not reproduced by the flux inversions with their relatively coarse vertical resolution (CAMS: 34 vertical layers; JRC: 25 vertical layers). Conversely, there are some cases where the CAMS "near real time analyses" (with 137 vertical layers) can partially reproduce the "fine structure" (e.g. at Boulder 01-12-2016). On average, the flux inversions show only relatively small biases in the troposphere (Figures 19a and 20), confirming the good performance of the inversions in simulating the CH_4 concentrations in the troposphere (as evaluated over the US by the regular NOAA aircraft profiles).

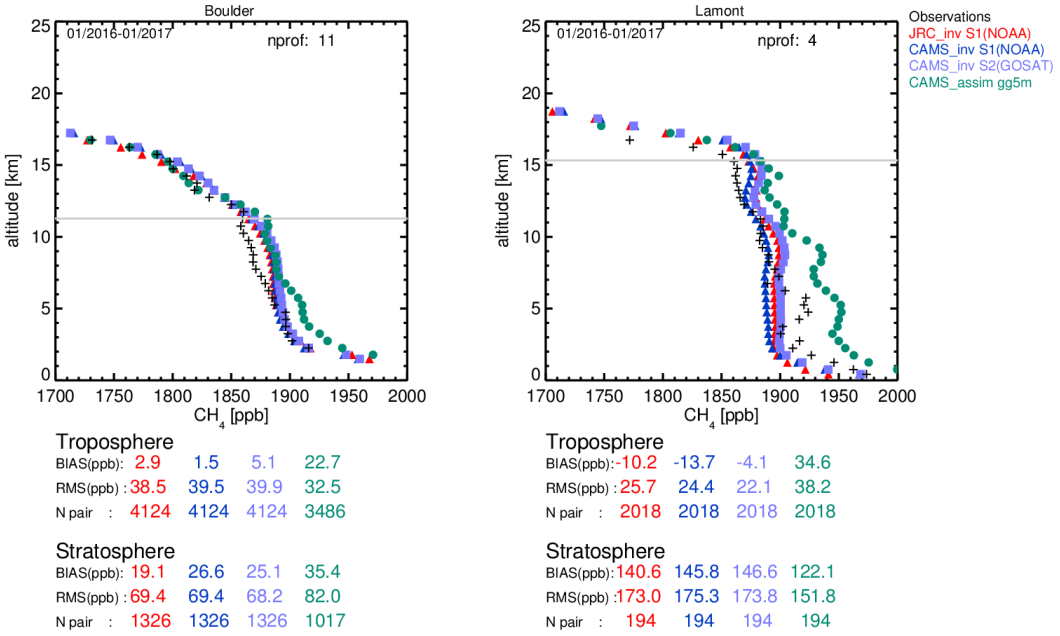

Figure 19a: Mean vertical profiles of modelled CH_4 mole fractions and AirCore observations at Boulder (left) and Lamont (right) for 2016. The bias and the root mean square (RMS) difference between the model simulations and observations are evaluated separately for the troposphere and stratosphere, respectively. N pair is the number of available paired data. The mean tropopause height as diagnosed by the TM5 model is shown by the grey line.

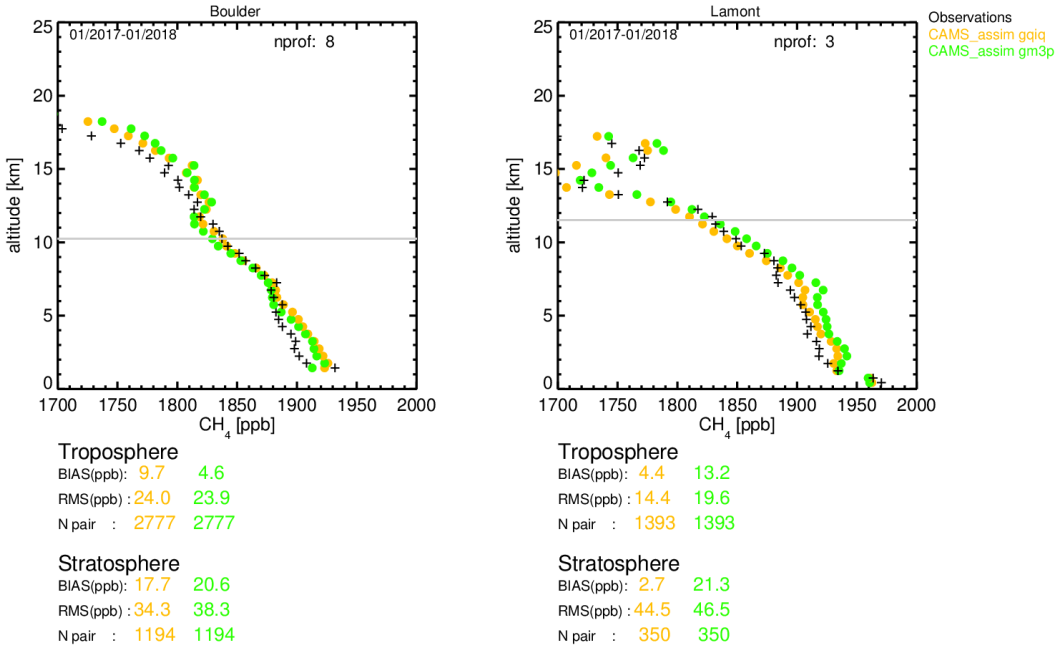

Figure 19b: As Figure 19a, but for the year 2017 for which CAMS "near real time analyses" are available for a large part of the year.

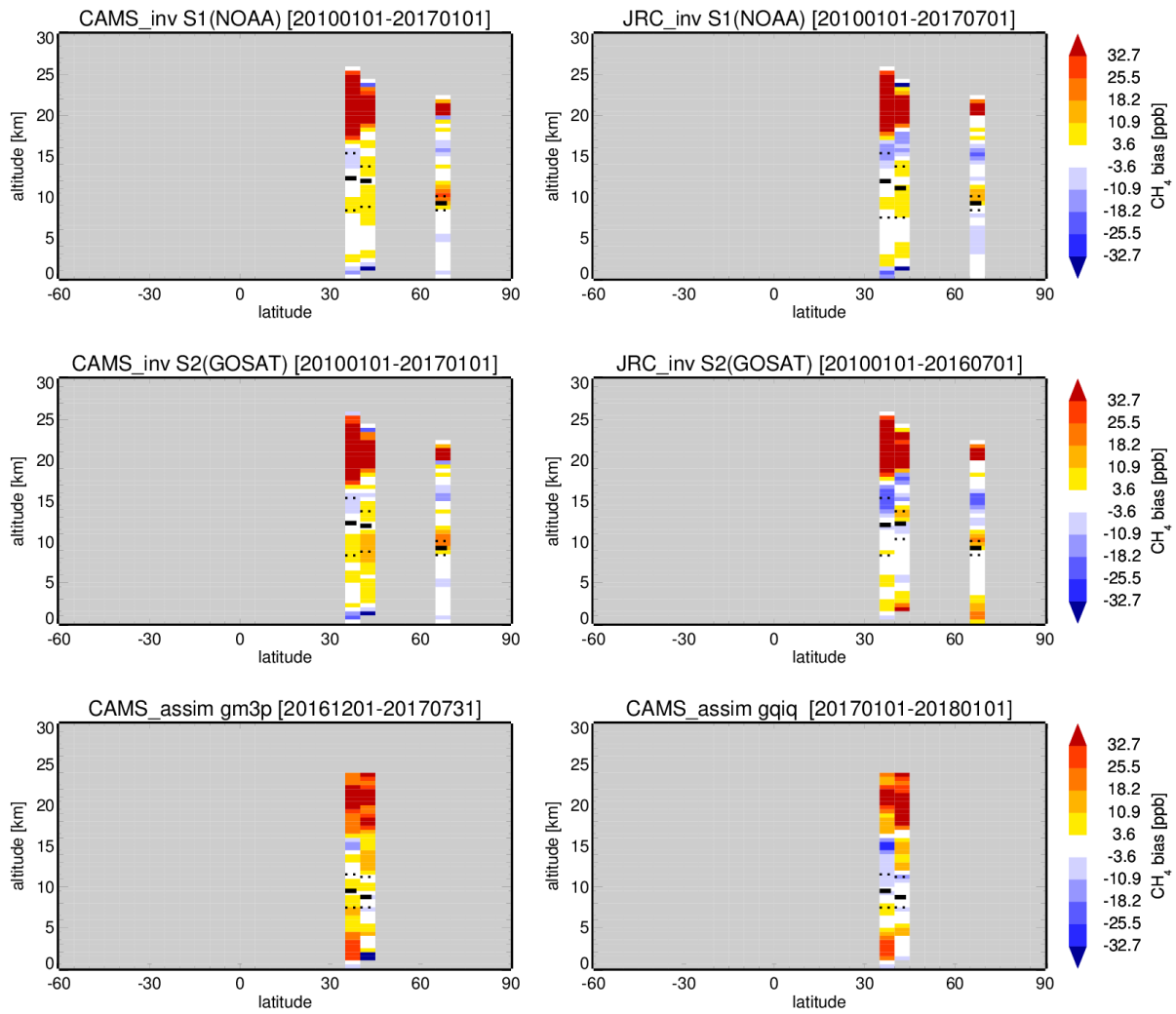

Figure 20: Average bias between simulated and observed CH_4 mole fractions as function of latitude and altitude using AirCore data. The bias is averaged in bins of 5° latitude and 500m altitude. The mean tropopause height as diagnosed by the TM5 model is shown by the black dash-dotted line (and minimum and maximum tropopause heights by black dotted lines).

4.4 Comparison with FTS observations

Figure 21 shows the time series of column-averaged CH_4 mole fractions at several TCCON FTS stations. The flux inversions reproduce the FTS observations in general relatively well, including the seasonal variations. However, at Sodankyla, the measurements often show relatively low XCH_4 values during spring, which are not reproduced by the models. Figure 22 displays the average bias as function of time and latitude and shows that the inversions overestimate the column averaged CH_4 mole fractions at high latitudes in the Northern Hemisphere, probably mainly due to the large bias of the models within the stratosphere, as discussed in the previous Sections (4.2 and 4.3). In the Southern Hemisphere (SH), the inversions show a small negative bias, which could partly reflect the small negative bias in the SH upper troposphere seen in the comparison with the aircraft data. Furthermore, the stratosphere (which is not validated independently in the SH, neither for the model simulations nor for the TCCON data) may contribute to the small bias.
The bias between the CAMS "near real time analyses" and the FTS data (Figures 21 and 22) largely reflects the bias of the CAMS "near real time analyses" in many areas of the globe, visible in the comparison with the surface and aircraft data (as discussed in sections 4.1, 4.2, and 4.3).

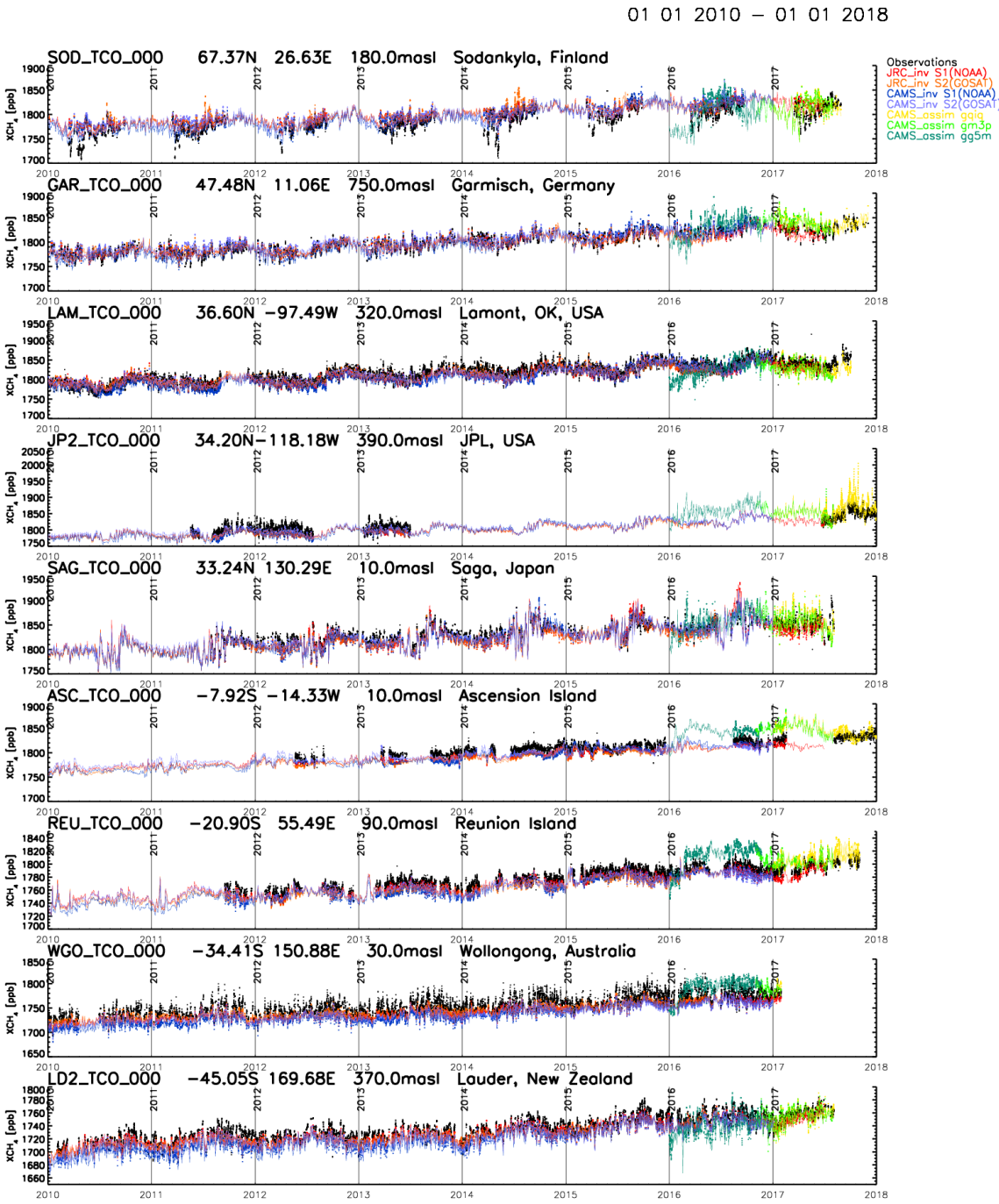

Figure 21: Comparison of simulated and observed column-averaged CH_4 mole fractions (XCH_4) at TCCON FTS stations.

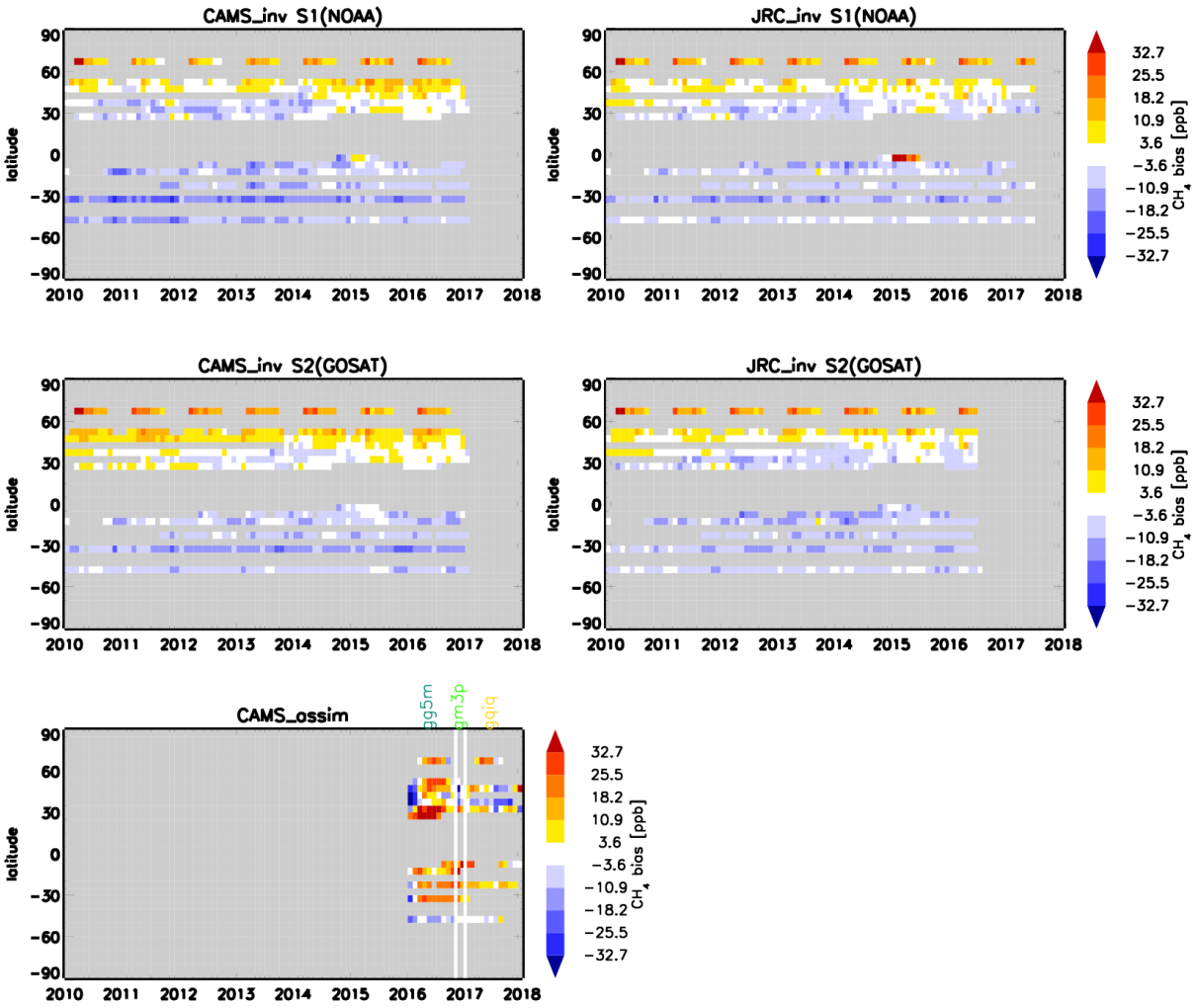

Figure 22: Average bias between simulated and observed column-averaged CH_4 mole fractions (XCH_4) as function of time and latitude using TCCON FTS data. Measurements and model simulations are averaged in monthly 5° latitude bins.

5 Evaluation of inverted surface CH_4 fluxes

Figure 23 shows the mean CH_4 emissions derived from the CAMS and JRC inversions, both for the "NOAA-only" inversions and for the inversions which use simultaneously the NOAA observations and GOSAT XCH_4 retrievals. There are some differences in "fine structure" of the spatial distribution of CH_4 emissions between the CAMS and JRC inversions (e.g. over the Hudson Bay Lowlands and over the Amazon), which are probably mainly due to the use of different a priori wetland emission inventories. The additional use of the GOSAT data results in some moderate changes in the spatial emission patterns (both for the CAMS and JRC inversions), e.g. somewhat higher CH_4 emissions over the south-central US and eastern Africa compared to the "NOAA-only" inversions. Compared to the JRC inversions, the CAMS inversions show somewhat higher emissions, especially in the Northern Hemisphere mid latitudes (between 30°N and 60°N, Figure 24). The small differences in the latitudinal distribution of the derived surface CH_4 fluxes could be (at least partly) related to the different convection schemes used in the two inversion systems (see section 2.2), which affects the inter-hemispheric mixing.

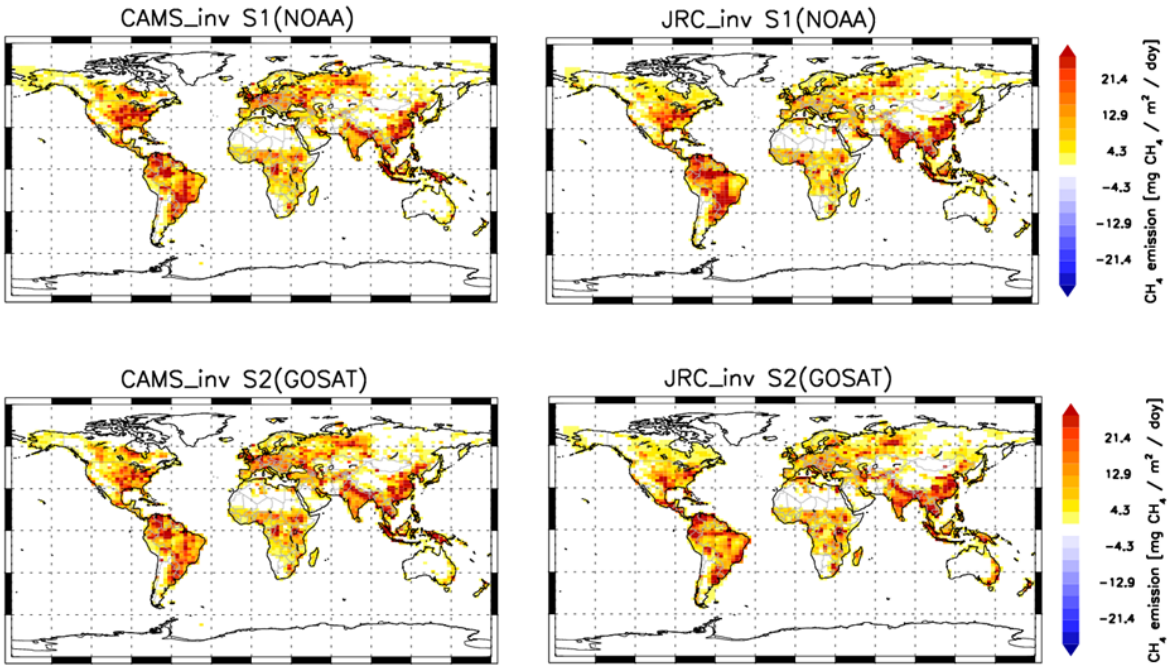

Figure 23: Mean CH_4 emissions derived from CAMS (left) and JRC (right) inversions, averaged over the 2010-2015 period. Top: inversions using only NOAA surface observations; bottom: inversions using both NOAA surface observations and XCH_4 satellite retrievals from GOSAT.

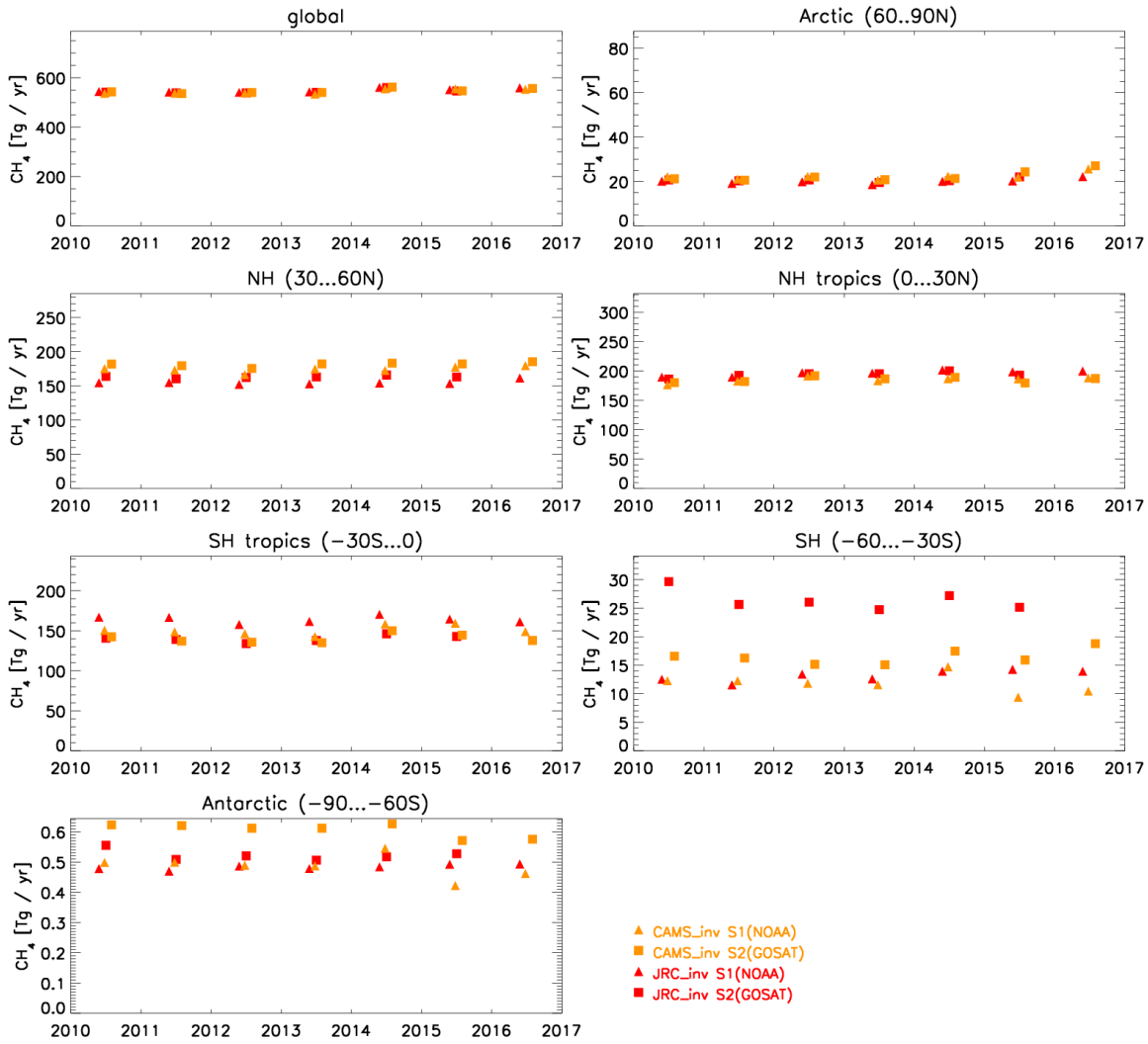

Figure 24: Global and regional annual total CH_4 surface emissions derived from the CAMS and JRC inversions.

6 Conclusions

We have evaluated the CAMS CH_4 "near real time analyses" (from the ECMWF IFS assimilation system) and the CAMS CH_4 flux inversions (from the TM5-4DVAR inverse modelling system, provided by TNO / SRON), using comprehensive observational data sets from surface monitoring stations, ship cruises, various aircraft programmes, AirCore balloon soundings, and FTS measurements of column-averaged CH_4 mole fractions. Furthermore, CH_4 flux inversions from the JRC TM5-4DVAR inversion system (which was used as prototype of the operational CAMS inversion system) were included in the analysis.

Figures 25 and 26 provide an overview of the performance of the different CH_4 products (in terms of simulated CH_4 mole fractions) compared to the different observational data sets. In general, the CAMS and JRC flux inversions show very similar performance and compare very well to the observations over remote regions near the surface and within the free troposphere (Figure 25), with an average bias close to zero and typical RMS differences around 10-20 ppb.

Due to the relatively coarse horizontal resolution of 3^ox2^o, however, both CAMS and JRC inversions show clear limitations in simulating the CH_4 mole fractions observed at regional monitoring stations (which are influenced by regional CH_4 emissions), showing negative biases (around -10 to -20 ppb) and RMS differences around 50 ppb.

Furthermore, the inversions significantly overestimate the CH_4 mole fractions in the lower stratosphere (measured by the different aircraft programmes; Figure 26). The comparison with the AirCore data in the lower and middle stratosphere also shows large differences, but since the biases of the individual profiles are highly variable in time (also varying in sign), the average bias is relatively small, but the RMS differences are around 50-60 ppb (for the comparison of the flux inversions with the AirCore data) and generally larger than ~40 ppb for all observations above the tropopause. The large biases in the stratosphere suggest that the current models have significant shortcomings to simulate the transport and/or chemistry in the stratosphere (and may have deficiencies to simulate the stratospheric-tropospheric exchange).

The CAMS "near real time analyses" show generally large biases in simulated CH_4 mole fractions, varying in space and time and visible in almost all global areas evaluated in this report. These large biases are probably mainly due to the assimilation strategy, including only satellite retrievals (but no surface observations) and potential biases in the assimilated satellite products (which are not corrected for in the IFS assimilations, while the flux inversions apply bias corrections for the satellite data). Furthermore, since the IFS assimilation system does not optimize the emissions, the "near real time analyses" are more sensitive (compared to the flux inversions) to errors in emission inventories.

The comparison of the CAMS "near real time analyses" with the AirCore data shows in some cases the benefit of much higher vertical resolution (with 137 vertical layers, as compared to 34 / 25 layers of the CAMS / JRC TM5-4DVAR inversion system). However, despite the higher vertical and horizontal resolution, the CAMS "near real time analyses" show - apart from their bias - also poorer performance to simulate the spatial and temporal variability (compared to the flux inversions) in areas which are affected by regional emissions (e.g. NOAA regional sites, NOAA aircraft), as apparent from the higher standard deviation and lower correlation coefficients (compared to the flux inversions). However, there are some

improvements in the recent "near real time analyses" for 2017 compared to the previous productions streams for 2016 (Figures 25 and 26).

The surface CH_4 fluxes derived from the CAMS inversion system are in general similar to the JRC estimates. However, the latitudinal gradients of the fluxes are slightly different between the two inversion systems, probably partly due to the two different convection schemes applied. Furthermore, there are also some differences in the "fine structure" of the spatial distribution of CH_4 emissions between the CAMS and JRC inversions, probably mainly due to the use of different a priori wetland emission inventories. In addition, the different bias corrections of the satellite retrievals applied in the CAMS and JRC inversions probably also have an impact on the derived emissions in the GOSAT inversion. The bias corrections (which partly also compensate the deficiencies of the models to simulate the stratosphere), should be further analysed and improved in the future. Furthermore, the improvements of the simulations of the stratosphere are essential to improve the model representation of the satellite retrievals, especially at mid to high latitudes. Despite the differences in the derived emissions, the CAMS and JRC inversions show very similar performance in the comparison of simulated CH_4 mole fractions with the different observational data sets used in this report (in terms of mean bias, correlation coefficient, standard deviation and RMS difference). Therefore, from the current analysis no clear conclusions can be drawn about which fluxes are more realistic.

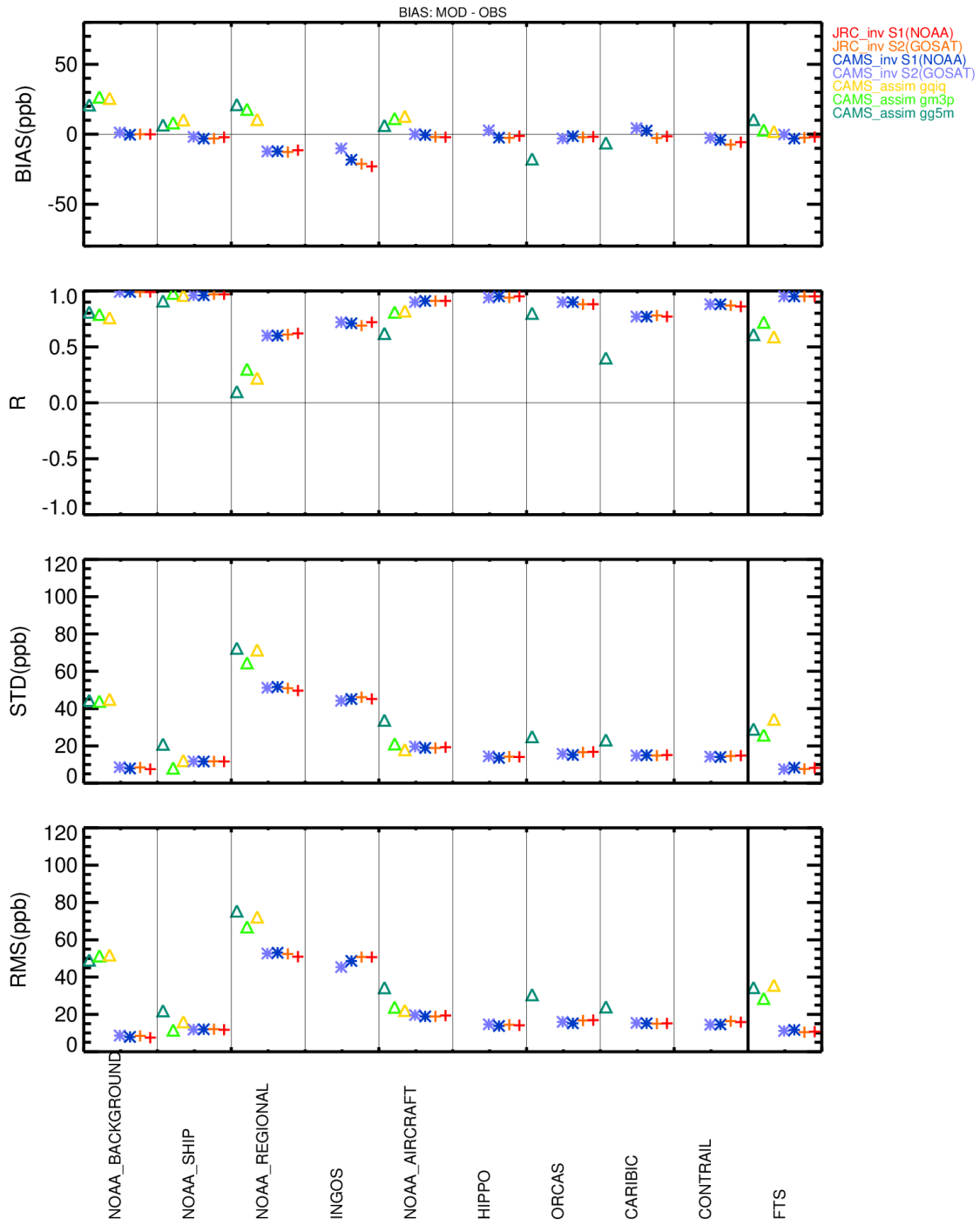

Figure 25: Summary of the evaluation of simulated CH_4 mole fractions of the different CH_4 products (CAMS and JRC flux inversions and CAMS 'near real time analyses"): mean bias, correlation coefficient R, standard deviation (STD), and root mean square (RMS) difference between model simulations and the observations in the troposphere and for the column averaged CH_4 mole fractions (at TCCON FTS sites).

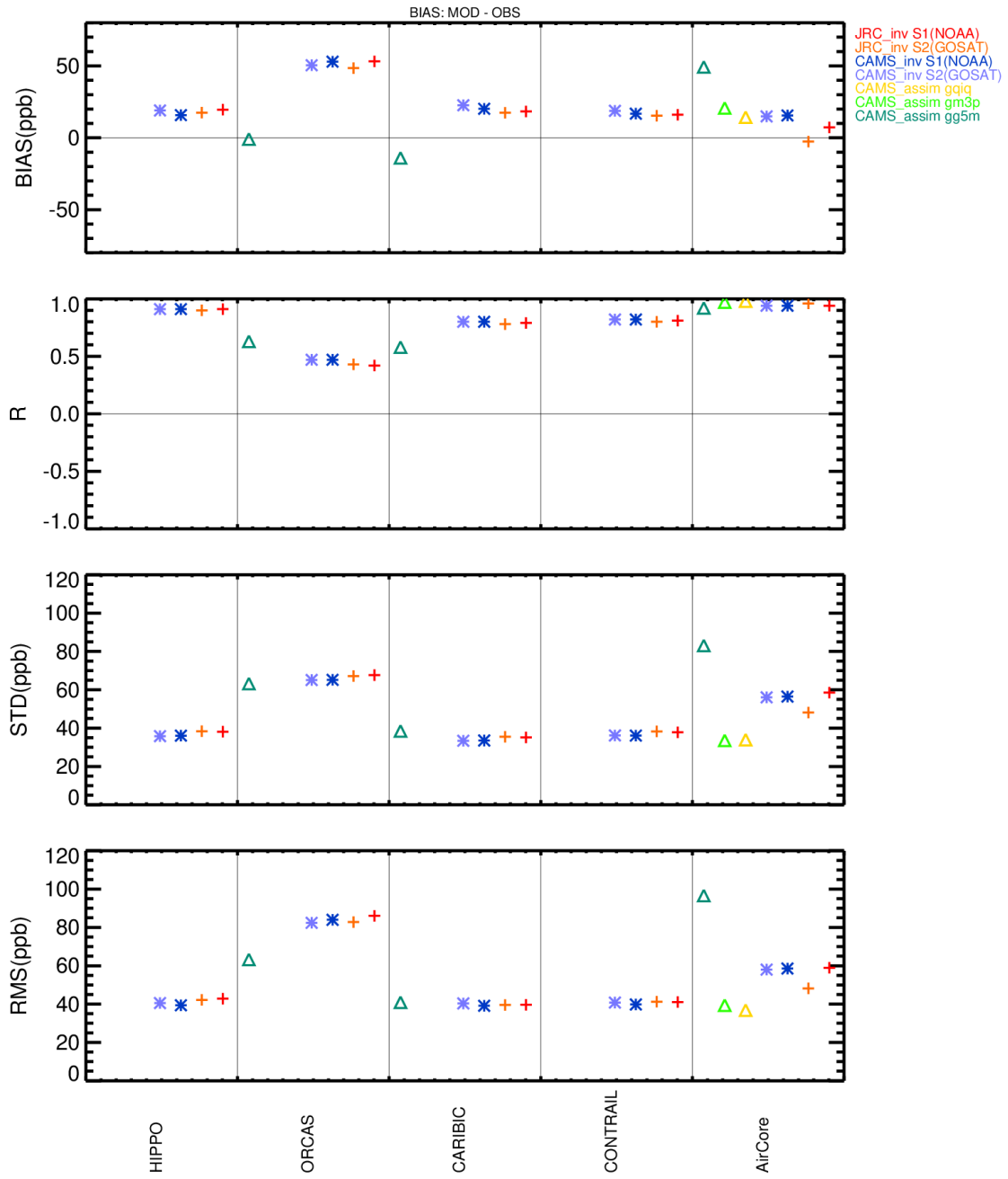

Figure 26: As Figure 25, but for the observations above the tropopause.

References

Agusti-Panareda, A., M. Diamantakis, V. Bayona, F. Klappenbach, and A. Butz, Improving the inter-hemispheric gradient of total column atmospheric CO2 and CH4 in simulations with the ECMWF semi-Lagrangian atmospheric global model, *Geosci. Model Dev.*, *10*(1), 1-18, doi:10.5194/gmd-10-1-2017, 2017.

Alexe, M., P. Bergamaschi, A. Segers, R. Detmers, A. Butz, O. Hasekamp, S. Guerlet, R. Parker, H. Boesch, C. Frankenberg, R. A. Scheepmaker, E. Dlugokencky, C. Sweeney, S. C. Wofsy, and E. A. Kort, Inverse modelling of CH_4 emissions for 2010-2011 using different satellite retrieval products from GOSAT and SCIAMACHY, *Atmos. Chem. Phys.*, *15*(1), 113–133, doi:10.5194/acp-15-113-2015, 2015.

Bergamaschi, P., C. Frankenberg, J. F. Meirink, M. Krol, F. Dentener, T. Wagner, U. Platt, J. O. Kaplan, S. Körner, M. Heimann, E. J. Dlugokencky, and A. Goede, Satellite chartography of atmospheric methane from SCIAMACHY onboard ENVISAT: 2. Evaluation based on inverse model simulations, *J. Geophys. Res.*, *112*(D02304), doi:10.1029/2006JD007268, 2007.

Bergamaschi, P., C. Frankenberg, J. F. Meirink, M. Krol, M. G. Villani, S. Houweling, F. Dentener, E. J. Dlugokencky, J. B. Miller, L. V. Gatti, A. Engel, and I. Levin, Inverse modeling of global and regional CH_4 emissions using SCIAMACHY satellite retrievals, *J. Geophys. Res.*, *114*, doi:10.1029/2009JD012287, 2009.

Bergamaschi, P., S. Houweling, A. Segers, M. Krol, C. Frankenberg, R. A. Scheepmaker, E. Dlugokencky, S. C. Wofsy, E. A. Kort, C. Sweeney, T. Schuck, C. Brenninkmeijer, H. Chen, V. Beck, and C. Gerbig, Atmospheric CH_4 in the first decade of the 21st century: Inverse modeling analysis using SCIAMACHY satellite retrievals and NOAA surface measurements, *J. Geophys. Res.-Atmos.*, *118*(13), 7350-7369, doi:10.1002/jgrd.50480, 2013.

Bergamaschi, P., U. Karstens, A. J. Manning, et al., Inverse modelling of European CH_4 emissions during 2006–2012 using different inverse models and reassessed atmospheric observations, *Atmos. Chem. Phys.*, *18*(2), 901-920, doi:10.5194/acp-18-901-2018, 2018.

Brenninkmeijer, C. A. M., P. Crutzen, F. Boumard, et al., Civil Aircraft for the regular investigation of the atmosphere based on an instrumented container: The new CARIBIC system, *Atmos. Chem. Phys.*, *7*(18), 4953-4976, doi:10.5194/acp-7-4953-2007, 2007.

Butler, J. H., and S. A. M. Montzka, The NOAA annual greenhouse gas index (AGGI), https://www.esrl.noaa.gov/gmd/aggi/aggi.html, last access: 19 September 2017, 2017, 2018.

Butz, A., O. P. Hasekamp, C. Frankenberg, J. Vidot, and I. Aben, CH4 retrievals from space-based solar backscatter measurements: Performance evaluation against simulated aerosol and cirrus loaded scenes *J. Geophys. Res.*, *115*(D24), doi:org/10.1029/2010JD014514, 2010.

Crevoisier, C., D. Nobileau, A. M. Fiore, R. Armante, A. Chédin, and N. A. Scott, Tropospheric methane in the tropics – first year from IASI hyperspectral infrared observations, *Atmos. Chem. Phys.*, *9*(17), 6337-6350, doi:10.5194/acp-9-6337-2009, 2009.

Crevoisier, C., D. Nobileau, R. Armante, L. Crépeau, T. Machida, Y. Sawa, H. Matsueda, T. Schuck, T. Thonat, J. Pernin, N. A. Scott, and A. Chédin, The 2007–2011 evolution of tropical methane in the mid-troposphere as seen from space by MetOp-A/IASI, *Atmos. Chem. Phys.*, *13*(8), 4279-4289, doi:10.5194/acp-13-4279-2013, 2013.

Dee, D. P., S. M. Uppala, A. J. Simmons, et al., The ERA-Interim reanalysis: configuration and performance of the data assimilation system, *Q. J. R. Meteorol. Soc.*, *137*, 553–597, doi:10.1002/qj.828, 2011.

Detmers, R., and O. Hasekamp, Product User Guide (PUG) for the RemoTeC XCH4 PROXY GOSAT Data Product v2.3.8, http://www.esa-ghg-cci.org/?q=webfm_send/219, 2016.

Dlugokencky, E. J., L. P. Steele, P. M. Lang, and K. A. Masarie, The growth rate and distribution of atmospheric methane, *J. Geophys. Res.-Atmos.*, *99*(D8), 17021-17043, doi:10.1029/94jd01245, 1994.

Dlugokencky, E. J., S. Houweling, L. Bruhwiler, K. A. Masarie, P. M. Lang, J. B. Miller, and P. P. Tans, Atmospheric methane levels off: Temporary pause or a new steady-state ?, *Geophys. Res. Lett.*, *30*(19), doi:10.1029/2003GL018126, doi:10.1029/2003GL018126, 2003.

Dlugokencky, E. J., R. C. Myers, P. M. Lang, K. A. Masarie, A. M. Crotwell, K. W. Thoning, B. D. Hall, J. W. Elkins, and L. P. Steele, Conversion of NOAA atmospheric dry air CH_4 mole fractions to a gravimetrically prepared standard scale, *J. Geophys. Res.*, *110*(D18306), doi:10.1029/2005JD006035, 2005.

Dlugokencky, E. J., L. Bruhwiler, J. W. C. White, L. K. Emmons, P. C. Novelli, S. A. Montzka, K. A. Masarie, P. M. Lang, A. M. Crotwell, J. B. Miller, and L. V. Gatti, Observational constraints on recent increases in the atmospheric CH_4 burden, *Geophys. Res. Lett.*, *36*(L18803), doi:10.1029/2009GL039780, 2009.

Etheridge, D. M., L. P. Steele, R. J. Francey, and R. L. Langenfelds, Atmospheric methane between 1000 A.D. and present: Evidence of anthropogenic emissions and climatic variability, *J. Geophys. Res.*, *103*(D13), 15979–15993, 1998.

IPCC, Climate Change 2013 The Physical Science Basis, Working Group I Contribution to the Fifth Assessment Report of the Intergovernmental Panel on Climate Change, edited by T. F. Stocker, D. Qin, G.-K. Plattner, M. Tignor, S. K. Allen, J. Boschung, A. Nauels, Y. Xia, V. Bex and P. M. Midgley, Cambridge University Press, Cambridge, United Kingdom and New York, NY, USA, 1535 pp. pp., 2013.

Karion, A., C. Sweeney, P. Tans, and T. Newberger, AirCore: An Innovative Atmospheric Sampling System *BAMS*, doi:org/10.1175/2010JTECHA1448.1, 2010.

Kort, E. A., P. K. Patra, K. Ishijima, B. C. Daube, R. Jiménez, J. Elkins, D. Hurst, F. L. Moore, C. Sweeney, and S. C. Wofsy, Tropospheric distribution and variability of N_2O: Evidence for strong tropical emissions, *Geophys. Res. Lett.*, *38*(L15806), doi:10.1029/2011GL047612, 2011.

Kort, E. A., S. C. Wofsy, B. C. Daube, M. Diao, J. W. Elkins, R. S. Gao, E. J. Hintsa, D. F. Hurst, R. Jimenez, F. L. Moore, J. R. Spackman, and M. A. Zondlo, Atmospheric observations of Arctic Ocean methane emissions up to 82^o north, *Nature Geoscience*, *5*, 318-321, doi:10.1038/NGEO1452, 2012.

Krol, M., S. Houweling, B. Bregman, M. van den Broek, A. Segers, P. van Velthoven, W. Peters, F. Dentener, and P. Bergamaschi, The two-way nested global chemistry-transport zoom model TM5: algorithm and applications, *Atmos. Chem. Phys.*, *5*, 417-432, doi:10.5194/acp-5-417-2005, 2005.

Machida, T., H. Matsueda, Y. Sawa, Y. Nakagawa, K. Hirotani, N. Kondo, K. Goto, T. Nakazawa, K. Ishikawa, and T. Ogowa, Worldwide Measurements of Atmospheric CO2 and Other Trace Gas Species Using Commercial Airlines *BAMS*, doi:org/10.1175/2008JTECHA1082.1, 2008.

Massart, S., A. Agusti-Panareda, I. Aben, A. Butz, F. Chevallier, C. Crevoisier, R. Engelen, C. Frankenberg, and O. Hasekamp, Assimilation of atmospheric methane products into the MACC-II system: from SCIAMACHY to TANSO and IASI, *Atmos. Chem. Phys.*, *14*(12), 6139-6158, doi:10.5194/acp-14-6139-2014, 2014.

Matsueda, H., T. Machida, Y. Sawa, Y. Nakagawa, K. Hirotani, H. Ikeda, N. Kondo, and K. Goto, Evaluation of atmospheric CO2 measurements from new flask air sampling of JAL airliner observations, *Pap. Meteorolo. Geophys*, *59*, 1-17, 2008.

Meirink, J. F., P. Bergamaschi, and M. Krol, Four-dimensional variational data assimilation for inverse modelling of atmospheric methane emissions: Method and comparison with

synthesis inversion, *Atmos. Chem. Phys.* , *8*, 6341–6353, doi:10.5194/acp-8-6341-2008, 2008.

Melton, J. R., R. Wania, E. L. Hodson, B. Poulter, B. Ringeval, R. Spahni, T. Bohn, C. A. Avis, D. J. Beerling, G. Chen, A. V. Eliseev, S. N. Denisov, P. O. Hopcroft, D. P. Lettenmaier, W. J. Riley, J. S. Singarayer, Z. M. Subin, H. Tian, S. Zürcher, V. Brovkin, P. M. van Bodegom, T. Kleinen, Z. C. Yu, and J. O. Kaplan, Present state of global wetland extent and wetland methane modelling: conclusions from a model inter-comparison project (WETCHIMP), *Biogeosciences*, *10*(2), 753-788, doi:10.5194/bg-10-753-2013, 2013.

Membrive, O., C. Crevoisier, C. Sweeney, F. Danis, A. Hertzog, A. Engel, H. Bönisch, and L. Picon, AirCore-HR: a high-resolution column sampling to enhance the vertical description of CH4 and CO2, *Atmos. Meas. Tech.*, *10*(6), 2163-2181, doi:10.5194/amt-10-2163-2017, 2017.

Pandey, S., S. Houweling, M. Krol, I. Aben, F. Chevallier, E. J. Dlugokencky, L. V. Gatti, E. Gloor, J. B. Miller, R. Detmers, T. Machida, and T. Röckmann, Inverse modeling of GOSAT-retrieved ratios of total column CH4 and CO2 for 2009 and 2010, *Atmos. Chem. Phys.*, *16*(8), 5043-5062, doi:10.5194/acp-16-5043-2016, 2016.

Sawa, Y., T. Machida, H. Matsueda, Y. Niwa, K. Tsuboi, S. Murayama, S. Morimoto, and S. Aoki, Seasonal changes of CO2, CH4, N2O, and SF6 in the upper troposphere/lower stratosphere over the Eurasian continent observed by commercial airliner *Geophys. Res. Lett.*, doi:10.1002/2014GL062734, 2015.

Schuck, T. J., C. A. M. Brenninkmeijer, A. K. Baker, F. Slemr, P. F. J. von Velthoven, and A. Zahn, Greenhouse gas relationships in the Indian summer monsoon plume measured by the CARIBIC passenger aircraft, *Atmos. Chem. Phys.*, *10*(8), 3965-3984, doi:10.5194/acp-10-3965-2010, 2010.

Schuck, T. J., K. Ishijima, P. K. Patra, A. K. Baker , T. Machida, H. Matsueda, Y. Sawa, T. Umezawa, C. A. M. Brenninkmeijer, and J. Lelieveld, Distribution of methane in the tropical upper troposphere measured by CARIBIC and CONTRAIL aircraft *J Geophys. Res.*, doi:org/10.1029/2012JD018199, 2012.

Segers , A., and S. Houweling, Description of the CH_4 Inversion Production Chain, https://atmosphere.copernicus.eu/sites/default/files/FileRepository/Resources/Validation-reports/Fluxes/CAMS73_2015SC2_D73.2.5.5-2017_201712_production_chain_v1.pdf, 2017a.

Segers, A., and S. Houweling, Validation of the CH_4 surface flux inversion - reanalysis 2000-2016, CAMS73_2015SC2_D73.2.4.4-2016_201712_validation_CH4_2000-2016_v1, 2017b.

Stephens, B. B., M. C. Long, E. A. Kort, et al., The O2/N2 Ratio and CO2 Airborne Southern Ocean Study *BAMS*, doi:org/10.1175/BAMS-D-16-0206.1, 2017.

Tiedtke, M., A comprehensive mass flux scheme for cumulus parameterization in large-scale models, *Monthly Weather Review*, *117*, 1779-1800, 1987.

Umezawa, T., T. Machida, K. Ishijima, H. Matsueda, Y. Sawa, P. K. Patra, S. Aoki, and T. Nakazawa, Carbon and hydrogen isotopic ratios of atmospheric methane in the upper troposphere over the Western Pacific, *Atmos. Chem. Phys.*, *12*(17), 8095-8113, doi:10.5194/acp-12-8095-2012, 2012.

Wofsy, S. C., H. S. TEAM, C. MODELLERS, and S. TEAMS, HIAPER Pole-to-Pole Observations (HIPPO): fine-grained, global-scale measurements of climatically important atmospheric gases and aerosols, *Phil. Trans. R. Soc. A* (369), 2073-2086, doi:10.1098/rsta.2010.0313, 2011.

Wunch, D., G. C. Toon, P. O. Wennberg, et al., Calibration of the Total Carbon Column Observing Network using aircraft profile data, *Atmos. Meas. Tech.*, *3*(5), 1351-1362, doi:10.5194/amt-3-1351-2010, 2010.

Wunch, D., G. C. Toon, J.-F. L. Blavier, R. A. Washenfelder, J. Notholt, B. J. Connor, D. W. T. Griffith, V. Sherlock, and P. O. Wennberg, The Total Carbon Column Observing Network, *Phil. Trans. R. Soc. A*, *369*, 2087-2112, doi:doi: 10.1098/rsta.2010.0240, 2011.

Zahn, A., C. A. M. Brenninkmeijer, M. Maiss, D. H. Scharffe, P. J. Crutzen, G. Heinrich, D. A. Wiedensohler, H. Giisten, M. Hermann, J. Heintzenberg, H. Fischer, J. W. M. Cuijpers, and P. F. J. van Velthoven, Identification of extratropical two-way troposphere-stratosphere mixing based on CARIBIC measurements of O3, CO, and ultrafine particles *J Geophys. Res.*, doi:org/10.1029/1999JD900759, 2000.

List of abbreviations and definitions

ASE	Automatic air Sampling Equipment
CAMS	Copernicus Atmosphere Monitoring Service
CARIBIC	Civil Aircraft for the Regular Investigation of the atmosphere Based on an Instrument Container
CONTRAIL	Comprehensive Observation Network for TRace gases by AIrLiner
ECMWF	European Centre for Medium-Range Weather Forecasts
EU	European Union
ESRL	Earth System Research Laboratory
FTS	Fourier Transform Spectrometers
GEMS	Global Monitoring for Environment and Security
HIPPO	HIAPER Pole-to-Pole Observations
IASI	Infrared Atmospheric Sounding Interferometer
IFS	Integrated Forecasting System
InGOS	Integrated non-CO_2 Greenhouse gas Observing System
IPCC	Intergovernmental Panel on Climate Change
JAL	Japan Airlines
JAL-F	Japan Airlines Foundation
JAMCO	JAMCO Corporation
JRC	Joint Research Centre
MACC	Monitoring Atmospheric Composition and Climate
MeTOp	Meteorological Operational
MRI	Meteorological Research Institute
MSE	Manual air Sampling Equipment
NOAA	National Oceanic and Atmospheric Administration
ORCAS	O_2/N_2 Ratio and CO_2 Airborne Southern Ocean Study
POC	Pacific Ocean
PROMOTE	PROtocol MOniToring GMES Service Element on Atmospheric Composition
SRON	Space Research Organisation Netherlands
TANSO	Thermal And Near-infrared Sensor for carbon Observation
TCCON	Total Carbon Column Observing Network
TNO	Toegepast Natuurwetenschappelijk Onderzoek (Netherlands Organisation for Applied Scientific Research)
USA	United States of America
WETCHIMP	Wetland and Wetland CH_4 Inter-comparison of Models
WMO	World Meteorological Organization

Annexes

Annex 1: Comparison of individual HIPPO campaigns

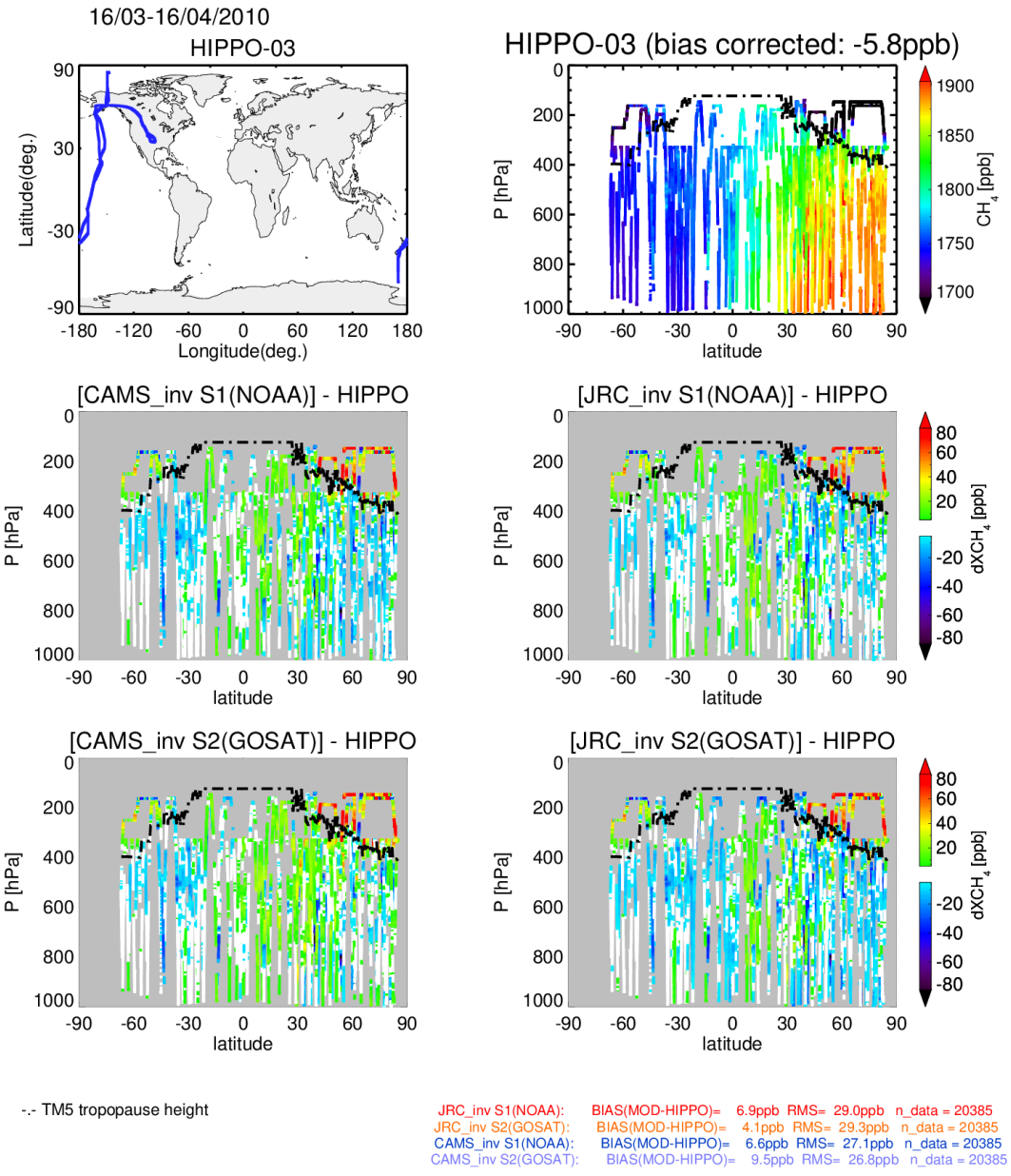

Figure A11: HIPPO-03 campaign (16/03 -16/04/2010): Top left: HIPPO flight track. Top right: measurements as function of latitude and atmospheric pressure. Middle and lower panel: Bias between modelled CH_4 mole fractions and HIPPO measurements. The level of the tropopause (as diagnosed from the TM5 model), is shown by the dashed dot lines.

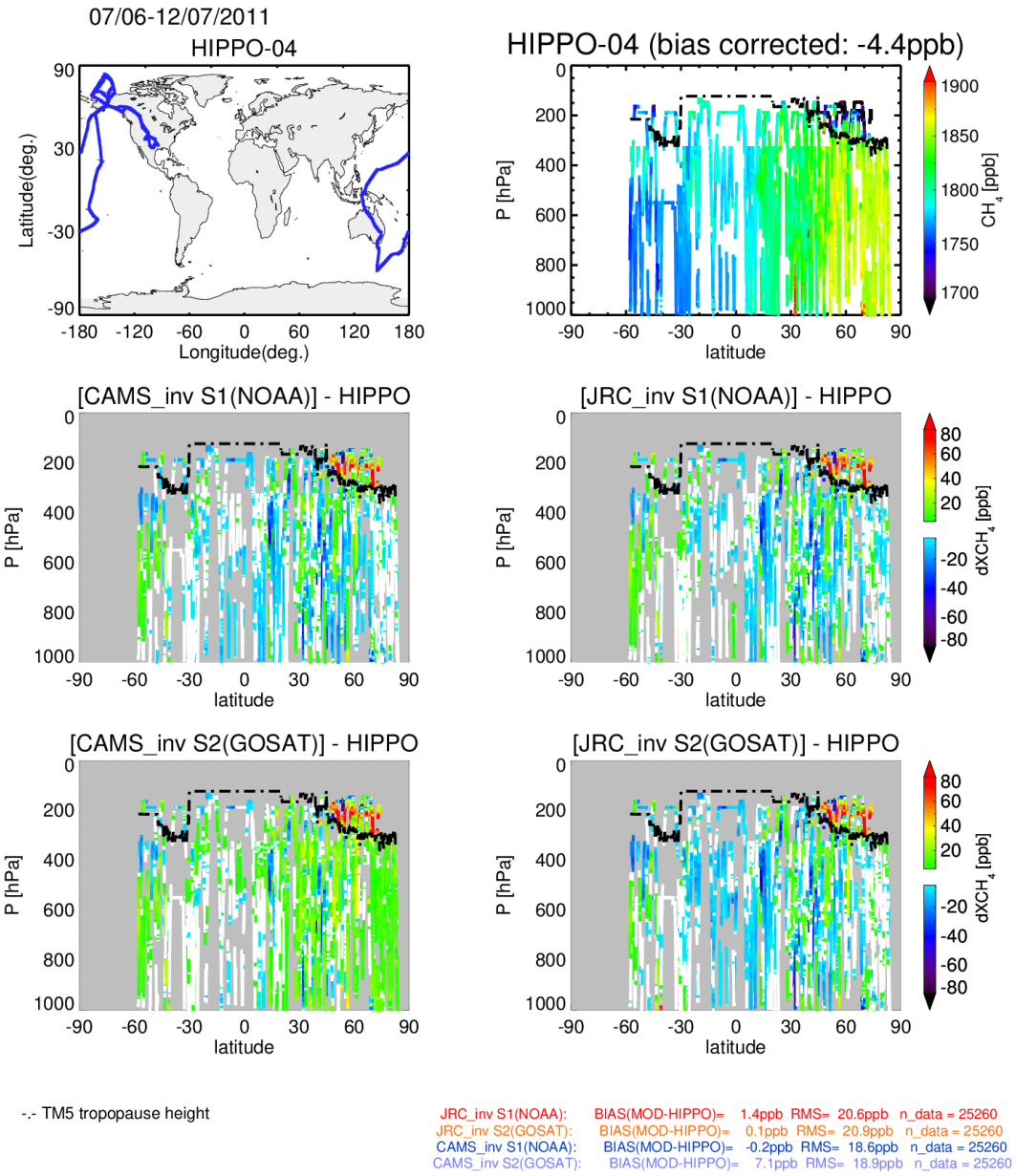

Figure A12: As Figure A11, but for the HIPPO-04 campaign (07/06 -17/07/2011).

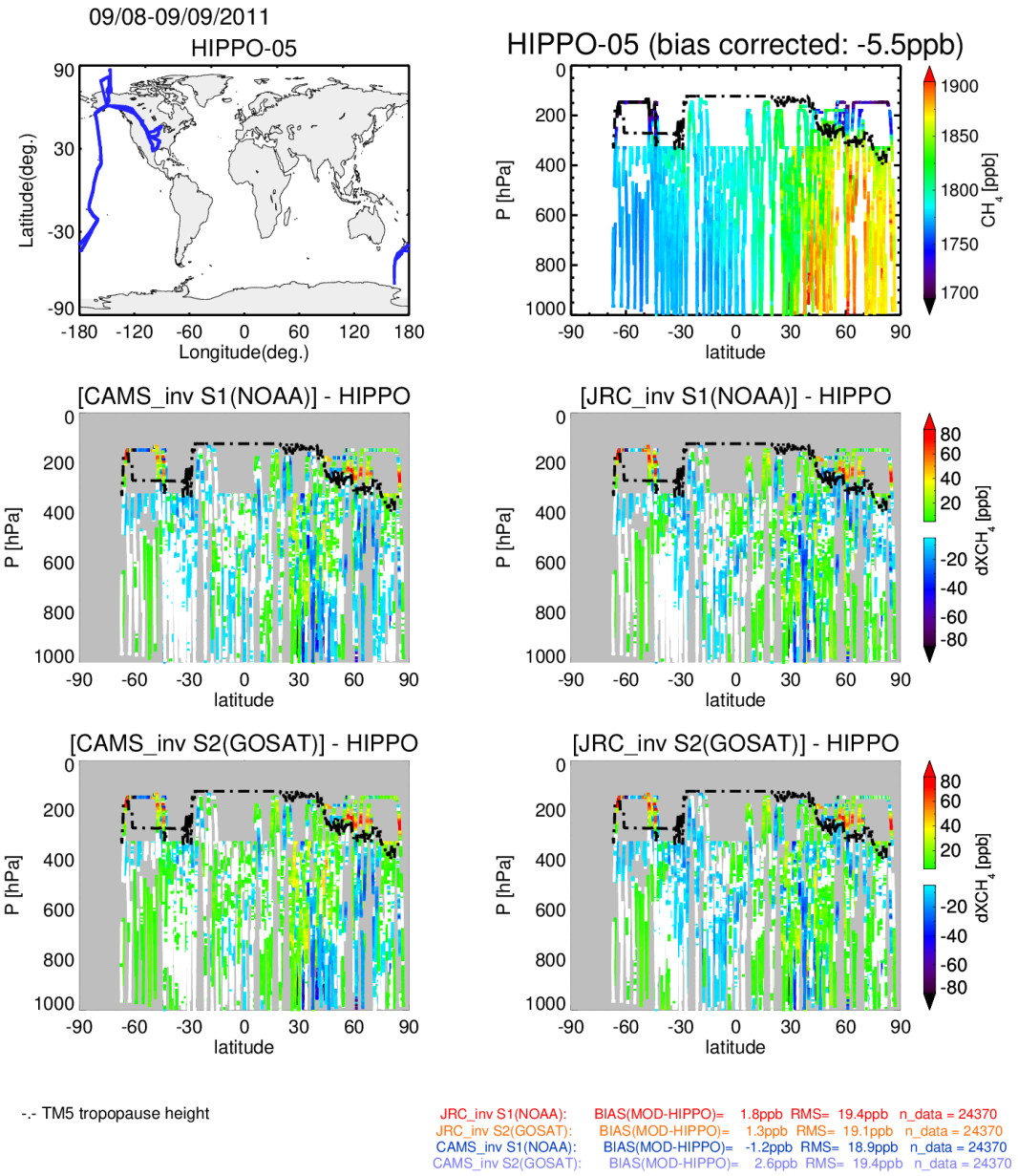

Figure A13: As Figure A11, but for the HIPPO-05 campaign (09/08-09/09/2011).

Annex 2: Comparison of individual ORCAS flights

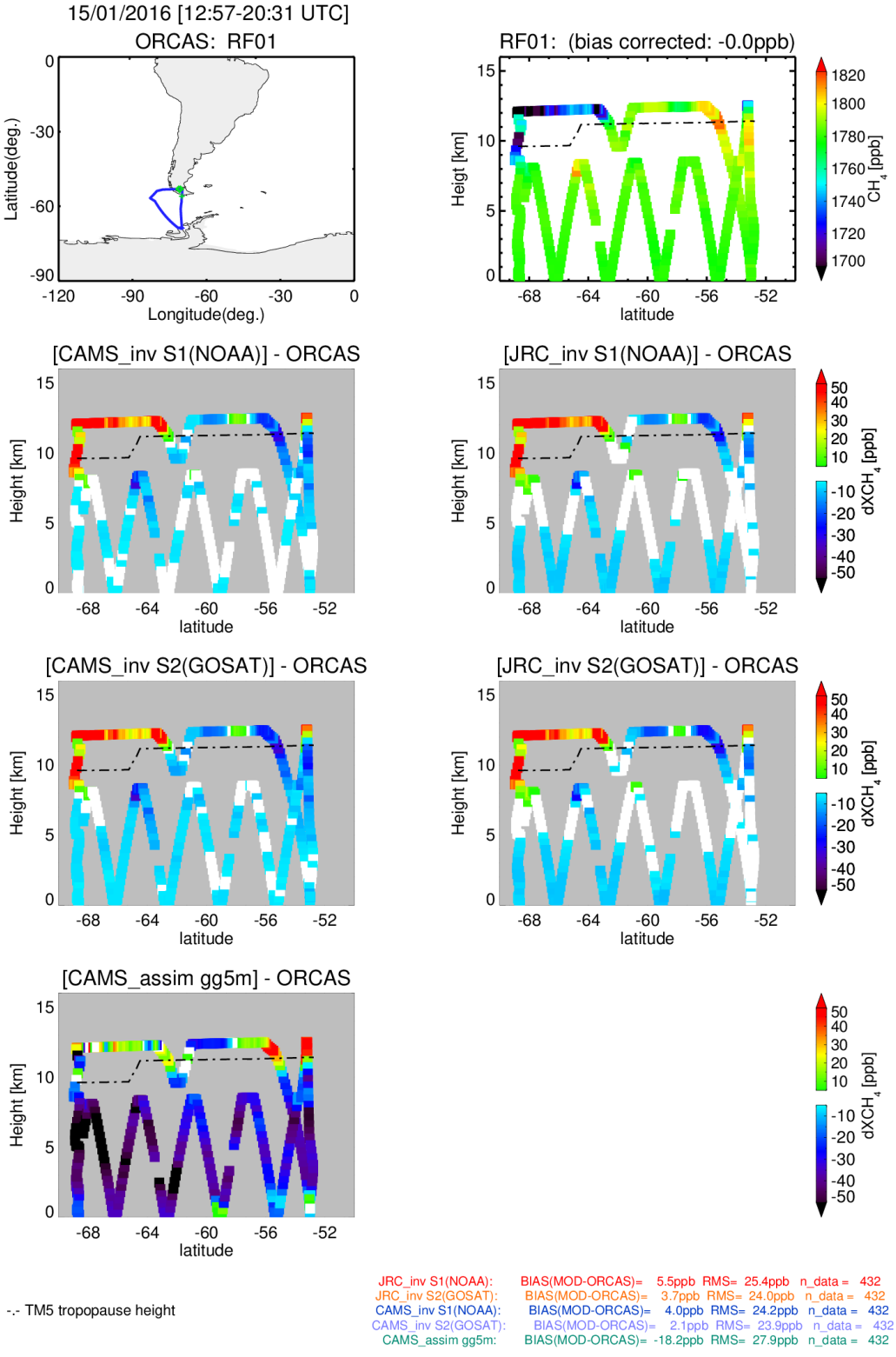

Figure A21: ORCAS flight RF01 (15/01/2016): Top left: flight route. Top right: Measured CH_4 mole fractions as function of latitude and flight altitude. The subsequent panels show the bias between the simulations for the different models and the measurements. The level of the tropopause, as diagnosed from the TM5 model, is shown by the dashed dot lines.

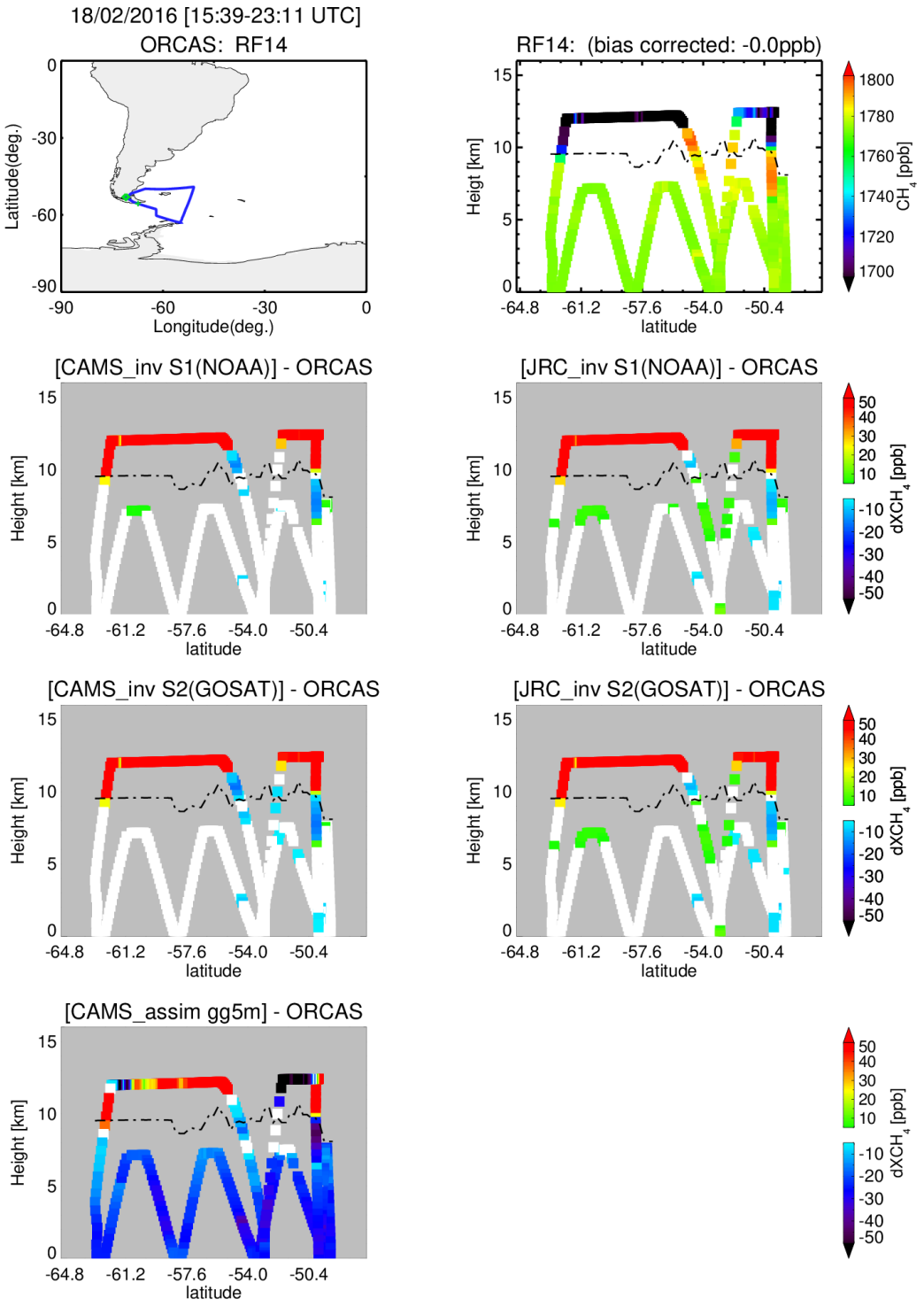

Figure A22: As Figure A21, but for the flight RF14 (18/02/2016).

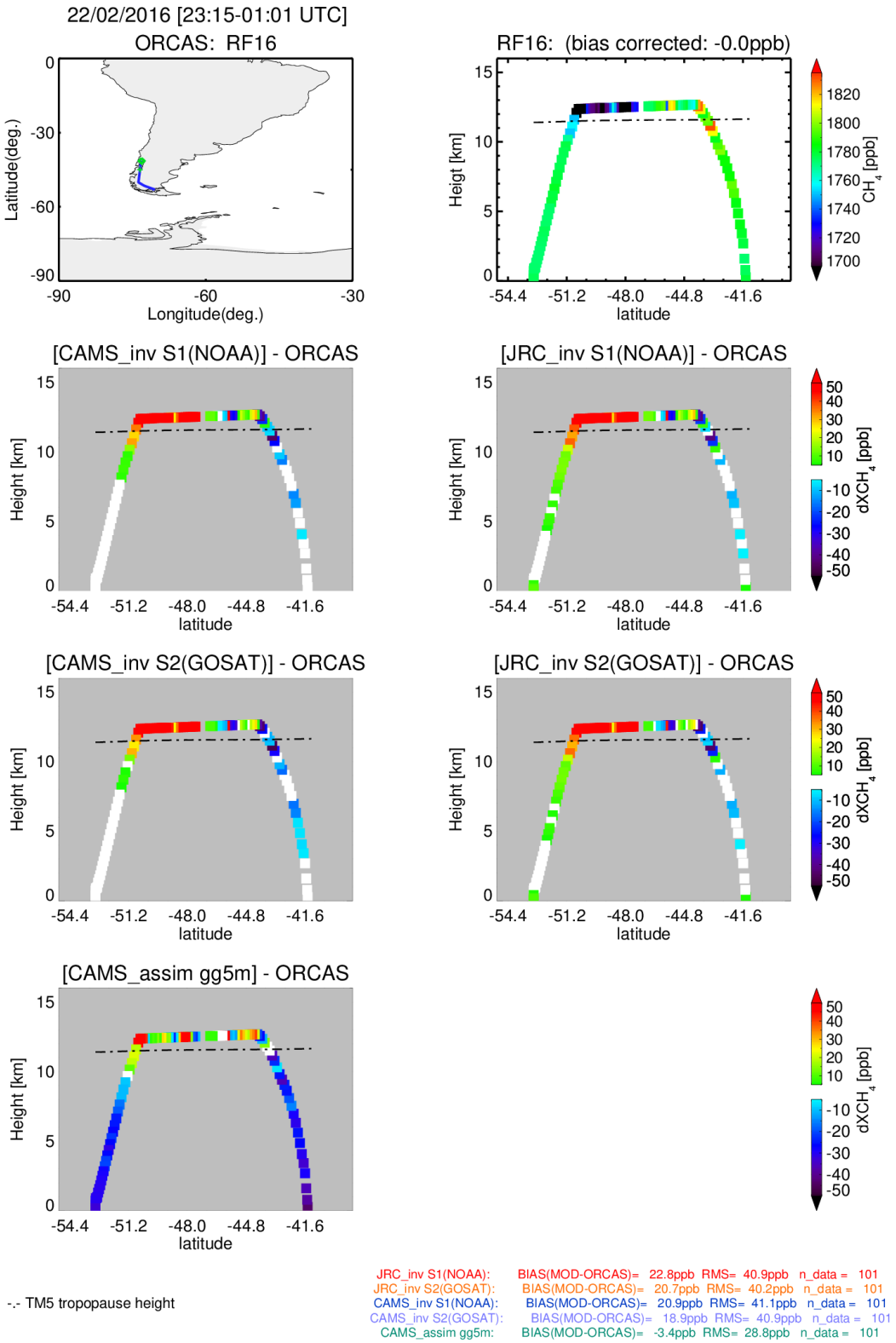

Figure A23: As Figure A21, but for the flight RF16 (22/02/2016).

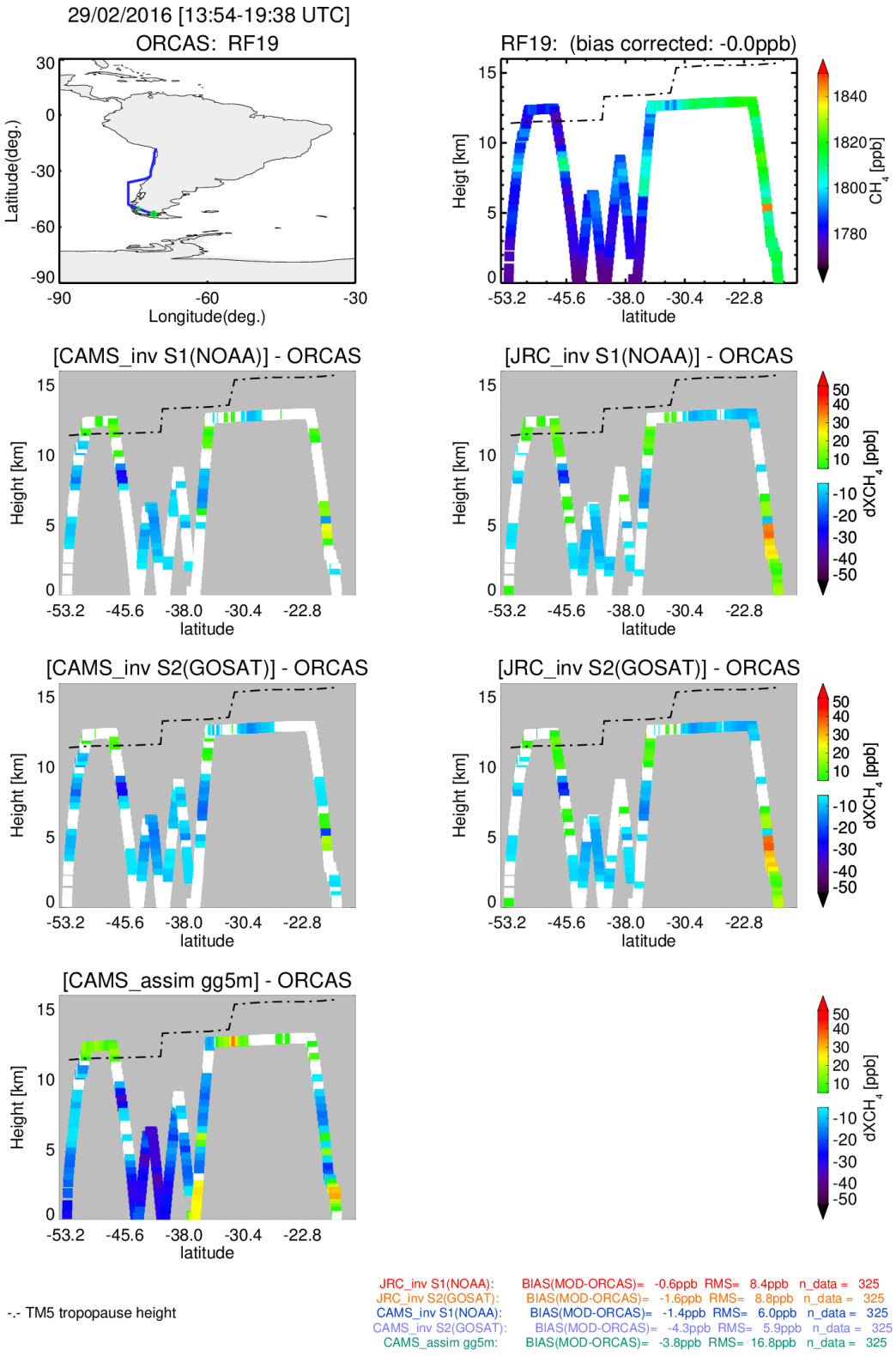

Figure A24: As Figure A21, but for the flight RF19 (29/02/2016).

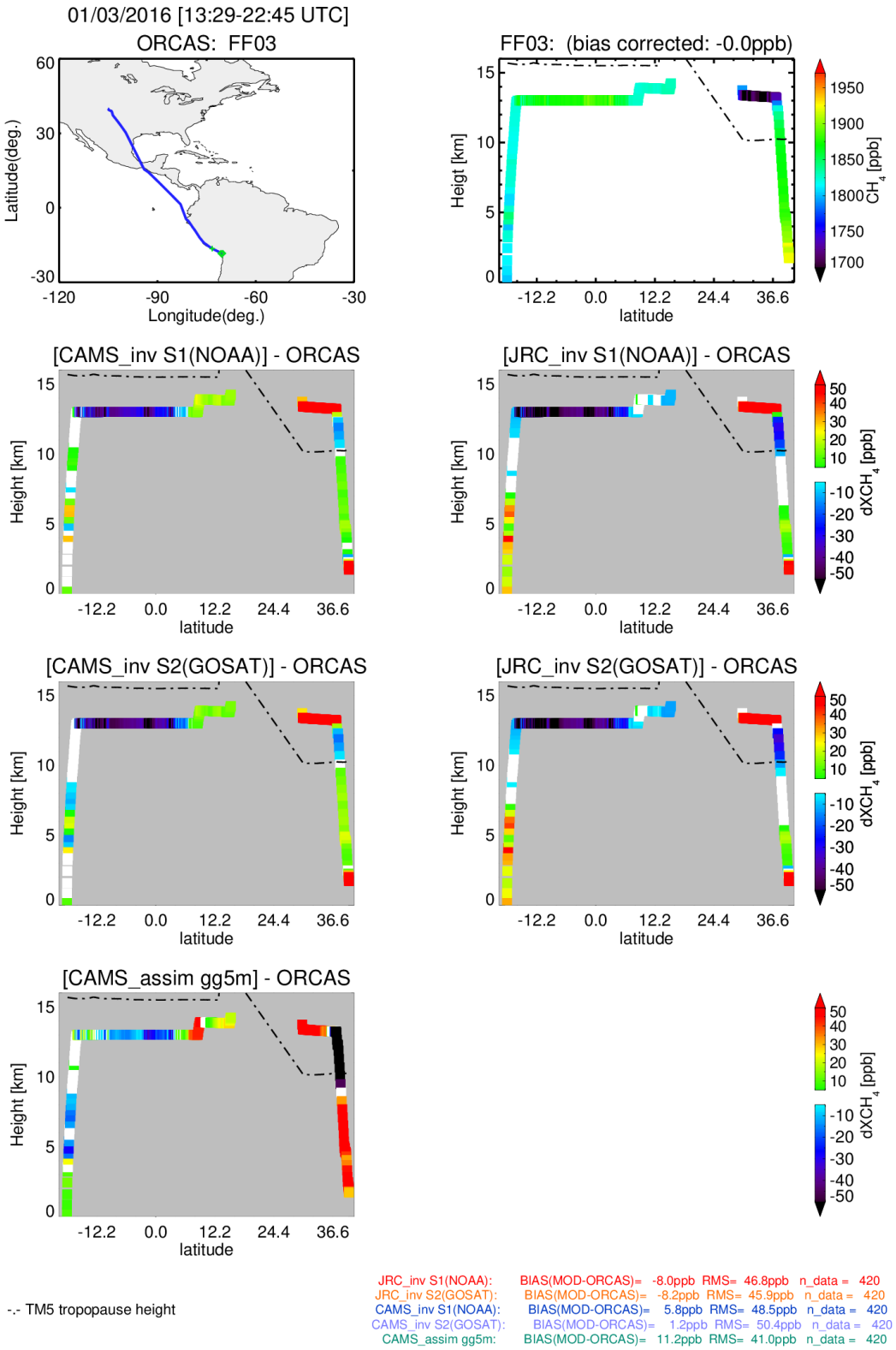

Figure A25: As Figure A21, but for the flight FF03 (01/03/2016).

Annex 3: Vertical profiles of AirCore data and statistics

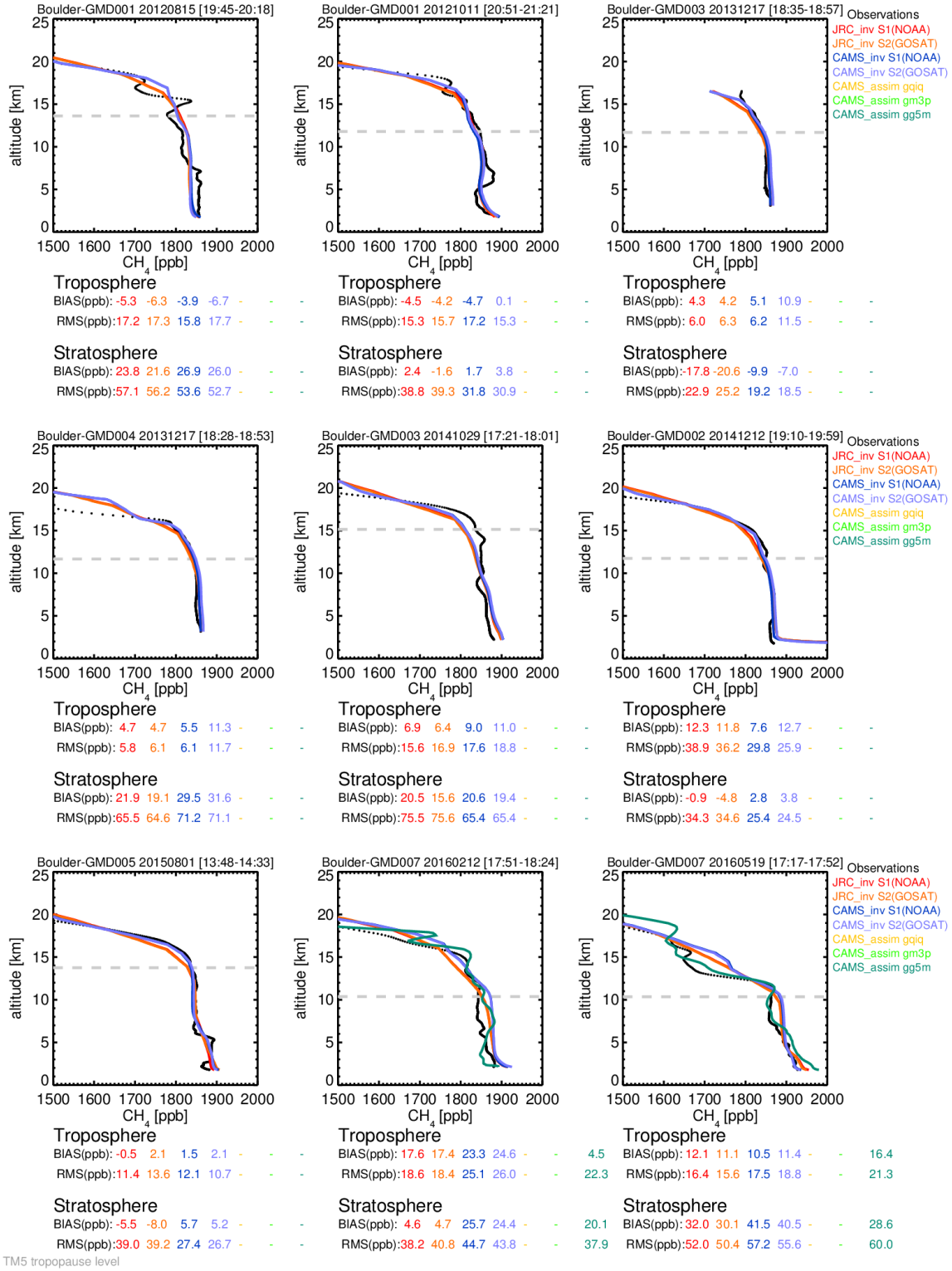

Figure A31: Vertical profiles of CH_4 mole fractions and model simulations (JRC and CAMS inversions and CAMS "near real time analyses") and observations collected during AirCore experiments at Boulder. The level of the tropopause, as diagnosed from the TM5 model, is shown by the dashed lines.

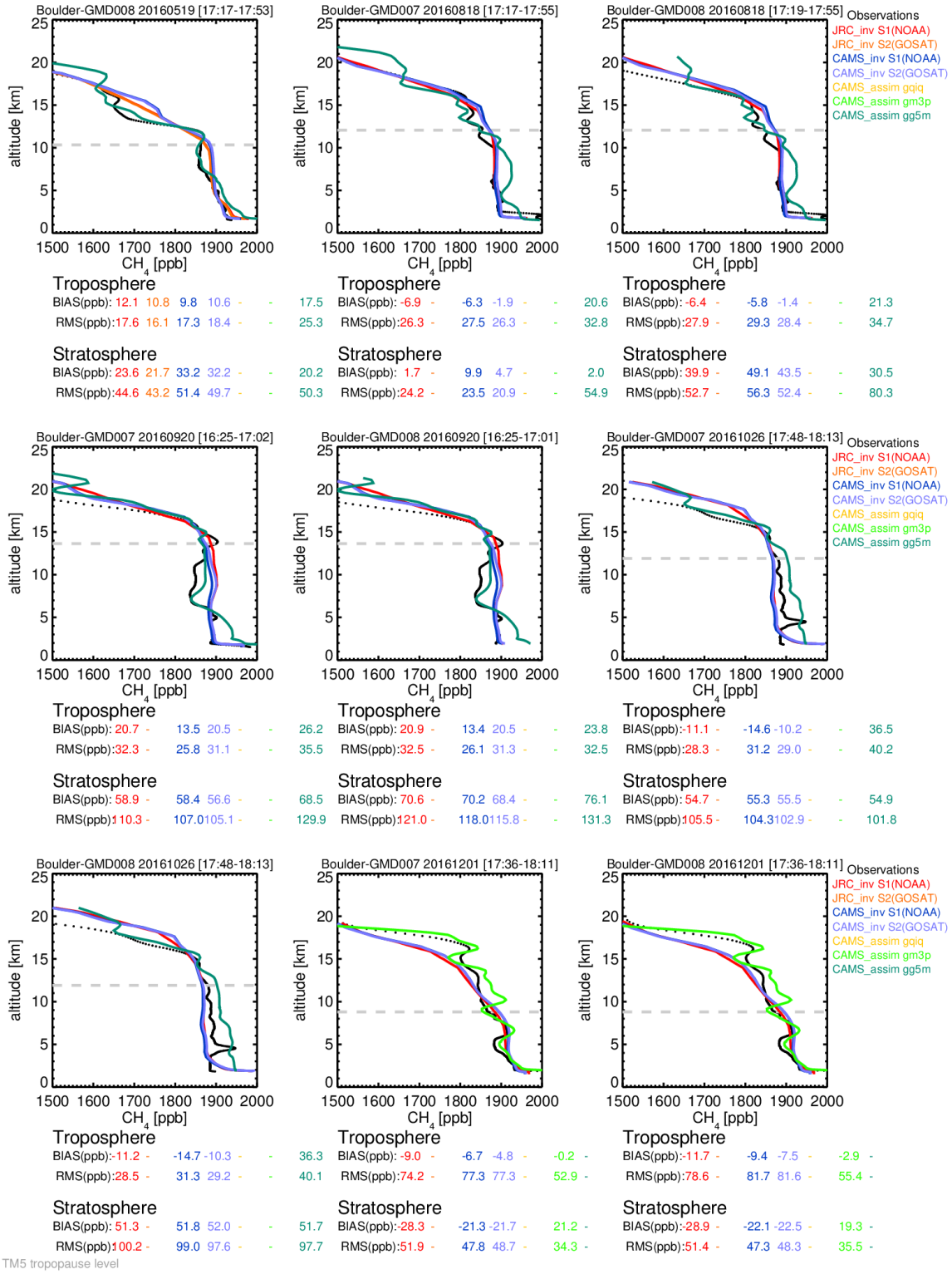

Figure A31: Continued

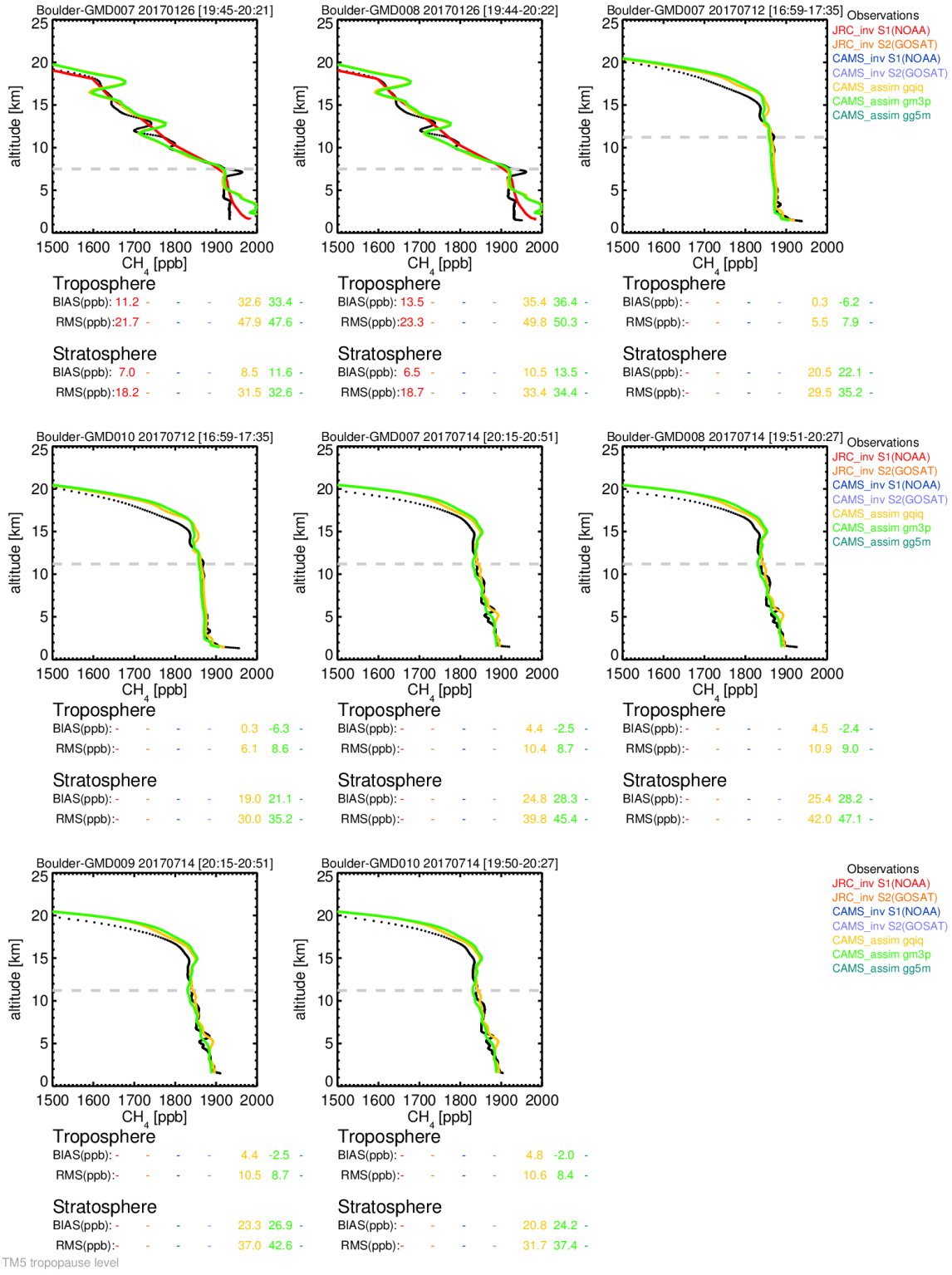

Figure A31: Continued

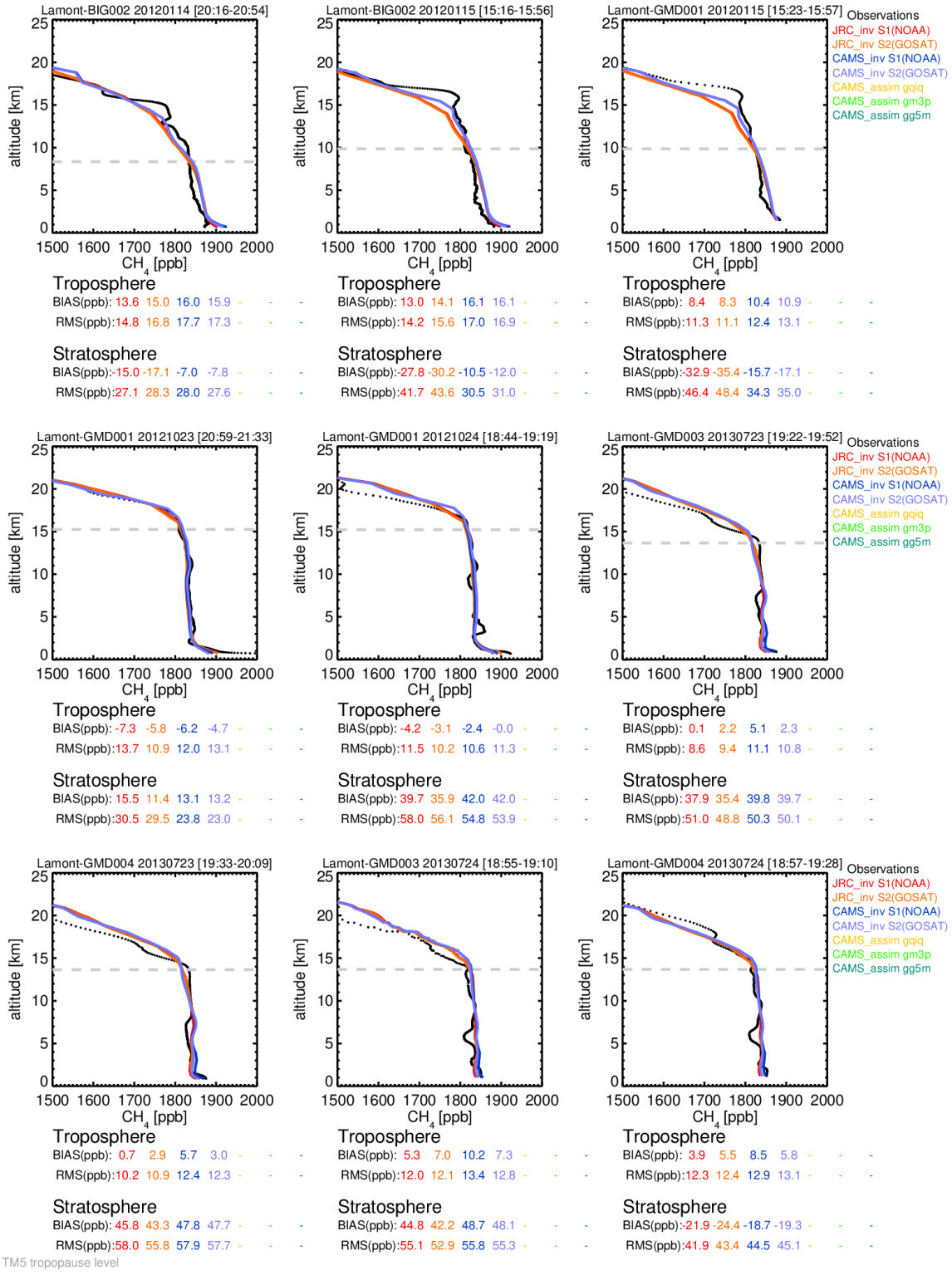

Figure A32: As Figure A31, but data at Lamont.

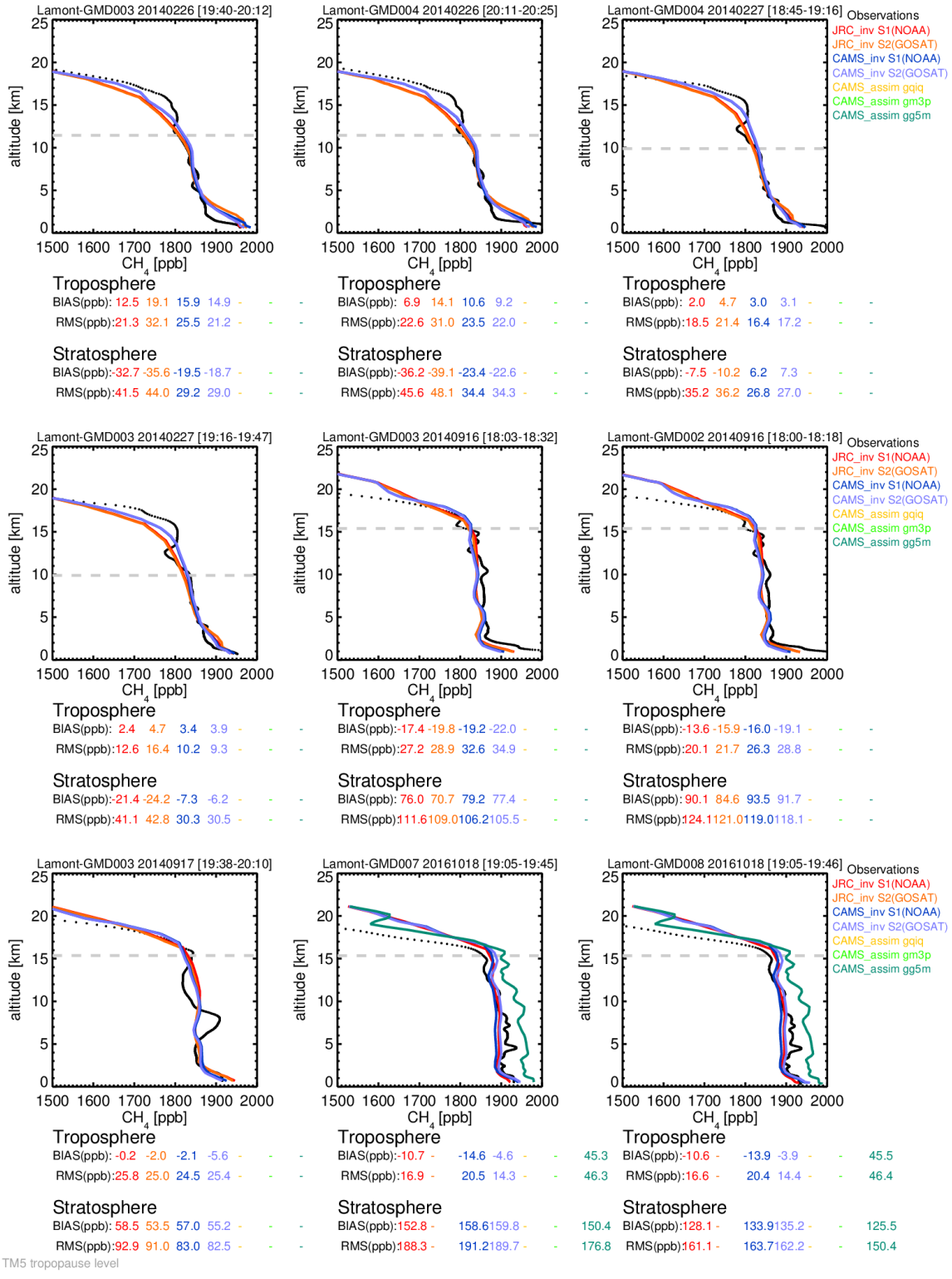

Figure A32: Continued

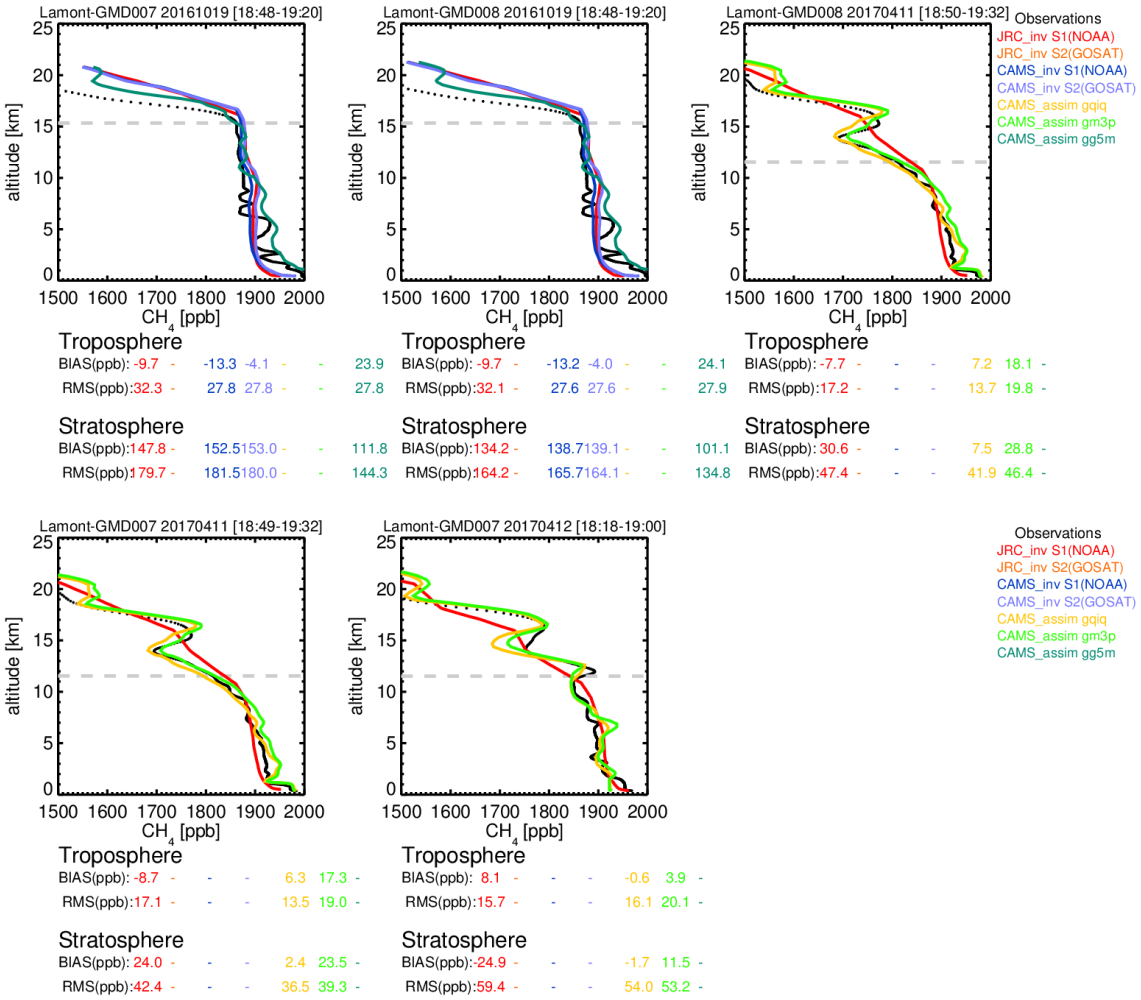

Figure A32: Continued

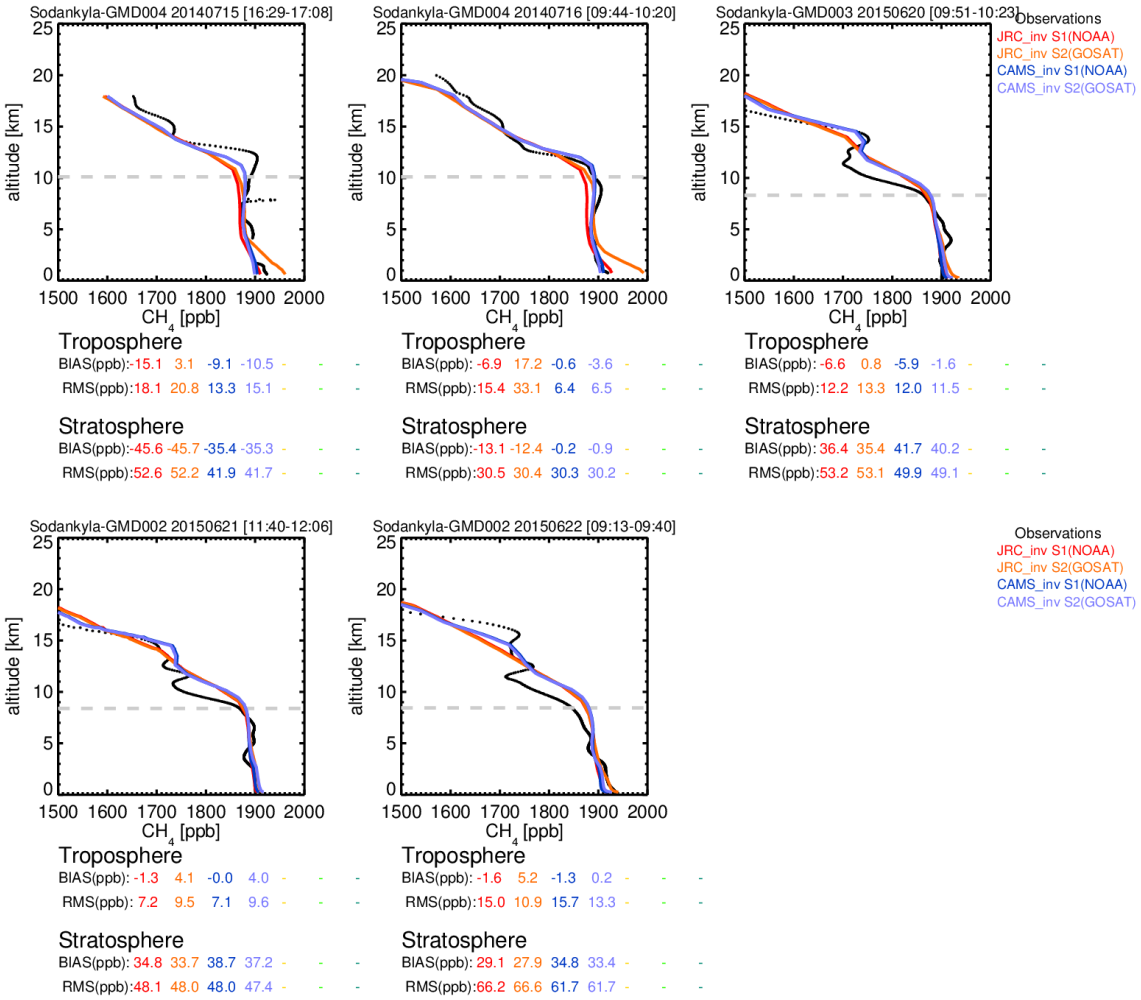

Figure A33: As Figure A31, but data at Sodankyla.

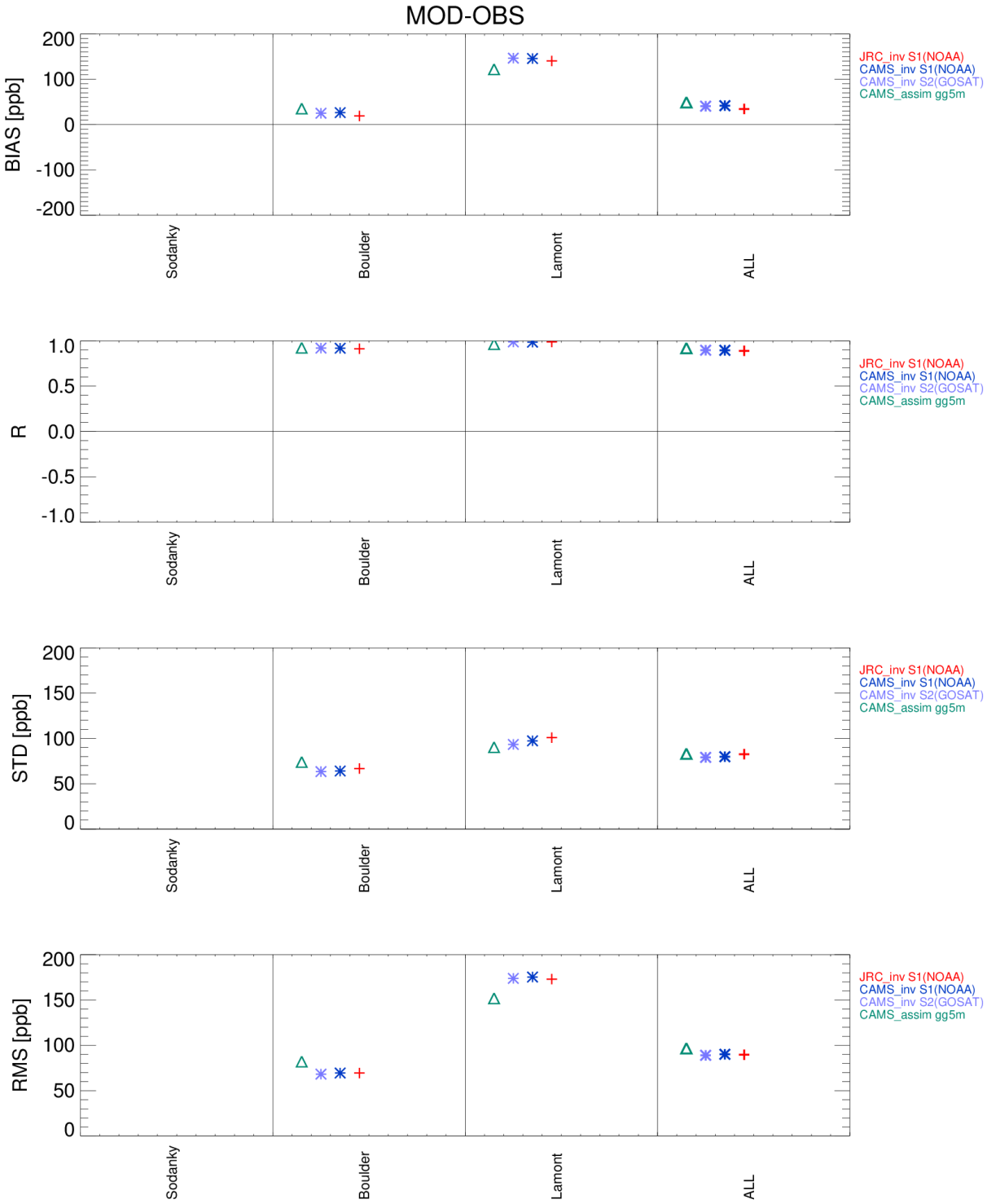

Figure A34: Summary of the evaluation of the different CH_4 products (CAMS and JRC flux inversions and CAMS "near real time analyses"): mean bias, correlation coefficient R, standard deviation (STD), and root mean square (RMS) difference between model simulations and the AirCore observations during 2016 above the tropopause and for each AirCore site.

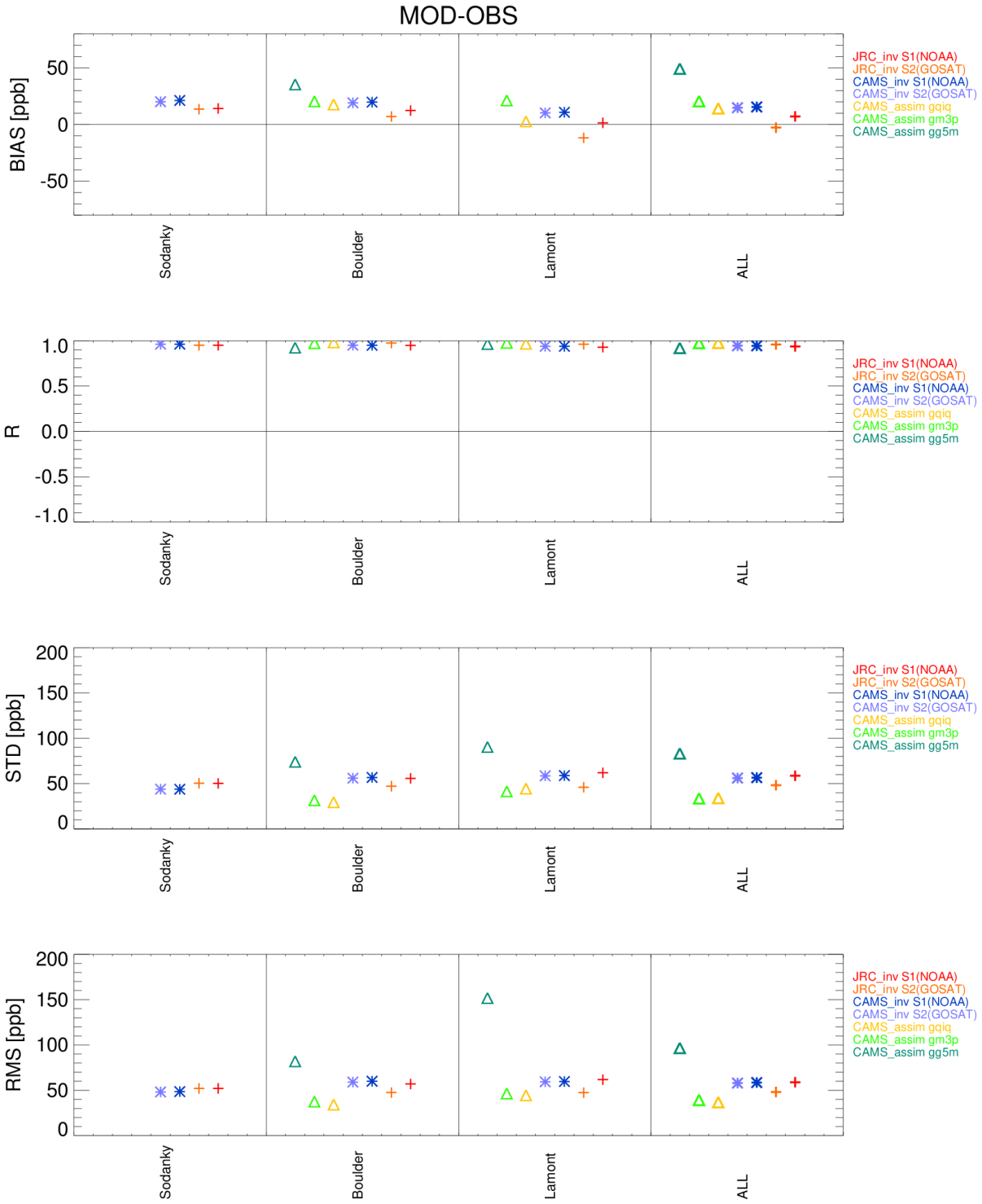

Figure A35: As Figure A34, but for the period 2012-2017.

GETTING IN TOUCH WITH THE EU

In person

All over the European Union there are hundreds of Europe Direct information centres. You can find the address of the centre nearest you at: https://europa.eu/european-union/contact_en

On the phone or by email

Europe Direct is a service that answers your questions about the European Union. You can contact this service:

- by freephone: 00 800 6 7 8 9 10 11 (certain operators may charge for these calls),

- at the following standard number: +32 22999696, or

- by electronic mail via: https://europa.eu/european-union/contact_en

FINDING INFORMATION ABOUT THE EU

Online

Information about the European Union in all the official languages of the EU is available on the Europa website at: https://europa.eu/european-union/index_en

EU publications
You can download or order free and priced EU publications from EU Bookshop at: https://publications.europa.eu/en/publications. Multiple copies of free publications may be obtained by contacting Europe Direct or your local information centre (see https://europa.eu/european-union/contact_en).

KJ-NA-29349-EN-N

The European Commission's science and knowledge service
Joint Research Centre

JRC Mission
As the science and knowledge service of the European Commission, the Joint Research Centre's mission is to support EU policies with independent evidence throughout the whole policy cycle.

EU Science Hub
ec.europa.eu/jrc

@EU_ScienceHub
EU Science Hub - Joint Research Centre
Joint Research Centre
EU Science Hub

Publications Office

doi:10.2760/906932
ISBN 978-92-79-93409-4